The Development of Enzyme Electrodes for Neurophysiology

Peter Timothy Galley

A thesis submitted in partial fulfilment for the degree of Doctor of Philosophy of the University of London and for the Diploma of Imperial College

Department of Chemistry, Imperial College

and

Department of Metabolic Medicine,
St Mary's Hospital Medical School

Abstract

In the past few years the real-time measurement of three important neurotransmitters acetyl choline (ACh), glutamate and γ-amino butyric acid (GABA) has continued to elude neuroscientists. This thesis presents a novel technique, an enzyme dialysis electrode, which can be used for their *in vivo* measurement. The invention combines the specificity of an enzyme biosensor with the micro-sampling techniques routinely used by neurophysiologists. Rather than monitoring neurochemicals as they are extracted from the brain, this probe eliminates the time delay and detects concentration changes at the point of implantation, with a detection limit presently at the 100 nM level and with a time response of ≈90% within 5 seconds. One of the many features of this sensor is its ability to measure background or 'control' levels immediately prior to the intended measurements. The technique has been shown to work for glutamate *in vivo* and for ACh in test solutions. By simply altering the enzymes the continuous measurement of GABA and other metabolites is possible.

The refinement of the electrodes to 200 μm diameter needle-like sensors is described and results are presented showing their *in vivo* performance. Changing levels of glutamate have been detected in the rat striatum during behavioural responses, in the rat hippocampus during long-term potentiation (a possible mechanism for learning and memory) and with epileptic activity.

These new sensors have great potential in a wide range of neurological studies such as behavioural activities, animal models of human diseases and for monitoring in neurosurgery.

Contents:

page

Abstract 3
Contents 5
List of figures 7
List of tables and plates... 11
Abbreviations 13
Acknowledgements 19

Chapter One: Introduction

1.1 The use of enzyme electrodes in neurophysiology ...21
1.2 Neurophysiological techniques 21
1.3 Enzyme electrodes and biosensors 27
1.4 The development of sensors 40
1.5 A sensor for glutamate 42
1.6 A sensor for ACh 46
1.7 The design of an *in vivo* probe 47
1.8 Neuroanatomy and neurophysiology of the rat brain...50
1.9 The aim of this study 50

Chapter Two: Materials and methods

Section 1: General procedures

2.1 Chemicals and solutions 57
2.2 Enzymes and biological reagents 57
2.3 Electrode fabrication 58
2.4 Enzyme immobilization and entrapment 59
2.5 Apparatus 61
2.6 Electronics 63

Section 2: Working electrode synthesis

2.7 Large electrodes 65
2.8 Electrosynthesis of organic salts 68
2.9 Organic salt paste coating 70
2.10 Platinum electrodes 71

Section 3: Probe construction

2.11 Immobilized and entrapped enzymes 72
2.12 Designing an implantable micro-probe 74

Chapter Three: The properties and lifetimes of the electrodes and probes

3.1 Tightly-packed, oil and polymer-bound organic salt ...87
3.2 Electrochemically synthesized organic salt electrodes..91
3.3 Organic salt paste coating 95
3.4 The platinum / peroxide system 98
3.5 Enzyme entrapment 104
3.6 The measurement of glutamate with the probes ...106
3.7 The measurement of acetyl choline 117
3.8 The removal of interference 118

Chapter Four: The measurement of glutamate in the Striatum

4.1 Striatal neural pathways 121
4.2 Probe implantation 122
4.3 The 'tail pinch' 124
4.4 The 'Control' run 128
4.5 Glutamate measurement during the tail pinch ...131
4.6 Catalase perfusion 135
4.7 Pharmacological effects 136
4.8 Conclusions 137

Chapter Five: The measurement of glutamate in the Hippocampus

5.1 Long-term potentiation and previous glutamate measurements 139
5.2 Probe construction 140
5.3 Probe implantation 142
5.4 Stimulus frequency procedures 143
5.5 In vivo 'control' or perfusion experiments 144
5.6 Measuring glutamate 145
5.7 Glutamate release during long-term potentiation ...148
5.8 Epileptic activity in the Hippocampus 151
5.9 Conclusions 153

References 155

List of Figures

Chapter One: Introduction

Figure 1.1 A recording of an epileptic fit in the dentate gyrus of the male rat

Figure 1.2 Electrochemical techniques

Figure 1.3 Push-pull cannulae and the cortical cup

Figure 1.4 A dialysis probe and a dialytrode

Figure 1.5 Schematic view of a biosensor

Figure 1.6 A first generation enzyme electrode for cholesterol

Figure 1.7 A second generation enzyme electrode

Figure 1.8 Two third generation enzyme electrodes

Figure 1.9 Organic and inorganic mediators

Figure 1.10 A mechanism for homogenous mediation

Figure 1.11 A mechanism for heterogeneous redox catalysis

Figure 1.12 A reaction scheme for NADH oxidation

Figure 1.13 Immobilized and entrapped enzymes

Figure 1.14 The set-up for potentiometric and amperometric experiments

Figure 1.15 Theoretical plots for potentiometric and amperometric analysis

Figure 1.16 A membrane covered electrode

Figure 1.17 Possible pathways for glutamate release, uptake and metabolism

Figure 1.18 Three glutamate sensors

Figure 1.19 Two acetyl choline sensors

Figure 1.20 An *in vivo* implantable microprobe

Figure 1.21 Saggital section through the rat brain

Figure 1.22 Overall shape of the rat brain, showing the hippocampus

Figure 1.23 Saggital section through the hippocampus

Figure 1.24 'Transverse' section through the rat brain showing the dorsal striatum

Chapter Two: Methods and Materials

Figure 2.1 Three immobilizing polymers, poly-N,N'-dimethyl piperidine, polystyrene sulphonic acid and nafion

Figure 2.2 The set-up for *in vivo* probe calibration

Figure 2.3 The set-up for the calibration of the large test electrodes

Figure 2.4 The electronic circuit for a purpose built potentiostat

Figure 2.5 Large cavity electrodes

Figure 2.6 254 μm Cavity-packed electrodes

Figure 2.7 A Design **1** probe

Figure 2.8 A Design **2** probe

Figure 2.9 A Design **3** probe

Figure 2.10 A Design **4** probe

Figure 2.11 A Design **5** probe for hippocampal implantation

Chapter Three: The properties and lifetimes of the electrodes and probes

Figure 3.1a Graph showing the lifetime of a 254 μm tightly-packed $TTF^{+}TCNQ^{-}$ electrode

Figure 3.1b The response time for a cavity packed electrode

Figure 3.2 Graph showing the recovery of activity for a $TTF^{+}TCNQ^{-}$ readsorbed Choline oxidase electrode

Figure 3.3 Graph showing activity of a 254 μm polystyrene-bound $NMP^{+}TCNQ^{-}$ electrode

Figure 3.4 Graph showing lifetime of a 254 μm silicone oil-bound $TTF^{+}TCNQ^{-}$ electrode

Figure 3.5 Graph showing the activity of a 254 μm electroplated $NMP^{+}TCNQ^{-}$ electrode

Figure 3.6 Graph showing the activity of an 50 μm electroplated $TTF^{+}TCNQ^{-}$ platinum electrode

Figure 3.7 Graph showing the potential dependence of the current

Figure 3.8 Graph showing the effect of polymer coating the electrode

Figure 3.9 Graph showing the activity of a graphite paste organic salt electrode

Figure 3.10a Graph showing the activity of an organic salt electrode bound with silicone oil only

Figure 3.10a Graph showing the activity of a graphite paste organic salt electrode

Figure 3.11 Graph showing the sensitivity of a glucose oxidase/ H_2O_2 electrode

Figure 3.12 Graph showing the activity of a glucose oxidase/ H_2O_2 electrode

Figure 3.13 Theoretical cyclic voltammograms of $NiFe_2(CN)_6$

Figure 3.14 A cyclic voltammogram for a glucose oxidase probe

Figure 3.15 A cyclic voltammogram for a glutamate oxidase probe

Figure 3.16 Graph showing the effect of electrode potential on the current

Figure 3.17 Graph showing the effect of electrode size on the current

Figure 3.18 Graph showing the response for PDP^+ / PSA^- immobilization

Figure 3.19 Graph showing the response for polyacrylamide gel immobilization

Figure 3.20 Graph showing the response of a design **1** probe

Figure 3.21 Graph showing the response of a design **2** probe

Figure 3.22 Graph showing the response of a design **3** probe

Figure 3.23 Graph showing the effect of a nafion coat on the lifetime

Figure 3.24 Graph showing the oxygen effect for glutamate oxidase on organic salt

Figure 3.25 Graph showing high sensitivity measurement for glutamate oxidase on organic salt

Figure 3.26a Graph showing high sensitivity measurement for glutamate oxidase on platinum

Figure 3.26b Response time for a glutamate oxidase / H_2O_2 electrode

Figure 3.27 Graph showing the dependence of enzyme concentration on the current

Figure 3.28 A Hanes plot for a glutamate oxidase probe

Figure 3.29 A 'Rho' plot for a glutamate oxidase probe

Figure 3.30 A comparison of glutamate and glutamine activity

Figure 3.31 Graph showing the activity of an 'untreated platinum' glutamate probe

Figure 3.32 Graph showing the sensitivity of an acetyl choline probe

Figure 3.33 Graph showing the repulsion of ascorbate by nafion

Figure 3.34 Graph showing the reduction of the glutamate current by nafion

Figure 3.35 Graph showing the reduction of electrode ascorbate oxidation by ascorbate oxidase

Chapter Four: The measurement of glutamate in the striatum

Figure 4.1 The basal ganglia-thalamocortical pathway

Figure 4.2 The arrangement for an implanted probe

Figure 4.3 A schematic view of the probe measuring interference

Figure 4.4 A Pre-implantation calibration of a microprobe

Figure 4.5 The 'Blank run' tail pinch

Figure 4.6 A schematic view of the probe removing interference

Figure 4.7 The effect of perfusing ascorbate oxidase into the probe

Figure 4.8 The 'Control run' tail pinch

Figure 4.9 A schematic view of the probe measuring glutamate

Figure 4.10 The effect of perfusing glutamate oxidase into the probe

Figure 4.11 *In vitro* glutamate calibration

Figure 4.12 The measurement of glutamate for a tail pinch

Figure 4.13 The effect of perfusing catalase into the probe

Figure 4.14 The effect of catalase on the tail pinch

Figure 4.15 The effect of an apomorphine injection on the glutamate release

Chapter Five: The measurement of glutamate in the hippocampus

Figure 5.1 The site of implantation of the probe in the dentate gyrus

Figure 5.2 A Pre-implantation ascorbate calibration

Figure 5.3 2 Hz stimuli of the perforant path in the absence of glutamate oxidase

Figure 5.4 The effect of adding glutamate oxidase to an implanted probe

Figure 5.5 2 Hz stimuli of the perforant path

Figure 5.6 Post-implantation ascorbate and glutamate calibration

Figure 5.7 The effect of LTP on the 2 Hz stimuli of the perforant path

Figure 5.8 The induction and maintenance of LTP in the dentate granule cells

Figure 5.9 Post-implantation glutamate calibration

Figure 5.10 Electrophysiological recording of evoked LTP

Figure 5.11 Glutamate release during kindling-induced epileptic activity

Figure 5.12 Electrophysiological recording of evoked response for kindling-induced epileptic activity

List of Tables

Chapter One: Introduction

Table 1.1 Electroactive metabolites in the brain measured on a carbon fibre electrode

Table 1.2 Classes of electron transfer enzyme

Table 1.3 Comparison of the two glutamate enzymes used

Table 1.4 Features of the *in vivo* micro enzyme electrode

Chapter Two: Methods and Materials

Table 2.1 Commercial enzyme preparations

Chapter Three: The properties and lifetimes of the electrodes and probes

Table 3.1 Comparison of electrode sizes and currents

Table 3.2 Substrate specificity of the glutamate probe

Chapter Five: The measurement of glutamate in the hippocampus

Table 5.1 The stimulus frequencies

List of Plates

Chapter Two: Materials and Methods

Plate 2.1 The five different probe designs **1** - **5**

Plate 2.2 Probe design **1** at 10-fold magnification

Plate 2.3 Probe design **2** at 10-fold magnification

Plate 2.4 Probe design **3** at 10-fold magnification

Plate 2.5 Probe design **4** at 10-fold magnification

Plate 2.6 Probe design **5** for striatal work (life size)

Plate 2.7 Probe design **5** for striatal work at 10-fold magnification

Plate 2.8 Probe design **5** for hippocampal work (life size)

Plate 2.9 Probe design **5** for hippocampal work at 10-fold magnification

Abbreviations

ACh	Acetyl choline
AChE	Acetyl choline esterase
Asc	Ascorbate
CA	Cornu Ammonis
ChOx	Choline Oxidase
CNS	Central Nervous System
CSF	Cerebral Spinal Fluid
DA	Dopamine
DDW	Double Distilled Water
DG	Dentate Gyrus
DOPAC	Dehydroxy phenyl acetic acid
DPV	Differential Pulse Voltammetry
EDTA	EthyleneDiamine Tetra Acetic acid
EGTA	Ethylene Glycol-bis(β-amino ethyl ether)
EPSP	Excitatory Post-Synaptic Potential
Er	Entorhinal Cortex
FAD / $FADH_2$	Flavin Adenine Dinucleotide (oxidized /reduced)
FMN	Flavin Mono Nucleotide
GABA	γ-amino butyric acid
HEPES	N-[2-hydroxyethyl] piperazine -N'-[2-ethanesulphonic acid]
5-HIAA	5-Hydroxy Indole Acetic Acid
HPLC	High Pressure Liquid Chromatography

IPSP	Inhibitory post synaptic potential
5-HT	5-hydroxytryptamine (serotonin)
HVA	Homo Vanillic Acid
LTP	Long-term potentiation
$NAD(P)^+$ / NAD(P)H ...	Nicotinamide Adenine (Phospho) Dinucleotide (oxidized / reduced)
NMP^+	N -Methyl phenazinium
PDP^+	Poly-N,N- Dimethyl Piperazine
PSA^-	Polystyrene Sulphonic Acid
PTP	Post-Tetanic Potentiation
SS	Stainless Steel
Sub	Subiculum
TEMED	N,N,N',N'- Tetra ethyl-4-butane diamine
TTF	Tetra Thio Fulvalene
TCNQ	Tetra Cyano Quinodimethane
UA	Uric Acid

To my family,
friends
and
other animals

'Sensitivity and trouble are proportional'

Primo Levi

(The Periodic Table, 1975)

Acknowledgements

I would like to express my thanks to my supervisors Professor John Albery and Dr John Jefferys for dreaming up such a challenging project !

My thesis has been funded entirely by The Wellcome Trust and I would like to thank all concerned.

I have also had the privilege of having three other 'foster' supervisors, Professor Desmond Johnston, Dr Marianne Fillenz and Dr Tim Bliss, who have given me every ounce of their support

My family and Nick Ken, Giles, Sput and Pat (+family) have always been there when needed

Martyn Boutelle, Mick Errington and Edmond Magner have provided all the help during the last three years and a lot of credit goes to them for the success (!?) of this project. Thanks guys !

I would also like to express my thanks to the Albery and Jefferys groups past and present for the friendliness and support they have shown: Andy M, Ged, George, Ben (GBM), Ying, Nick, Bernie, Arshad, Imran, Barry Anne, Brian, Lindy, Ruth Alison, Sarahs J &W, Gerald..+ Andy, Jenny, Paul K, Mark G, David W, Lesley, Vahab and Greg...

The following at St Mary's have entertained me for the last year: Pete M, Corla, Kamsiah, Johnny, Steve, Liz, Chris, Dawn, Cathy, Jill, Debbie, Karen, Victor, Jane, Ann, Pete G, Jane, Sue, Victor, Nithy..*et al.*

All my flat-mates at 'The Bramber Road Institution': Andy, Keith, Simon, Brian, Matt, Johnny P, JP, JF, Fergus, Marcus, Andy & Dave F, Wally, Simon H and the 'Joint Honours Boys' Dave , Eamonn, Andy R and Andy B have put up with me so well. Sez and Meriel *et al* for introducing me to the delights of 'TV drinking' !!

Jeremy and family (& Baldrick) for helping me enjoy 21hr 52min of curled-up jam butties, deep heat and nausea !

And last but not least the three other wallies for making life in 549 so great: Monsignor Oi Oi, Rat and Bear..... I could n't have made it without you all.

Peter Galley October 1991

Chapter One

Introduction

1.1 The use of enzyme electrodes in neurophysiology

The need to measure the concentrations of important neurotransmitters and metabolites in the nervous system is a fundamental requirement in order to gain an understanding of the complex mechanisms involved. The last twenty years has seen much progress in the field of electrochemical and spectroscopic measurements, with new and improved techniques being presented constantly.

The variety of such techniques, described in the next section, is wide and reflects the attention that these neurotransmitters and metabolites have received. *In vivo* enzyme electrodes have seldom been used in neurochemistry, because of various problems, such as loss of enzyme activity, but as this thesis shows, they now have a great potential for neurophysiological use.

1.2 Neurophysiological techniques

Early neurophysiological studies were carried out using glass micro-electrodes and markers to study and map out the neuronal connections and these electrophysiological techniques are still widely used. The electrodes used for these experiments are glass capillaries filled with an ionic solution, which acts as an electrolyte, drawn out to give a fine tip of approximately 1 μm (Halliwell and Whitaker 1987). The components of the ionic solution vary depending on the experiment being performed. For example Finch and Jackson (1990) used 140 mM

K^+gluconate, 1 mM NaCl, 1mM $MgCl_2$, 0.5mM $CaCl_2$, 5mM EGTA and 10mM HEPES at pH 7.2. The tips have a high resistance, ranging from 30 to 500MΩ and can be used for potential recording, current injection and also free ion measurement. The glass/electrolyte system is not the only way of fabricating electrodes. Armstrong-James and Millar (1979) used fine carbon fibres, 7 μm across with a resistance of between 200k and 2MΩ, inside glass capillaries for electrophysiological recordings. These electrodes record from both *in vivo* and *in vitro* slice preparations and can be inserted into single neurons for intracellular recordings or they can be used to measure 'field potentials', the voltages at various points around the neuron, a technique called current density analysis (Lømo 1971). Cell labelling using markers is widespread for (1) cell identification after recording, (2) revealing cell structure and neuronal pathways and identification of free ion concentrations. Many different markers can be loaded into the electrolyte of a drawn microelectrode and then perfused into a cell. Examples of these are fluorescein, rhodamine, labelled dextrans, enzymes with chromagens, heavy metals, dyes and radioligands (Warner and Bate 1987). Figure 1.1 shows an *in vivo* electrophysiological recording from the hippocampus of a male rat.

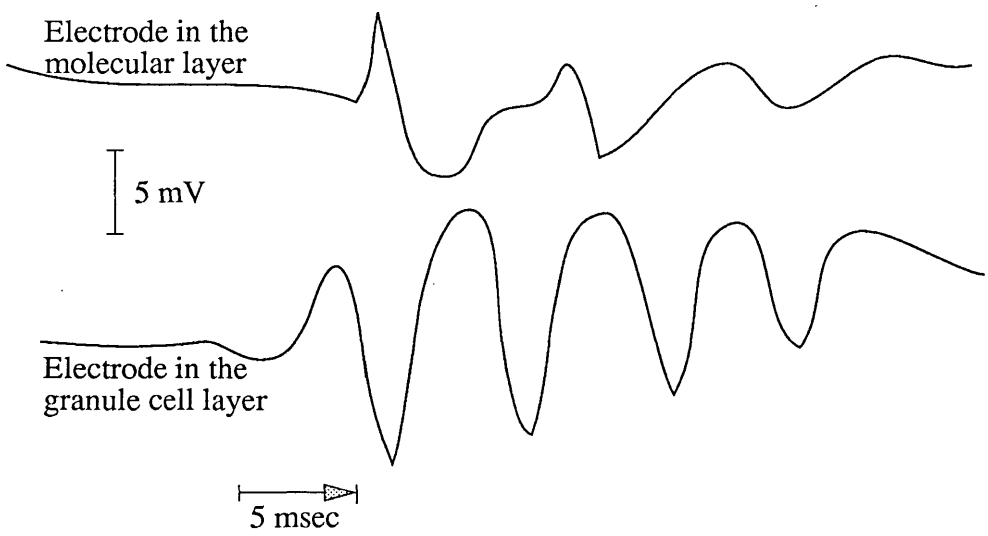


Figure 1.1 A recording of an epileptic fit in the dentate gyrus of the male rat. The downward spikes on the lower trace represent the cells 'firing. This experiment can be found in Chapter Five.

The power of electrophysiological recording is that it reveals a large amount of information about the cell's character, such as its firing rate, its strength of activation and the effects of particular agonists and antagonists. With the use of drugs and toxins, electrophysiology can indicate which neurotransmitter is released by the neuron, however this is not the only technique that has been used.

Since the first *in vivo* electrochemical studies in the 1970's (Kissinger *et al* 1973) carbon paste, carbon fibre, graphite and platinum electrodes have been used to measure electroactive species such as ascorbate and the catecholamines (Gonon *et al* 1981). The relative sizes of these electrodes varies considerably; carbon paste electrodes are typically 300 μm in diameter (O'Neill *et al* 1982), whereas carbon fibre electrodes are 1 to 10 μm across (Armstrong-James and Millar 1979).

When these sizes are compared to the synapse, the junction between two nerve cells, which has been measured as 1 -10 nm (Marsden *et al* 1988), it can be seen that the electrodes cannot measure activity in the synapse itself, rather it is the overflow of neurotransmitters and other metabolites into the extracellular fluid (ECF) from a group of synapses that is measured.

Just as there are many types of electrode, many electrochemical techniques have been described for studying these compounds both *in vivo* and *in vitro* (figure 1.2). In linear sweep voltammetry (LSV), for example, the current is measured as the potential of the electrode is swept at a constant rate between two values. Boutelle and his colleagues swept a carbon paste electrode from 0 to +700 mV at 5 mV s^{-1} at short intervals , figure 1.2a (Boutelle *et al* 1989); whereas differential pulse voltammetry (DPV, figure 1.2b) involves voltage 'pulses' on ramp of increasing potential and this has been used widely for analyzing the electroactive monoamines (Crespi 1990) and for DNA probes (Turner 1991).

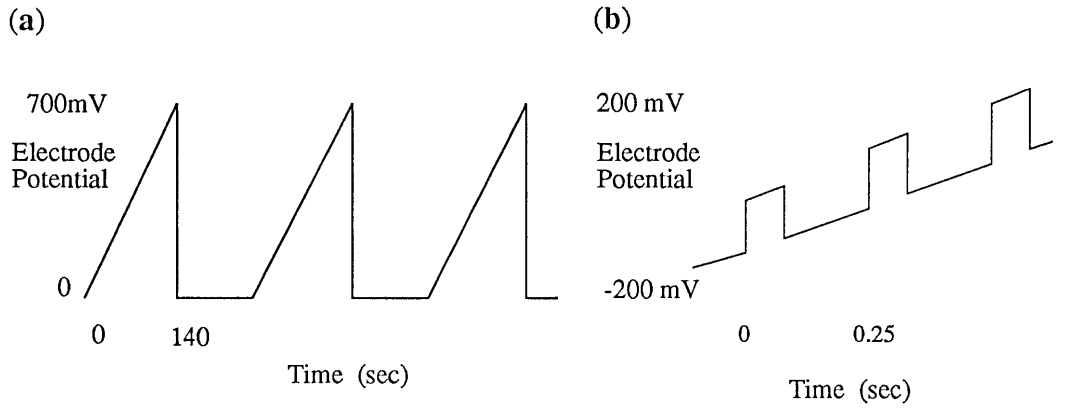


Figure 1.2a & b, Electrochemical techniques (a) LSV linear sweep voltammetry (taken from Boutelle *et al* 1989 and (b) DPV differential pulse voltammetry (adapted from Gonon *et al* 1981)

Many of the electroactive species in the EC F oxidize at close or similar potentials and so these elaborate electrochemical techniques have been developed to differentiate between the signals. A selection of these compounds is presented in table 1.1 (taken from Crespi 1990)

Table 1.1 Electroactive metabolites in the brain measured on a carbon fibre electrode

Compound:	Potential mV
Ascorbate (Asc)	-50
Dopamine (DA) and Di hydroxy phenyl acetic acid (DOPAC)	80-100
Uric acid (UA), 5-hydroxy tryptamine (5-HT) 5-hydroxy indole acetic acid (5-HIAA)	280-310
Homo vanillic acid (HVA)	400-430

An alternative to direct *in vivo* and *in vitro* recording with micro-electrodes is the removal of samples from the brain, a review of these techniques can be found in Abdul-Ghani *et al* (1981) and Benveniste (1989). Early on, 'Push-pull' cannulae and the cortical cup technique were the two most preferred, figure 1.3. Push-pull cannulae consist of two concentric tubes, with an outer diameter of 1mm, down

which buffer is perfused and withdrawn. This has the effect of 'pulling up' any analytes near the probe, which can then be analysed downstream. Cortical cups were superfusion chambers, made from 1.5cm nylon tubes, which were cemented onto the pial surface of the exposed cortex. The chambers were superfused at 1ml/min with O_2 saturated artificial CSF (ACSF) maintained at 37°C. Electrodes were inserted for stimulating and recording and any analytes diffusing up from the cortex could then be studied in the pool above the skull.

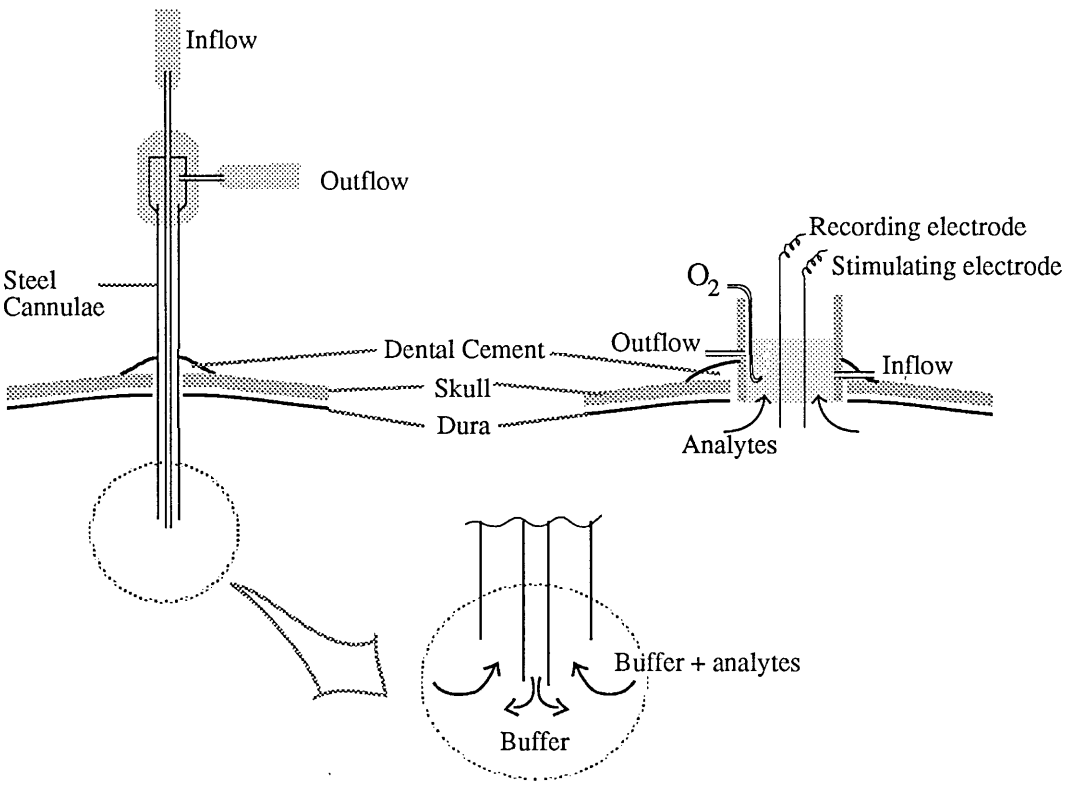


Figure 1.3 Push-Pull cannulae (left) and the cortical cup (right), both adapted from Abdul-Ghani *et al* (1981)

The advent of microdialysis coupled to electrochemical or spectroscopic detection introduced a more delicate sampling technique for *in vivo* work, compared to push-pull cannulae, and two probes are shown in figure 1.4. The microdialysis probe is more refined, with a semi-permeable membrane covering the open ends and

it has been described as an 'artificial blood vessel'. As buffer is perfused through the probe, analytes in the ECF are drawn through the membrane by a concentration gradient, removed by the flow of buffer and then analysed. A 'dialytrode' (Delgado *et al* 1984), shown in figure 1.4, was one of the first such probes. It consisted of a permanently implanted outer cannula, 1.2mm in diameter, down which a finer gauge tube could be inserted. The outer cannula was angled at its tip and covered with a permeable membrane. Buffer was then perfused through the in and outflows, drawing analytes through the membrane. The dialytrode also had fine electrodes stuck to the outer cannula, for stimulating and recording purposes. Microdialysis is now extremely prevalent in the neurosciences, because of its small size and its reduced disturbance on its environment.

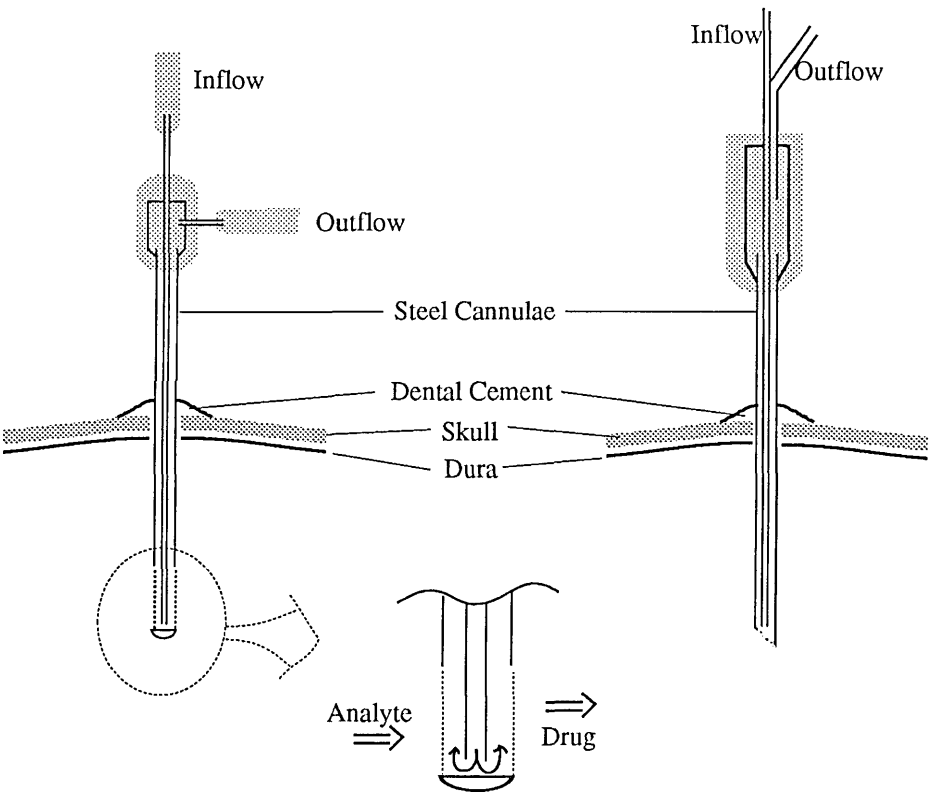


Figure 1.4 A dialysis probe (left) adapted from Ungerstedt (1984) and a 'Dialytrode' (right) adapted from Delgado *et al* (1984)

As described, samples of perfusion fluid were removed from the brain and then analysed downstream. This analysis takes many forms, the outflow can be linked directly to an HPLC column, separating the ECF components which can then be analyzed. Low levels of DA and DOPAC, for example, have been measured electrochemically in the rat striatum after HPLC separation (Wheeler 1991). However, there are a number of chemicals such as glutamate, γ-amino butyric acid (GABA) and acetyl choline (ACh) which are neither electroactive nor directly measurable using HPLC with spectroscopic measurement. Derivatization with o-phthalaldehyde/t-butylthiol prior to separation and either UV fluorimetry (Errington *et al* 1987) or electro-chemical detection (Kissinger and Shoup 1990) is a commonly used method for measuring amino acid levels.

An HPLC column linked to an enzyme packed-bed with a wall-jet electrode (Durrant 1988) and enzyme assays (Nicholls 1988) are also other analytical methods that have been tried for ACh and glutamate respectively. Probably the most significant drawback with these techniques is the sampling time required. In order to accumulate enough analyte, sampling must be done every 10 to 20 minutes, reducing the resolution of these methods considerably. Enzyme electrodes, which have a much faster response time, should reduce this delay significantly, making them an useful technique for studying some of these important neurochemicals.

1.3 Enzyme electrodes and biosensors

Another more specific electrochemical method for measuring compounds is enzyme electrochemistry. Enzyme electrodes are a type of biosensor, whose properties are outlined in figure 1.5. The biosensor centres around a complex biological molecule, such as an enzyme, an antibody or a receptor, whose specificity

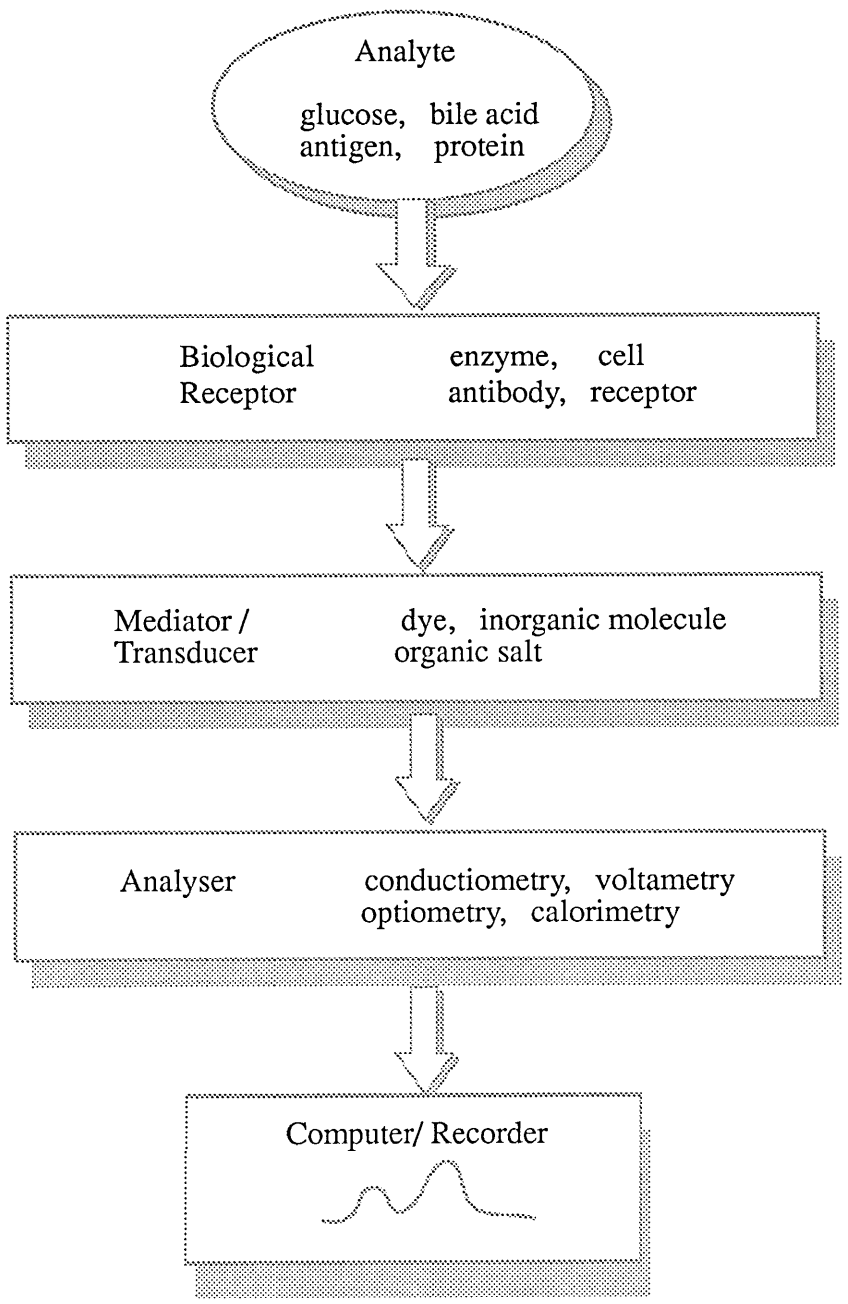


Figure 1.5 Schematic view of a biosensor

and response to the binding of its substrate is converted by the transducer/ mediator to give a measurable electronic, optical or calorimetric signal.

An enzyme electrode consists of an enzyme (or enzymes) in close proximity to a suitable electrode, which converts the turnover of the enzyme's substrate into a quantifiable electronic signal, usually through a chemical mediator. The enzyme electrode uses an oxido-reductase enzyme; there are four main classes of electron-transfer protein and these are shown below in table 1.2; the enzyme electrodes used in this study derive their enzymes predominantly from the first two groups, the pyridine and the flavin linked enzymes.

Table 1.2 Classes of electron transfer proteins

(1) Pyridine linked dehydrogenases using
NAD^+ or $NAD(P)^+$ as the co-enzyme:
alcohol, glutamate, lactate and glycerol dehydrogenase

(2) Flavin linked oxidases using FAD or FMN as the prosthetic group:
glucose, glutamate, choline and L-amino acid oxidase

(3) Cytochromes : Cytochrome b_2

(4) Metal and ion centred proteins
ascorbate oxidase (multi Cu)
ferrodoxin (Fe-S)

Three generations of enzyme electrodes have arisen over the years, where the first generation involved no mediation. In this case, a product of the reaction was itself electroactive and could be measured on a bare electrode. An example, shown overleaf in figure 1.6, is a sensor for cholesterol which produces H_2O_2, which can then be oxidized on a bare platinum electrode at +650 mV.

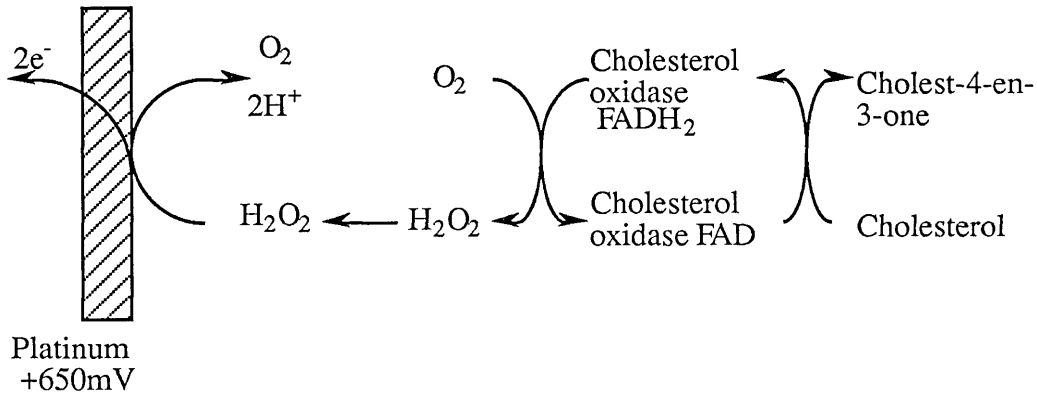


Figure 1.6 A first generation enzyme electrode for cholesterol

Second generation electrodes, figure 1.7, use an aqueous mediator such as ferrocene to oxidize the reduced enzyme or co-enzyme (Cass *et al* 1984). One advantage of using mediators is that the potential of the working electrode can be lowered, reducing the interference due to the oxidation of other electroactive species present.

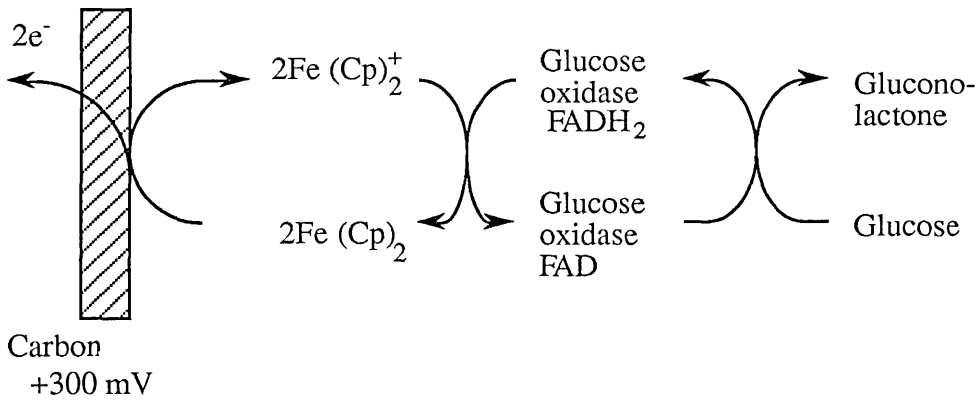


Figure 1.7 A second generation enzyme electrode using ferrocene/ ferrocinium to mediate glucose oxidase (adapted from Cass *et al* 1984)

In the third generation, figure 1.8, the reduced form of the enzyme or co-enzyme is directly oxidized on the surface of the electrode. In the first example shown, the oxidation of choline oxidase on $TTF^{+}TCNQ^{-}$ (Driscoll 1988), the oxidation of the choline produces the reduced form of the enzyme, choline oxidase-$FADH_2$. The reduced flavin group $FADH_2$, is then oxidized directly on the electrode, rather than by oxygen, the natural electron acceptor.

The second example shows an bile acid sensor (Rao 1990) figure 1.8b, using 3α-hydroxy steroid dehydrogenase as its enzyme. The dehydrogenases use NAD^{+} as the electron accepting moiety, forming NADH which is reoxidized back to NAD^{+} under physiological conditions by other enzymes, such as NADH dehydrogenase. With the enzyme electrode, a mediator such as ($NMP^{+}TCNQ^{-}$) is required to reoxidize the NADH, as direct oxidation on a conventional electrode produces harmful radicals that poison the electrode.

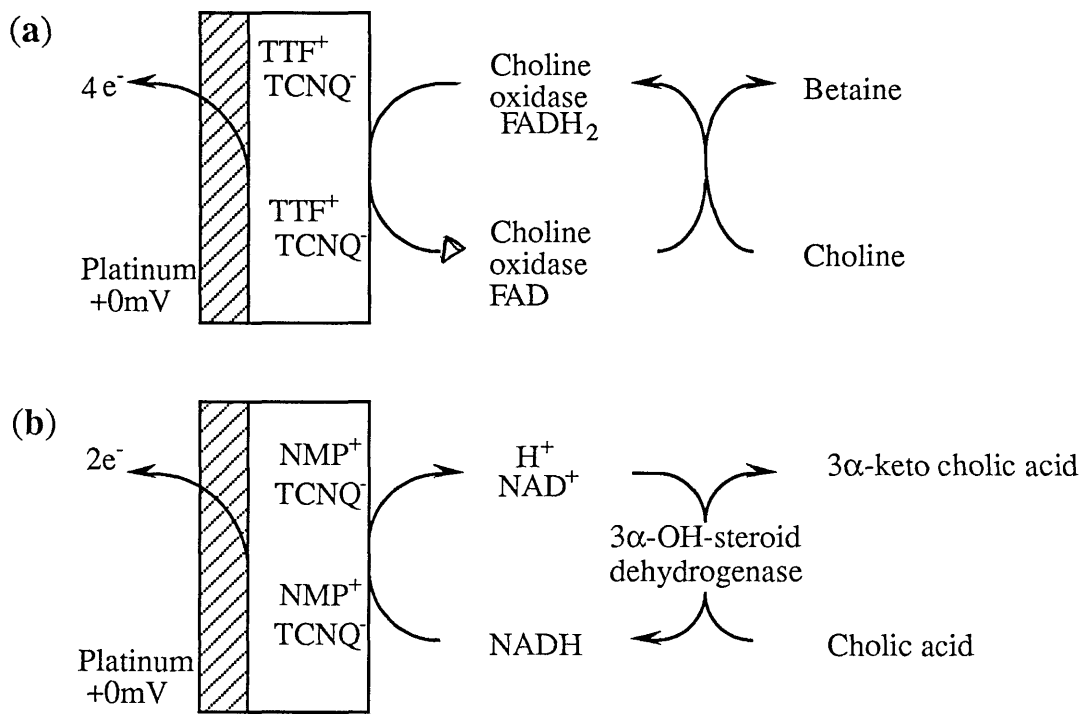
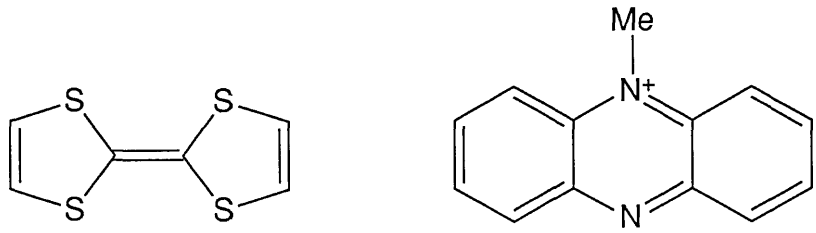


Figure 1.8 Third generation enzyme electrodes, (**a**) a choline oxidase electrode mediated by $TTF^{+}TCNQ^{-}$ (taken from Driscoll 1988) and (**b**) a cholic acid sensor using $NMP^{+}TCNQ^{-}$ (Rao 1990)

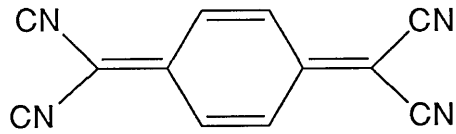
Mediation

A multitude of mediators have been described for oxidizing reduced forms of enzymes and co-enzymes and they range from small inorganic molecules, such as ferrocyanates, to complex organic and biological molecules such as conducting organic salts and dyes, figure 1.9.

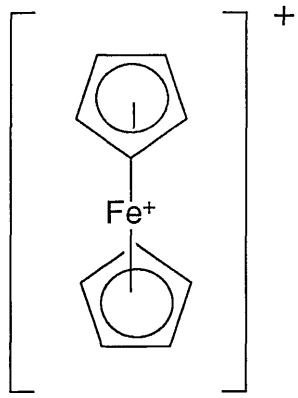


TTF

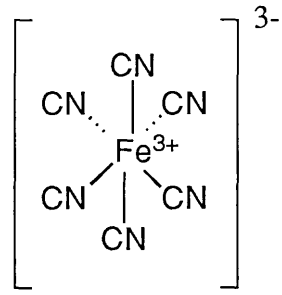
NMP+



TCNQ



Ferricinium



Ferrocyanate

Figure 1.9 Various mediators, the organic mediators NMP^+, TTF and TCNQ are shown at the top, ferricinium and ferrocyanate two inorganic mediators are pictured below.

Two forms of electrode mediation, homogeneous and heterogeneous, have been proposed and the former is pictured in figure 1.10. Homogeneous mediators are by their action soluble in aqueous conditions, since they must diffuse from enzyme to electrode to allow the passage of electrons. Examples of such mediators are the ferrocene/ ferricinium and the ferri/ ferrocyanate couples.

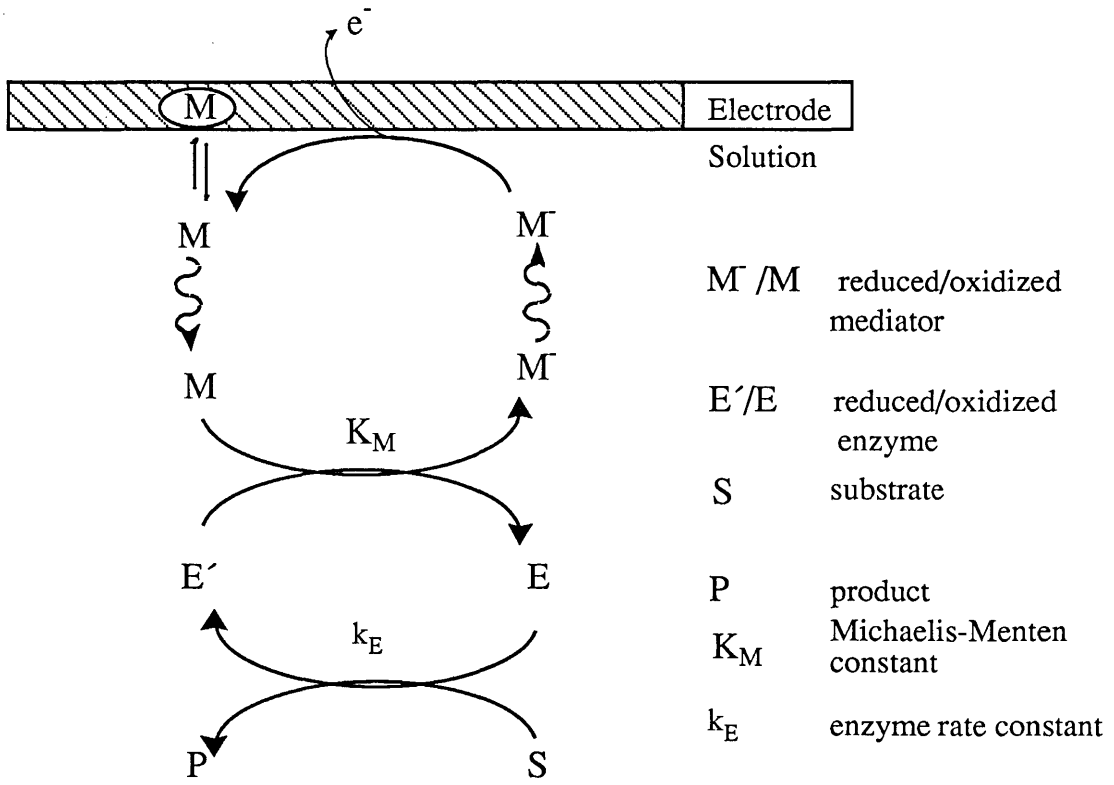
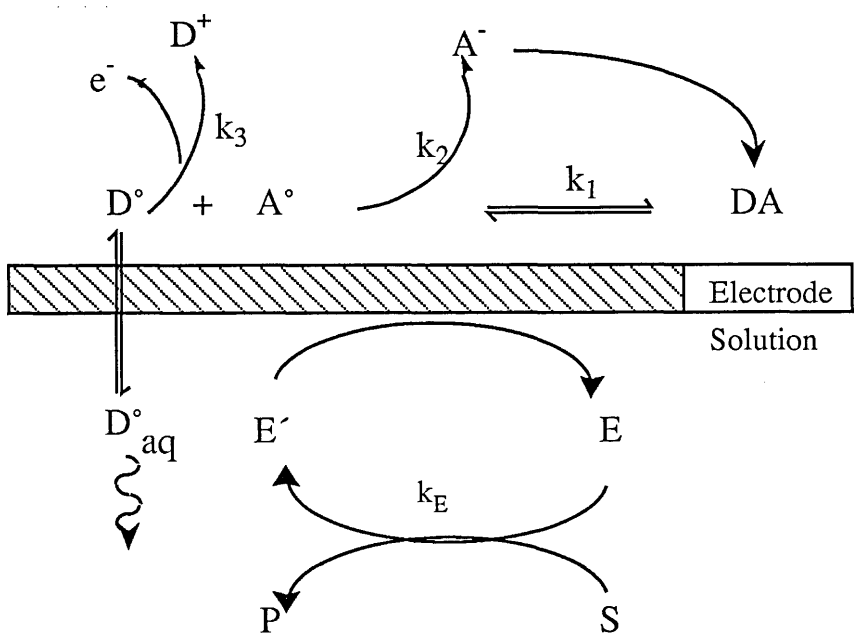


Figure 1.10 Homogeneous mediation of an enzyme mediated reaction

Heterogeneous mediation has been seen with the enzymes on organic salts (Kalia 1990 and Magner 1991) and using modified enzymes on bare electrodes (Heller 1990). The heterogeneous redox catalysis proposed for the organic salt oxidation is more complex and as figure 1.11 shows, assumes a dissociation of the two mediator components, the donor (D^+) and the acceptor (A^-) into their neutral forms, for example TTF°TCNQ°. The reduced form of the enzyme E' is then

oxidized by the acceptor giving E and A^- ($TCNQ^-$) ion. Donation of the the donor's electron to the electrode gives D^+ (TTF^+) and then combination of the ionic forms of the donor and acceptor, in a fast reaction step, gives the mediator in its D^+A^- form (TTF^+TCNQ^-).



DA	mediator in its ionic form
$D°/D^+$	reduced /oxidized donor
$A^-/A°$	reduced /oxidized acceptor
E'/E	reduced /oxidized enzyme
k_1, k_2, k_3	rate constants
S	substrate
P	product
k_E	enzyme rate constant

Figure 1.11 Heterogeneous redox catalysis of an enzyme mediated reaction

At present, the oxidation of biological molecules such as the flavins ($FADH_2$) and the pyridines (NAD(P)H) follow both mechanisms depending on the nature of the surface of the electrode. Recent studies (Kalia 1990) have shown that

glucose oxidase is oxidized homogeneously on both a 'silicone oil paste TTF TCNQ' and a 'pressed-pellet' TTF TCNQ electrode and heterogeneously on a polystyrene-bound TTF TCNQ electrode. The oxidation of NAD(P)H is more complicated as the co-enzyme must diffuse away from the dehydrogenase and then be oxidized by the mediator, the reaction scheme is depicted in figure 1.12.

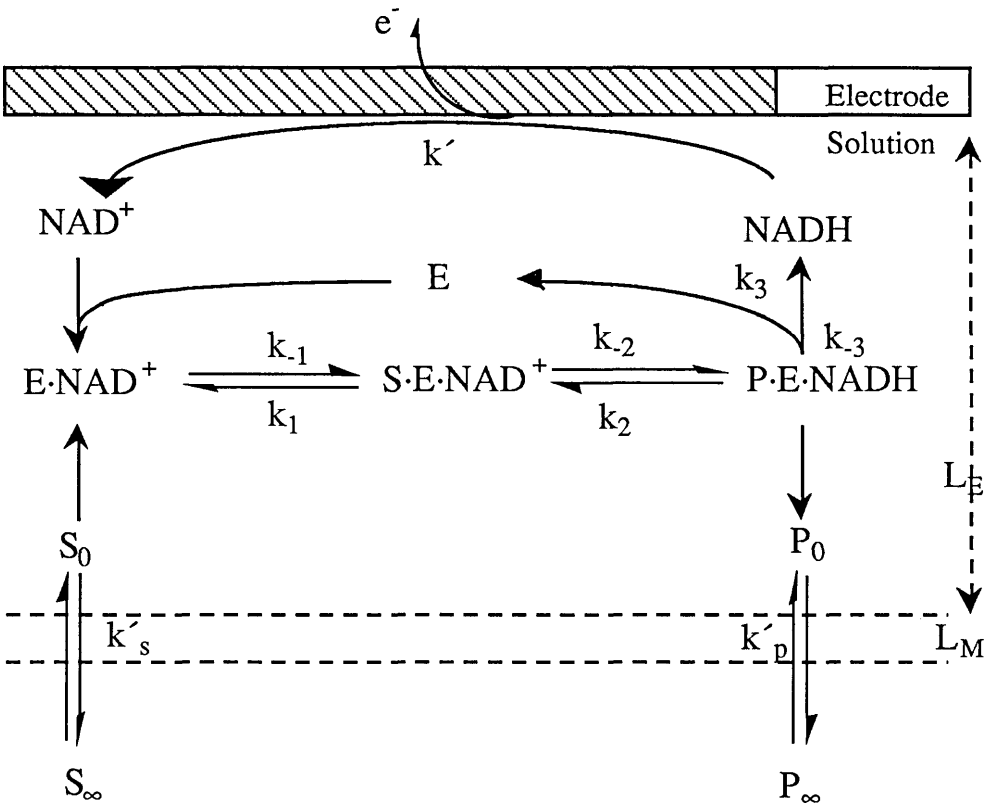


Figure 1.12 Reaction scheme for the oxidation of NADH on a mediated electrode

Enzyme immobilization

As the definition of an enzyme electrode states, the enzyme must be in close proximity to the electrode, otherwise no reaction will be detected. There are a number of methods for doing this, ranging from restraining the enzyme behind a membrane (Wilson & Thévenot 1990) to immobilization on a protein or polymer (Sternberg *et al* 1988) or within a gel (Korenbrot *et al* 1987), figure 1.13.

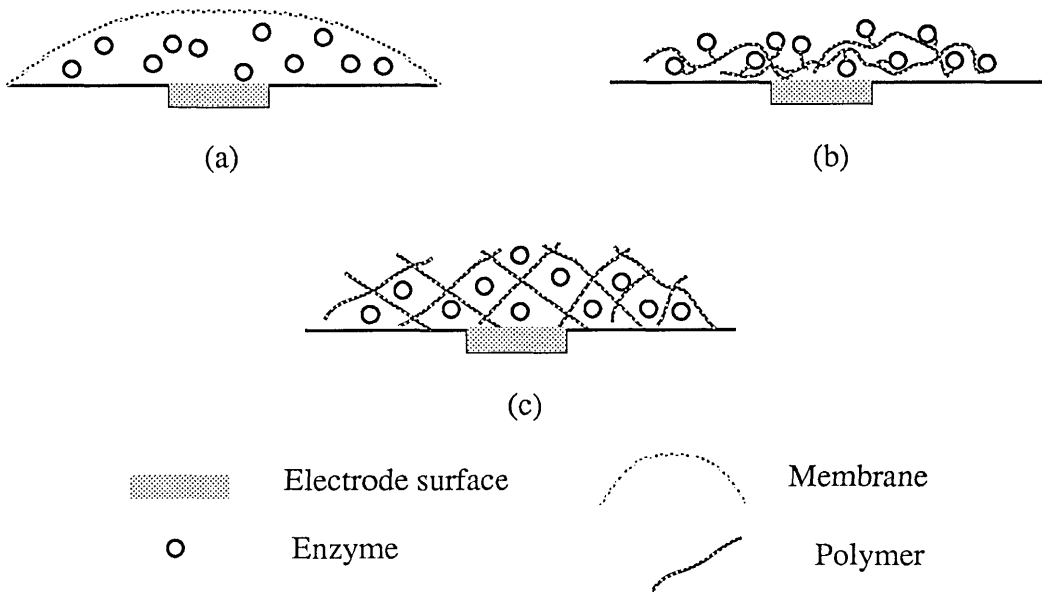


Figure 1.13 (a) a membrane entrapped enzyme (Wilson & Thévenot 1990), (b) polymer-bound enzyme (Sternberg *et al* 1988) and (c) enzyme immobilized inside a polyacrylamide matrix (Korenbrot *et al* 1987)

Signal measurement

The electronic signal is normally measured in one of two ways, amperometrically or potentiometrically. Potentiometric analysis is the simpler technique and involves measuring the potential difference generated between the sensing electrode, called the working electrode, and a standard reference electrode when no current is flowing, figure 1.14. The exponential of the potential measured is

proportional to the concentration of the electroactive analyte in solution, as shown in the redox potential equation 1.1 below, where E is the potential measured, E^o the redox potential, [O] the concentration of oxidant and [R] the concentration of reductant.

$$E = E^o + \frac{RT}{nF} \ln\left[\frac{O}{R}\right] \qquad 1.1$$

Hence, $\ln[O] \propto E$.

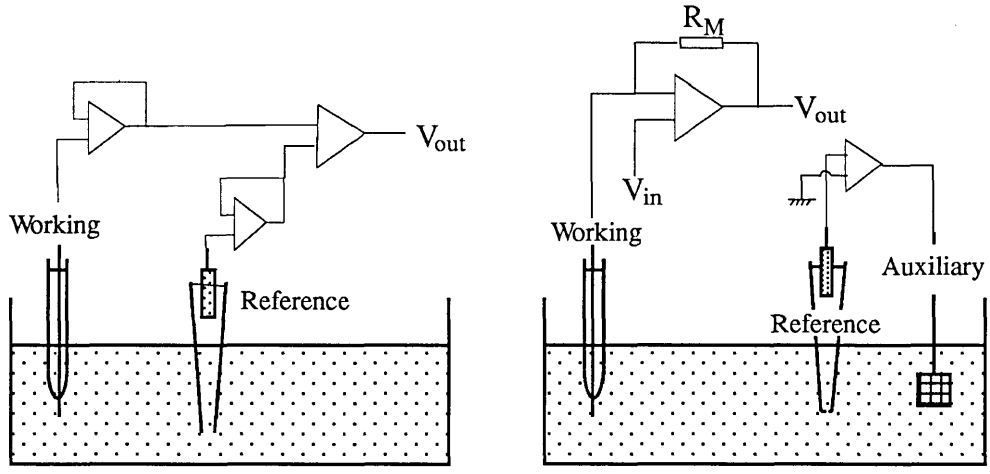


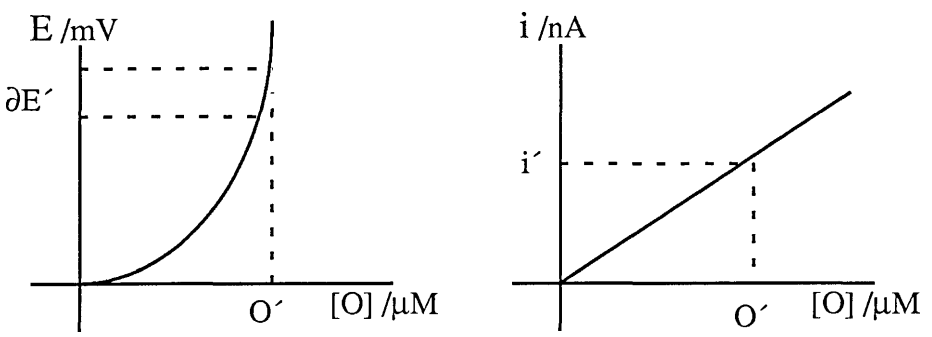
Figure 1.14 The set-up used for potentiometric (left) and amperometric (right) experiments

Amperometry is more complicated in that it usually requires a third electrode, the auxiliary or counter electrode. In this technique, also shown in figure 1.14, the reference electrode is used to hold the working electrode at a fixed potential. The current generated by oxidation or reduction of an electroactive species is measured on the working electrode and flows not through the reference, down which no current flows, but through the counter electrode. The current is related to the concentration of electroactive species, as shown in equation 1.2.

$$i = nFAk^{o}\left[O\right]e^{(-n(E-E^{o}))} \qquad 1.2$$

Where **i** is the current measured and k^{o} is the heterogeneous rate constant

As E is held constant, the exponential term becomes fixed, and so the current is proportional to the concentration of analyte present . This is the main advantage of amperometric over potentiometric detection and figure 1.15 illustrates this. With potentiometry any small change in analyte concentration will produce a much larger corresponding change in the potential measured inducing much larger errors in the system. Whereas with amperometry, the current concentration relationship is directly proportional and so errors are not so large, providing mass transport, the concentration gradient of [O], is controlled. The lower errors involved with amperometry mean that it is the technique used in the work described in this thesis.



(**a**) potentiometric analysis

(**b**) amperometric analysis

Figure 1.15 Theoretical plots for potentiometric and amperometric analysis

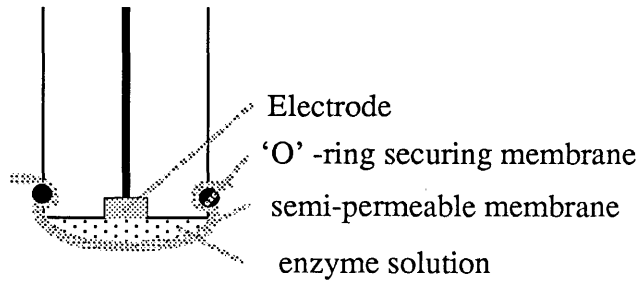


Figure 1.16 membrane covered enzyme electrode

Kinetics

For a typical membrane enzyme electrode shown in figure 1.16, the overall rate determining step in the system is dependent on one of three individual kinetic steps (Albery *et al* 1986):

(i) the rate of oxidation at the electrode
(ii) the enzyme kinetics
(iii) the diffusion of substrate through the membrane.

If one of these steps is slow it will control the kinetics of the reaction; the equations shown below describe the three cases.

(i) electrode control

$$j = k' [M_{red}]$$

where j is the flux, k' the First order rate constant and M_{red} the reduced mediator (NADH, $Fe(Cp)_2$ or H_2O_2)

(ii) enzyme control, at low substrate concentration

$$\frac{e_\Sigma}{j} = \frac{K_M}{L\, k_{cat}\, [S]_\infty}$$

with saturated enzyme

$$\frac{e_\Sigma}{j} = \frac{1}{L\, k_{cat}} \left[1 - \frac{j}{k'_S\, [S]_\infty} \right]$$

where e_Σ is the total enzyme concentration, K_M the Michaels constant, k_{cat} the maximum velocity and $[S]_\infty$ the bulk substrate concentration.

(iii) membrane diffusion

$$k_S = \frac{D_S K_S}{L}$$

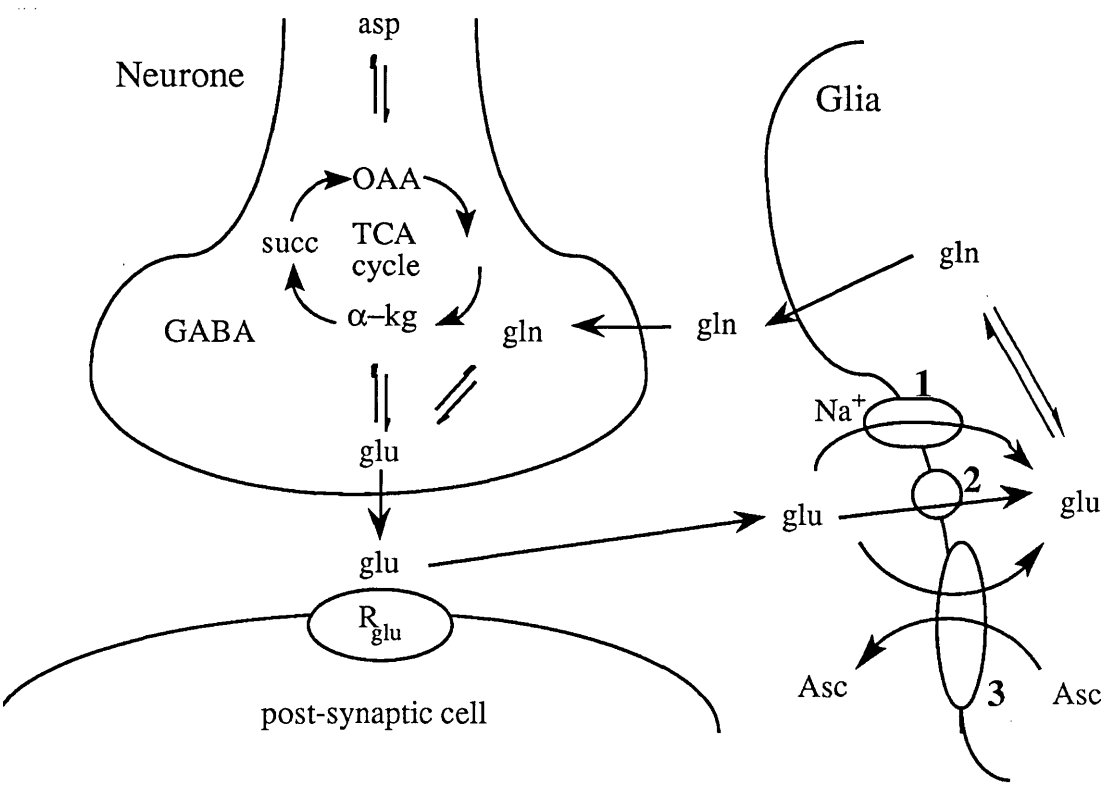
where k_S is the rate of diffusion of S, D_S the diffusion coefficient, K_S the partition coefficient and L the membrane thickness

1.4 The development of sensors

The enzyme electrodes developed in the course of this work are devoted to studying some of the neurotransmitters that cannot be easily measured by existing techniques. ACh, Glutamate and GABA are three very important molecules to neurophysiologists, but they have previously required long sampling and complex analysis. A real-time sensor for all of these chemicals would be a distinct advantage in furthering neurochemistry. As discussed previously, endogenous glutamate has been measured by one of four methods: (1) derivatization with o-phthalaldehyde/t-butyl thiol with UV fluorimetry (Errington *et al* 1987), (2) automated amino acid analysis , (3) enzyme assay with glutamate dehydrogenase, measuring NADPH fluorimetrically and (4) [^{14}C]-glutamate incubation, followed by scintillation counting (Nicholls 1989 and Nicholls *et al* 1987).

When applied to *in vivo* measurements, these methods require lengthy sampling times typically twenty minutes, depending on the sensitivity of the assay. This presents several problems in that any changes in the levels of the neuro-transmitters being measured must be both prolonged, to allow 20 min sampling to detect this effect and big enough to be significantly above basal levels and not be averaged out into 20 min of basal values as a small change may be. For example, Bliss and his colleagues have shown that long term potentiation (LTP) produces

long-lasting increases in glutamate in the hippocampus, which can be detected using method (1) shown above (Dolphin *et al* 1982 & Errington *et al* 1987). However stimulus dependent changes in glutamate levels have previously not been seen after 2 minute increases in stimulation of the perforant path (Errington 1991). These changes have been hard to pick up because of the lack of resolution. The advantage of using enzyme electrodes is the improvement on the resolution, which will make it feasible to measure these short term 'behavioural' changes in neurotransmitter levels.



glu	glutamate
gln	glutamine
R_{glu}	glutamate receptor
Asc	ascorbate
α-kg	α-keto glutarate

GABA	γ-amino butyrate
OAA	oxalo acetate
asp	aspartate
1	Na+ dependent uptake
2	Na+ independent uptake
3	ascorbate/ glutamate exchange

Figure 1.17 Possible pathways for the release, uptake and metabolic pathways for glutamate (adapted from Fillenz *et al* 1986)

The uptake of glutamate is a problem for *in vivo* measurement, for there are three uptake mechanisms situated either on the glia or on the neurons, which provide a fast and efficient removal of neuronally released glutamate. There is reported to be a Na^+ dependent, high affinity uptake, K_M >500μM, and a low affinity Na^+ independent uptake, K_M 20 μM, (Fillenz *et al* 1986) .

There is also thought to be an ascorbate/glutamate exchange for glutamate uptake (Fillenz *et al* 1986). This system is Na^+ dependent and releases ascorbate as glutamate is uptaken, figure 1.17. This released ascorbate is then likely to interfere with any electrochemical measurement of glutamate. Any *in vivo* sampling probe will be measuring glutamate (or another neurotransmitter) that has spilled out into the ECF pool surrounding the probe, missing any uptake channels.

Uptake is a problem for measurement of any neurotransmitter, uptake blockers can be used, but for glutamate uptake, blockers such as kainic acid and L-aspartate-β-hydroxamate are likely to cause epileptogenesis (Fillenz 1991).

1.5 A sensor for glutamate

As well as having different mediators for oxidizing the reduced form of enzymes or coenzymes, there are three enzymes that have been employed in glutamate sensors, an NADH dehydrogenase (EC 1.4.1.2, Korenbrot *et al* 1987), secondly an NADPH dehydrogenase (EC 1.4.1.4, Kuhr 1991) and thirdly an FAD oxidase (EC 1.4.3.11, Wollenberger *et al* 1989). The dehydrogenases can be obtained from animal tissue, beef heart and liver, and being intracellular, are stable for about 24 hours at room temperature (Sigma 1990).

As the oxidase comes from fungal and bacterial sources and is excreted as an extracellular enzyme, it thus has a much higher stability, being able to withstand temperatures of 60°C for 15 minutes at pH 7 (Kusakabe *et al* 1983). The properties of the two types of enzyme are compared below in table 1.3.

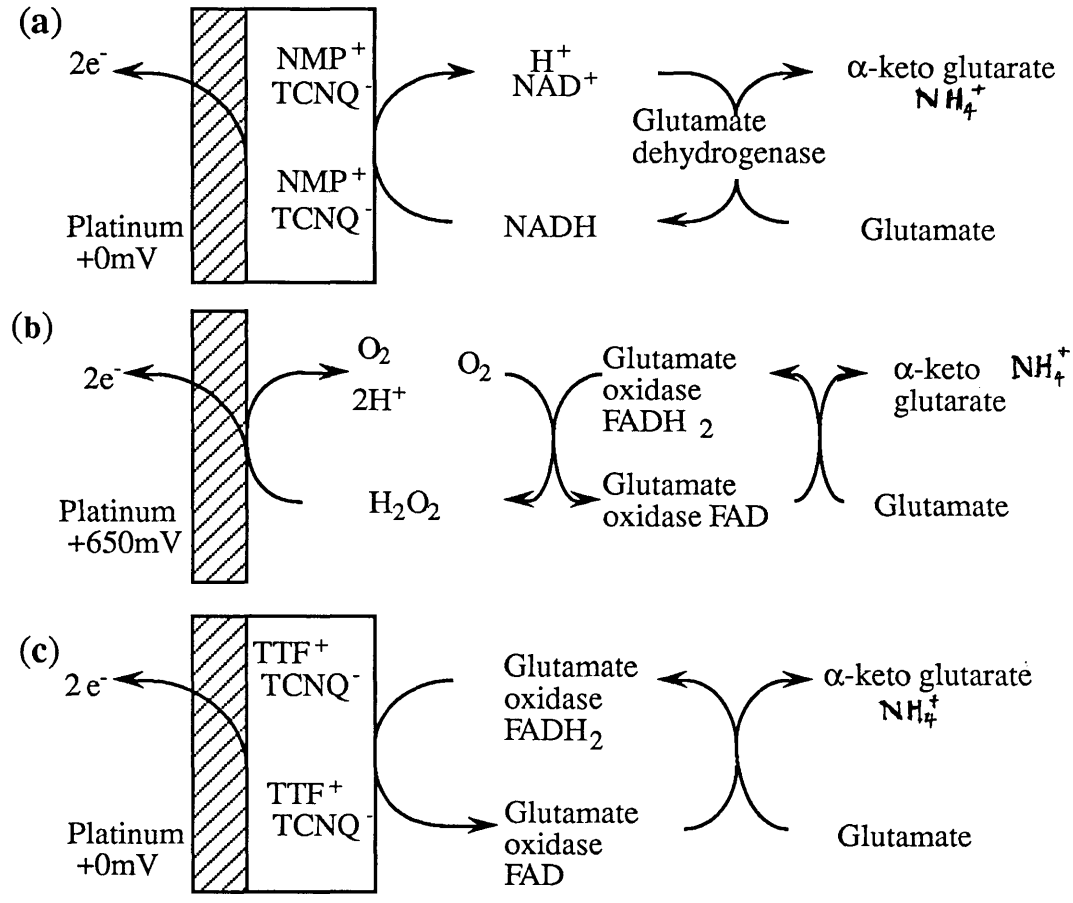


Figure 1.18 Three different schemes for the oxidation of glutamate, (a) glutamate dehydrogenase on NMP^+TCNQ^-, (b) Glutamate oxidase on platinum and (c) glutamate oxidase on TTF^+TCNQ^-

Table 1.3 Comparison of the two glutamate enzymes used

	NAD(P)H Dehydrogenases	FAD Oxidase
1.	require soluble co-enzyme	tightly bound FAD prosthetic group
2.	short lifetime at room temperature	very stable
3.	no Oxygen effect	Oxygen effect with some mediators
4	small aspartate response for some preparations	0-80 μM glutamine signal

Both types of enzyme were used to make sensors, figure 1.18. The initial work studied the use of conducting organic salt (NMP^+TCNQ^- and TTF^+TCNQ^-) mediated electrodes with both the dehydrogenase and the oxidase enzymes. As table 1.3 shows, with a mediated system the oxidase enzyme can suffer from an 'O_2 effect', that is a competition between oxygen and some mediators for the reduced form of the enzyme at low substrate concentrations, resulting in a reduced current seen at the electrode. Ferrocene is a mediator that has been shown to compete well with oxygen and exhibits no oxygen effect, except in oxygen-saturated buffer (Hill & Sanghera 1990). However with the organic salts, the oxygen effect was seen with glutamate oxidase.

Being smaller, the natural electron acceptor and in higher concentration than mediator, oxygen has a higher probability of oxidizing electrons. The concentration of oxygen in physiological conditions is about 50μM (Boutelle 1991) and glutamate concentrations must exceed this before good sensitivity is achieved. The resting glutamate concentrations in the brain lie around 2-20 μM (Benveniste 1989), so it obvious that the organic salt-mediated oxidase system will be a poor method for this type of low substrate measurement, since the oxygen has a greater affinity for the enzyme than the mediator.

The oxidation of NADH, the reduced co-enzyme form of the dehydrogenase, has no side reaction with oxygen and ideally is the better system to use for the lower concentration range. However both the short enzyme lifetime and the solubility and instability of the coenzyme prevents any realistic *in vivo* measurements from being made, because fresh NAD^+ would always have to be supplied to the electrode to replace any diffusing away, which would not only be costly but may also be harmful to the tissue under investigation.

In trying to measure μM glutamate concentrations, each system is greatly disadvantaged, making *in vivo* monitoring of glutamate very difficult. The only

solution to greater sensitivity, reproducibility and lifetime is to either find another insoluble mediator or to find a different system for detecting the reduced enzyme. Since a large number of mediators are soluble, they will encounter similar problems to the dehydrogenase system, and any mediator used with the oxidase will be susceptible to the oxygen effect.

As oxygen can never be eliminated in an *in vivo* system, the only sensible alternative is to use it as the mediator for the oxidase, making a glutamate sensor similar to that of Wollenberger and coworkers (`Wollenberger *et al* 1989). The H_2O_2 produced on oxidation of the $FADH_2$ can be easily measured on a bare platinum electrode at a potential of +300 to +650 mV. Initially this method was dismissed as the high potential would oxidize other electroactive species and might cause fouling of proteinaceous matter on the platinum surface. Both of these problems were in fact surmountable. The electroactive interferents were either in too low a concentration or could be removed using specific enzymes and charged polymers, carefully selected to screen out similarly charged interferents. The platinum/peroxide system gave much greater electrode sensitivity and life-time, 100nM with a 7 day activity against 10 μM over 24 hours for the organic salt mediated system. This platinum/peroxide system had the following advantages:

(1) greater sensitivity and life-time

(2) no added mediator required

(3) very stable oxidase enzyme

(4) no soluble cofactors

(5) high enzyme specificity,

and disadvantages:

(1) high working potential.

The advantages of this system far outweigh the disadvantages and have made this system a successful *in vivo* mediated enzyme electrode. Both glutamate systems are described fully in chapters two and three.

1.6 A sensor for Acetyl Choline (ACh)

An acetyl choline sensor requires a multi-enzyme system to produce a measurable electrical signal. Two enzymes are used for the electrode, acetylcholine esterase (AChE, EC 3.1.1.7), which cleaves the acetyl group from the choline, and choline oxidase (ChOx EC 1.1.3.17), which oxidizes choline to betaine via betaine aldehyde, figure 1.19. Initial work on a choline sensor used the conducting organic salt $TTF^{+}TCNQ^{-}$, but this mediated electrode suffered similar problems to the mediated glutamate electrode, namely the oxygen effect. However, as choline

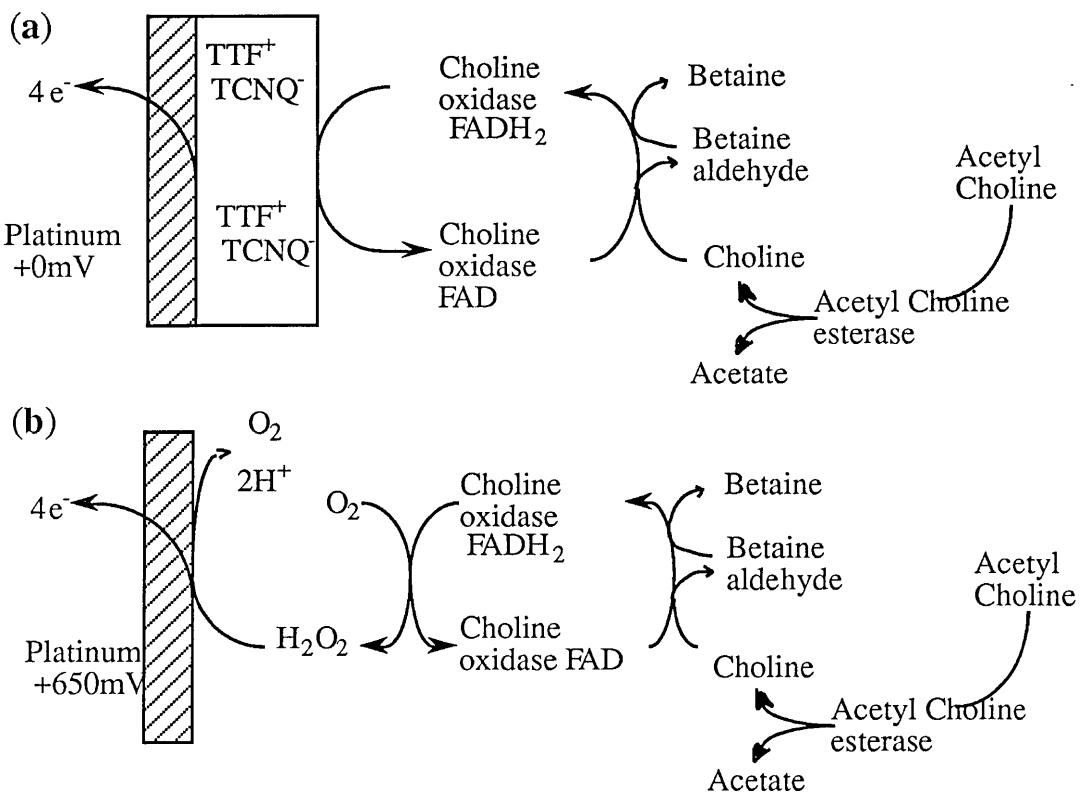


Figure 1.19 Two schemes for an acetyl choline sensor, (**a**) a $TTF^{+}TCNQ^{-}$ mediated reaction and (**b**) a platinum/ peroxide mediated system

oxidase produces H_2O_2, its oxidation and the advantages that it carries can be used to measure ACh.

The basal levels of ACh in the rat brain have been estimated at 15 nM (estimation from Kawashima *et al* 1991), 1000 times lower than the glutamate, requiring the electrode to work at its highest sensitivity. Instead of having an uptake mechanism for ACh directly, endogenous esterase (AChE) present in the synaptic cleft breaks the neurotransmitter down to choline which is then taken up into the neurons and glia (Bradford 1986). To aid ACh detection, μM quantities of neostigmine and physostigmine have been perfused into the nervous tissue, which inhibit the endogenous esterase preventing ACh breakdown and increase its recovery by approximately 100-fold (Nilsson *et al* 1990 & Kawashima *et al* 1991). However, this would not work for the enzyme electrode as the neostigmine and physostigmine would inhibit not only the endogenous AChE but also the electrode-bound enzyme. Another problem for endogenous ACh measurement is the level of choline present in ECF, which has been found to change with nutritional uptake and metabolism, thus altering the background currents. (Klein *et al* 1990).

The *in vitro* sensitivtiy of the enzyme electrode, shown in chapter three, was 100 nM, making the probe unlikely to detect basal Ach levels; however it may be possible to detect elevated levels with either pharmacological stimulation, by atropine for example, or with physiological stimulation by epileptic activity.

1.7 The design of an *in vivo* probe

The biggest problem faced with developing an implantable *in vivo* sensor was the miniaturization. Initial attempts to make such a probe focused on producing an open-ended electrode with the appropriate enzymes immobilized or entrapped on the surface. For a number of reasons, discussed in chapter three, this proved very unsatisfactory and a different system had to be found. The idea of retaining the

electrode with its appropriate enzyme or enzymes inside a small dialysis fibre, with, if possible, an inflow and outflow system was adopted. The design of such a probe was very challenging and underwent many different forms and guises. An implantable *in vivo* sensor,whose final form is shown in figure 1.20, required the following features (table 1.4):

Table 1.4 Features of the *in vivo* micro enzyme electrode

(1) small internal size (500 μm at most), to prevent damaging the tissue under study,
(2) easily implantable,
(3) rigid, so as to reach the precise area target,
(4) a small external size to allow free movement of the animal,
(5) an internal plumbing system to allow replenishment and replacement with alternative solutions,
(6) durable to avoid damage during calibration and implantation,
(7) easily fabricated.

The probe could be filled with either buffer or enzyme solution using the inflow and outflow tubes. With the probe full of solution the three electrodes are then in electrical contact through the electrolyte. The analyte under study diffuses through the dialysis membrane, reacts with any enzymes present and the product, H_2O_2, is oxidized on the electrode between +300 and +650 mV. The background current can be studied alone by eliminating the specific enzymes, i.e. glutamate oxidase or AChE and ChOx, from the perfusion medium. An external platinum electrode is held at +350 mV and measures H_2O_2 only at high concentrations, as it is outside the probe and away from any enzyme, and also electroactive species such as ascorbate and uric acid.

The probe also had to remove all traces of electroactive interferents from the internal volume, especially those whose levels fluctuated during normal behaviour. This was done by firstly coating the electrode in Nafion, a sulphonated polymer that has an overall negative charge repelling negative ions, and secondly by using

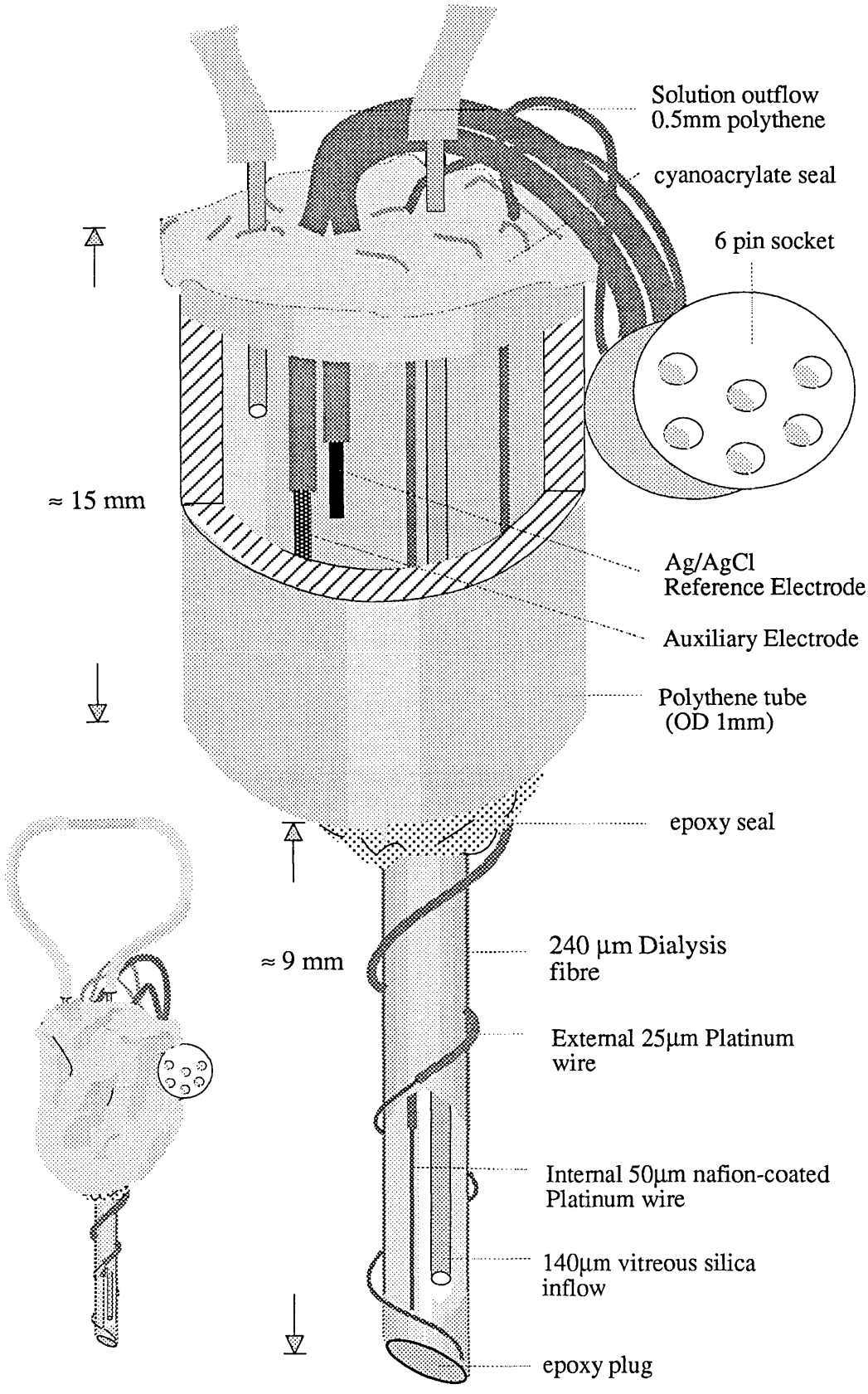


Figure 1.20 The *in vivo* micro enzyme probe; a cut away section is shown on the right and an acrylate-sealed probe, ready for implantation is illustrated on the left

ascorbate oxidase and uric acid oxidase to remove two of the main interferents, ascorbate and uric acid respectively. Initial *in vivo* tests showed that the uric oxidase would not be necessary as only the ascorbate levels changed to any great extent. These points are discussed further in chapter four.

1.8 Neuroanatomy and neurophysiology of the rat brain

The rat brain is used widely in neurological work and a large amount of information has come form its study. A generalized plan of the main regions is shown in figure 1.21, a sagittal section through the rat central nervous system (CNS). Although there are many important areas, it is not possible to discuss them all; Angevine and Cotman (1981) provide a comprehensive text. The two areas studied in this thesis are described in more detail below.

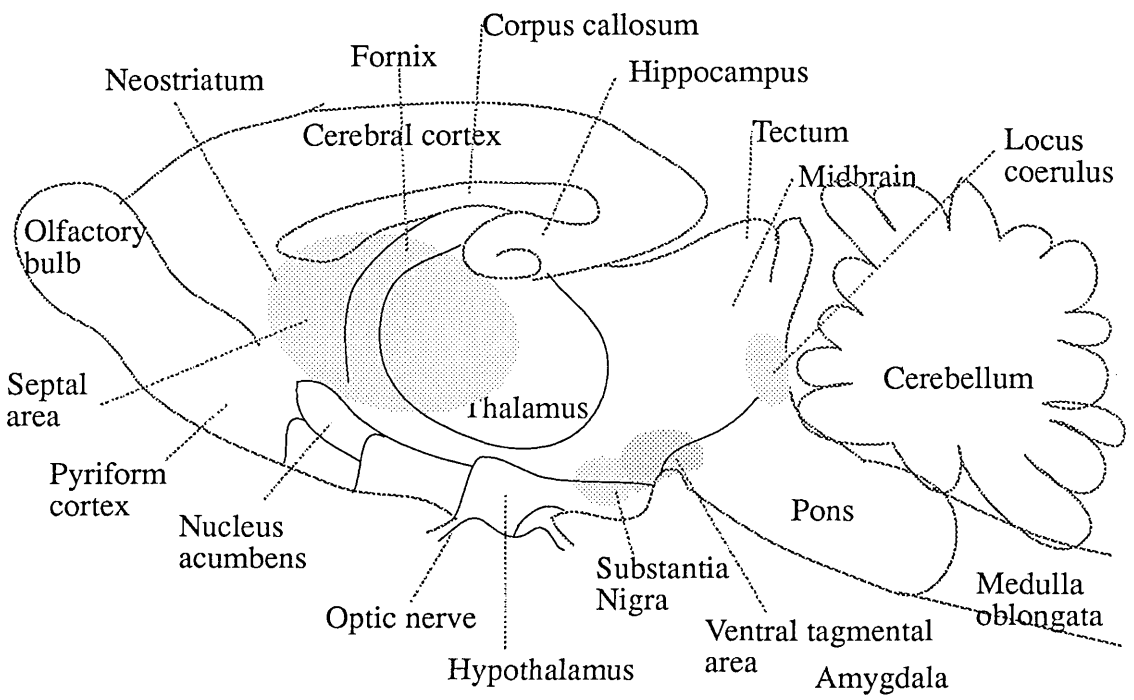


Figure 1.21 Saggital section through a rat brain (adapted from Angevine & Cotman 1981)

The Hippocampus

Much is known about the hippocampus and there is a large body of evidence to show that it is involved with the basis of learning and memory. It is situated in the middle of the brain, lying under the neocortex and projecting into both sides of the brain, see figures 1.21 & 1.22. It has the appearance of being coiled over on itself and has well defined layering. Having a high degree of organisation has resulted in it being the subject of much research.

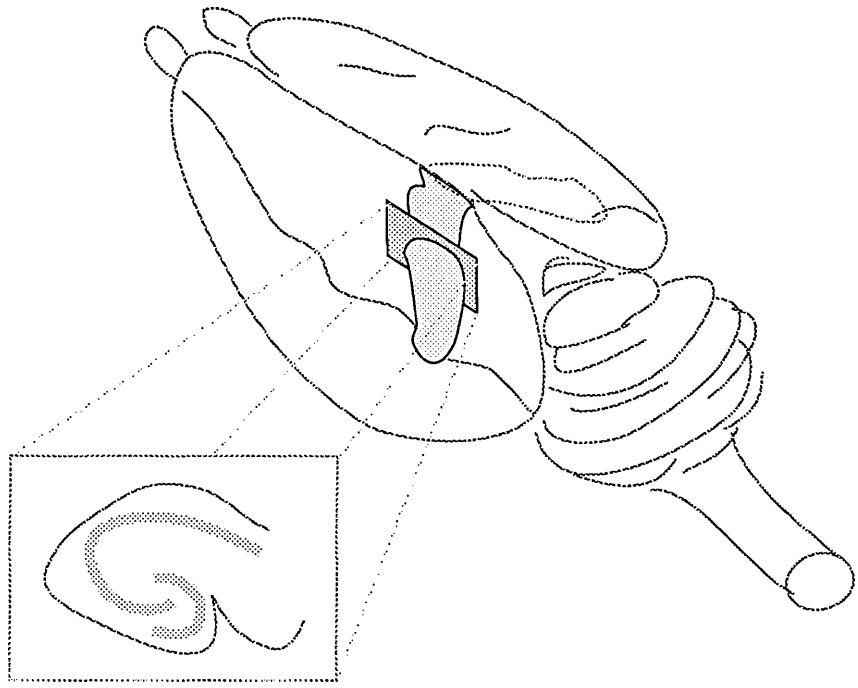


Figure 1.22 Overall shape of the rat brain showing the position of the hippocampus and a saggital section through it (adapted from Jefferys 1990)

The hippocampus itself consists of four regions CA1-CA4 (CA- Cornu Ammonis or Ammon's horn), although the CA2 region is quite small and often ignored. Other structures, namely the dentate gyrus (DG), the subiculum (Sb) and the entorhinal cortex (Er) can be included in the 'hippocampal region', figure 1.23.

Both the hippocampus and the dentate gyrus comprise of three cell layers; the polymorphic, the pyramidal and the molecular layers make up the hippocampus and the dentate gyrus comprises of the hilus, a polymorphic layer, the granular and the molecular layer.

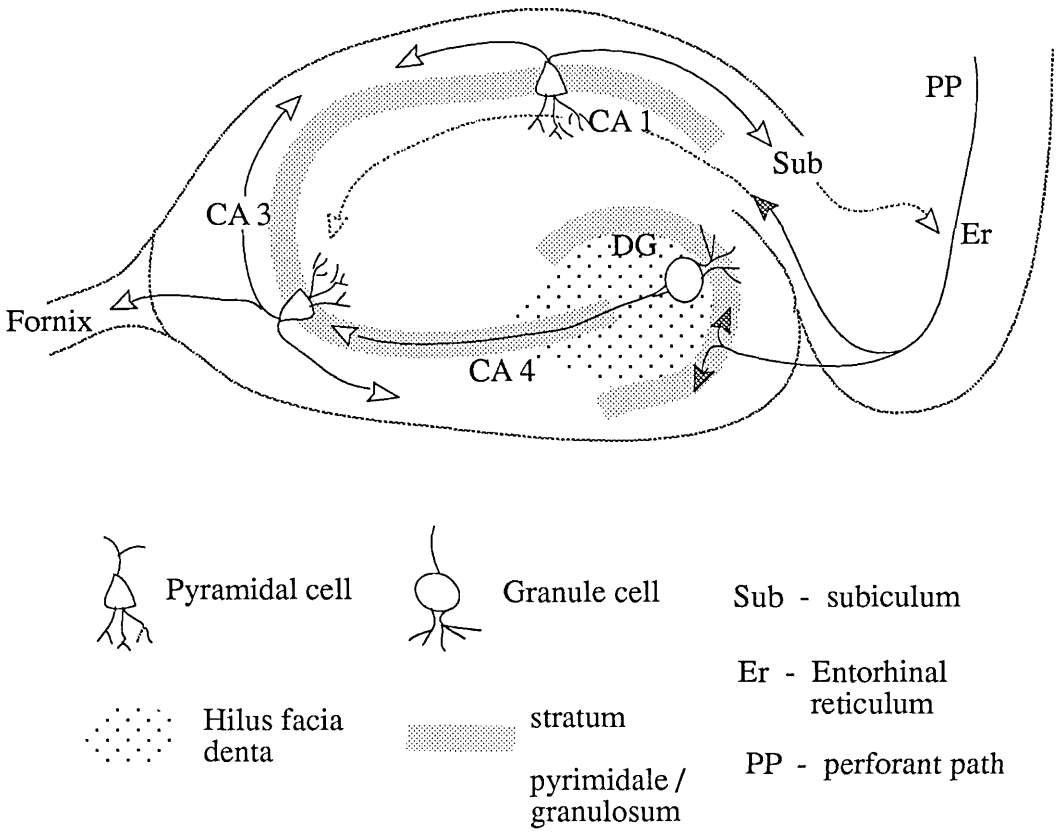


Figure 1.23 A saggital section through the hippocampus and its accompanying regions (adapted from Jefferys 1990 and Angevine & Cotman 1981))

The main sensory inputs come from the neocortex, via the entorhinal region, the septum and the contralateral hippocampus. Although the circuitry is very complicated, there is an overall pathway for the processing of information, figure 1.23. The major input from the entorhinal cortex, the perforant path (PP), stimulates the granule cell layer of the dentate gyrus and also synapses in the CA1 and CA3 regions. The mossy fibre axons from the granule cells project through the hilar region onto the dendrites of the CA3 pyramidal cells. The CA3 axons project into

other CA3 cells, to the CA1 pyramidal region via the Schaffer collaterals and through the alveus to the contralateral hippocampus. The dominant efferent pathway leads out of the hippocampus via the fimbria and the fornix. Axons from the CA1 pyramidal region also feed back to a large degree into the subiculum and to a lesser extent into the entorhinal cortex. As there are connections between the subiculum and the entorhinal cortex, information is passed back into the hippocampus, forming a closed-loop.

The hippocampus is part of an arbitrary collection of closely interrelated brain areas termed the limbic system, which is comprised of regions such as the visceral lobe of the cortex, the hypothalamus, septum and habernula. It is important in regulating visceral (internal organ) activity and emotional behaviour. There are various theories that suggest the hippocampus is the most important of the structures in the limbic system. Its involvement in the encoding of memories and the ability of the animal to adapt to change have been demonstrated by lesioning. The hippocampus is subject to a large degree of regulation, through both hormonal effects form the blood and from direct neural feed-back from the hypothalamus.

The hippocampus has been implicated in the process of learning and memory for almost two decades (Bliss and Lømo 1973, Errington *et al* 1987). Long lasting changes in synaptic plasticity have been observed in nervous tissue, the best examples being neurons in the hippocampus. This effect, called long term potentiation (LTP), caused by an increase in frequency and strength of stimulation of the afferent fibres, over a certain threshold, produces a long-lasting enhancement in synaptic efficacy and this is thought to be a mechanism for learning. Strong repeated tetani give LTP that lasts for days to weeks, although there is no evidence for any permanent change, and weaker stimuli result in shorter-lived potentiation which lasts for minutes to hours and is similar to post tetanic potentiation (PTP).

LTP requires both associativity and cooperativity among the neurons. Induction requires increased presynaptic activity and post-synaptic depolarization, making the process associative, and a sufficient number of fibres must be stimulated to induce the effect, giving the process its cooperativity. A more detailed discussion is given in chapter five.

The Striatum

The striatum is non-cortical and has two distinct regions, the dorsal and the ventral areas. Along with the globus pallidus (GP), the sub-thalamic nucleus (STN) and the substantia nigra (SN), the striatum forms the basal ganglia, a large area in the core of the cerebral hemi-sphere. The dorsal striatum (or neostriatum) contains the caudate nucleus and the putamen and receives dense glutamatergic and dopamin-ergic inputs from the neocortex and the substantia nigra respectively (these pathways are discussed more in chapter four). The ventral striatum comprises of the nucleus accumbens, the septal areas, the olfactory tubercle, and the basal fore-brain.

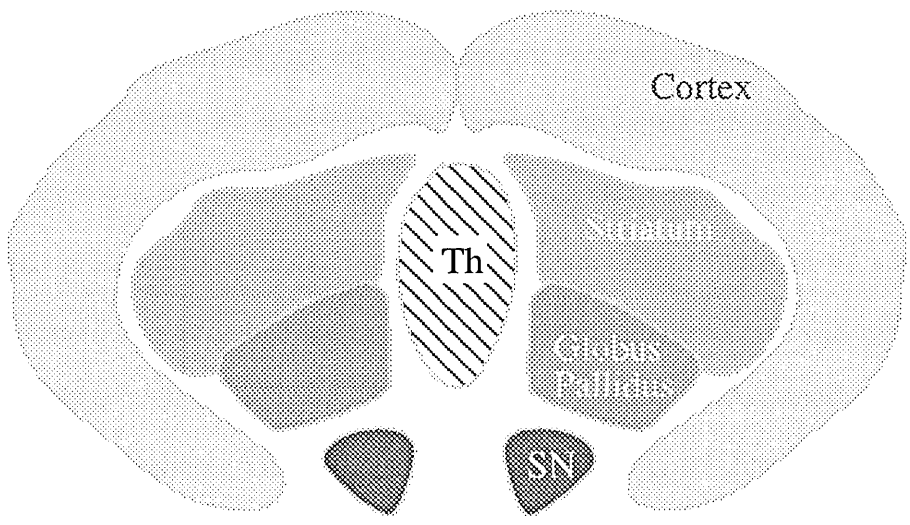


Figure 1.24 A 'transverse' section through the rat brain, showing relative positions of the dorsal striatum and four other closely related regions that are connected to it. The substantia nigra lies posteriorly to the other three, with the nigrostriatal pathway joining them Adapted from Zeman & Innes (1963) SN - substantia nigra, Th - Thalamus. The ventral striatum would lie in front, as shown in figure 1.21

It has close affiliations with the hippocampus and the limbic system (Angevine & Cotman 1981). The precise role of the striatum in motor activity is still not clear, however it is thought to be involved both in maintenance of motor control as well as in its planning and initiation (Graybiel 1990). There is also a large body of evidence linking dopamine increases in the nucleus accumbens with reward behaviour, not just with the motor activity related to it, but also with the arrival of a new and important stimulus such as perception of food or water (Joseph *et al* 1991 and Hernandez *et al* 1991).

Any imbalance or degeneration in the neurotransmitter pathways leads to well-known disorders such as Schizophrenia, Parkinson's Disease and Huntington's Chorea, high-lighting the basal ganglia's role in mental and physical control (Graybiel 1990, Bradford 1986 and Carlsson & Carlsson 1990).

1.9 The aim of this study

The aim of this work was to develop novel, implantable enzyme biosensors to allow real-time monitoring of behavioural events such as long-term potentiation and the 'tail pinch' response and also to study animal models of human diseases, such as epilepsy. As the present methods only allow 10 - 20 minute analyte sampling, the increased time resolution for measuring glutamate and acetyl choline will enable these neurotransmitters to be studied on the behavioural time-scale.

Chapter Two

Materials and Methods

Section 1: General procedures

2.1 Chemicals and Solutions

Chemicals were usually of AnalaR quality and purchased from Aldrich, BDH or Sigma. They were used without further purification. All solutions were prepared using double distilled water (DDW) from a Millipore Milli-Q system, with a minimum resistivity of 18 MΩ cm. Each solution was stored in the 'fridge at +4°C.

2.2 Enzymes and biological reagents

A list of the enzymes and their technical information is given in table 2.1. All enzymes and some biological reagents were stored, as instructed, at either +4°C or frozen at -20°C. Fresh electroactive reagents and enzyme substrates were, where possible, prepared daily using Krebs buffer, the main exception being D-glucose, which was prepared a day earlier to allow equilibration of the anomers. In all cases, enzymes were used without any further purification. The L-glutamate oxidase was a generous gift from Dr Hitoshi Kusakabe of Yamasa Shoyu, Japan.

Krebs-Ringer buffer was used mostly as it is the standard buffer used by neurophysiologists. Its consists of NaCl (136 mM), KCl (2.54 mM), KH_2PO_4 (1.18 mM), $NaHCO_3$ (16 mM),$CaCl_2$ (1.18 mM), Mg_2SO_4 (1.18 mM) and glucose 10mM. The pH was adjusted by either bubbling a mixture of Oxygen (95%) and

CO_2 (5%) (BOC gas) through the buffer or concentrated HCl was added adjusting the pH to 7.4. pH adjustment; was carried out on a Kent EIL pH meter. When probes were perfused with glucose oxidase, the 10 mM glucose was omitted from the buffer.

Table 2.1 Commercial enzyme preparations

Enzyme	EC number	Supplier	Activity U /mg	Source
glucose oxidase	1.1.3.4	Sigma	132	Aspergillus niger
glutamate oxidase	1.4.3.11	Yamasa Shoyu	8	Streptomyces
glutamate dehydrogenase	1.4.1.2	Sigma Boehringer	35 10	Beef liver
ascorbate oxidase	1.10.3.3	Sigma Boehringer	170 169	Cucurbita sp.
choline oxidase	1.1.3.17	Sigma Boehringer	10 10	Arthrobacter globiformis
acetyl choline esterase	3.1.1.7	Sigma Boehringer	190 1000	Electrophorus electricus

2.3 Electrode fabrication

Each electrode was made from insulated wire and was connected to the external circuit by 1mm gold contacts supplied by A.W.P. Electronics. The procedures for constructing organic salt and platinum (working) electrodes are described in section 2. Both TTF^+TCNQ^- and NMP^+TCNQ^- crystals were a generous gift from Dr Kalia at Imperial College. The TTF^+TCNQ^- was synthesized following the method of Ferraris *et al* (1973) and that of Melby (1965) for the NMP^+TCNQ^-.

Ag/AgCl reference electrodes were made by electro-depositing silver chloride onto teflon-coated silver wire, purchased from Clark Electromedical Instruments. This method was used for both 254 μm (0.01") and 75 μm (0.003") diameter wire and follows the procedure of Prohaska (1987).

Typically, a 5mm length of silver was exposed on a 20mm electrode. The reference electrode to be plated was then placed in a solution of 10% NaCl with a silver wire as the cathode and an anodizing current density of 10 $\mu A\ mm^{-2}$ was applied for 3 minutes, forming silver chloride:

$$2Ag + Cl^- \text{ ------> } Ag/Ag^+Cl^- + e^-$$

Initially the electrodes had a plum colour, but this became darker when exposed to light. Each electrode was washed with DDW and was then ready for use. Counter electrodes were prepared by exposing a 5mm length of teflon coated silver wire, again from Clark Electromedical Instruments, and were then ready for use.

2.4 Enzyme immobilization and entrapment

Various methods for restraining enzymes on electrodes were attempted. Physical adsorption of some enzymes onto the electrode surface involved placing the electrode in 100 μL of enzyme in Krebs-Ringer solution, usually 0.5 to 5 U/μL for 2 to 24 hours at 4°C. The electrodes were removed from the solution, washed carefully with DDW and assayed in the manner described below. This method was very efficient for some types of enzyme, such as glucose oxidase which presumably possess groups on their surface favouring adsorption, but for others, activity only remained for 24 hours after removal from the enzyme solution.

Coating the surface-adsorbed enzyme with polymers was performed using two different polymers, firstly nafion, an alcohol-based sulphonated polymer available from Sigma, and secondly a mixture of poly-N,N-dimethyl piperidine

(PDP^+) and polystyrene sulphonic acid (PSA^-), figure 2.1. When mixed together, the latter two polymers, which are soluble in aqueous conditions on their own, precipitate out to form an insoluble gel. In both cases, a solution of polymer, 2 to 5 µL, was added to the electrode surface and allowed to dry, before being assayed.

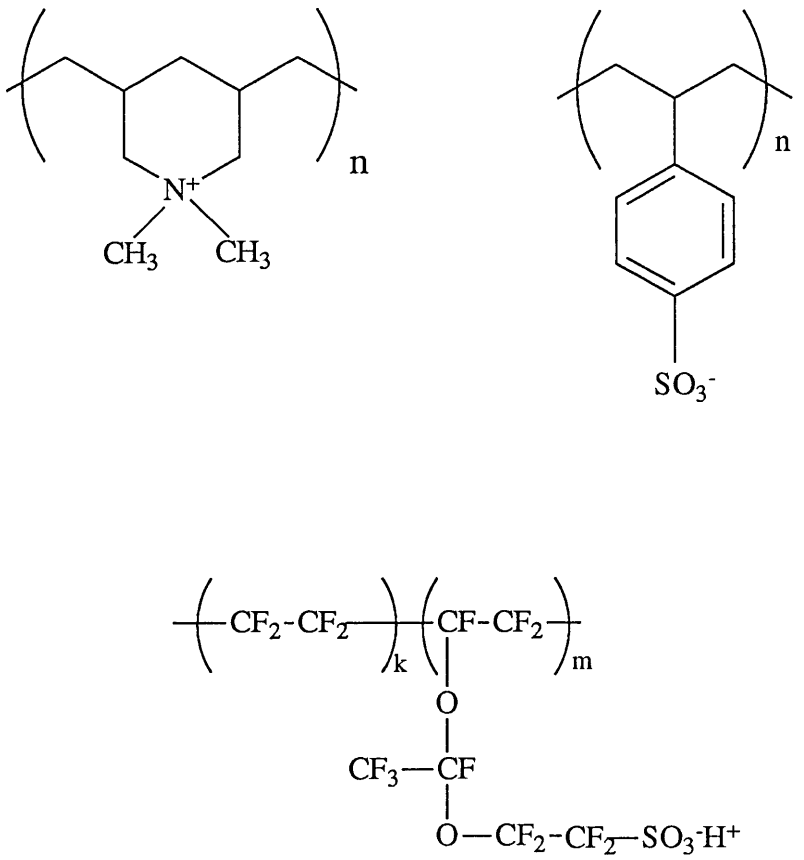


Figure 2.1 poly-N,N-dimethyl piperidine (PDP^+) and polystyrene sulphonic acid (PSA^-) above and nafion below

Enzymes were also immobilized in polyacrylamide gel, according to the procedure of Korenbrot *et al* (1987). This involved polymerising a solution of acrylamide and enzyme onto an electrode at +4°C under nitrogen, using exactly the same conditions and times as quoted in the reference. The following solutions were mixed in the order given

0.32 mL	0.65 M PIPES, 0.65mM EDTA adjusted to pH 6.5 with NaOH
200 µL	L-glutamate dehydrogenase in 30 mM K_2HPO_4 at pH 7
100 µL	20 mM NADH
400 µL	20 mM N-acrylamide succinate in Dimethyl Sulphoxide (DMSO)

after 10 minutes with mixing, the following solutions were added in order:

270 µL	acrylamide at 295 mg/mL, bis-acrylamide at 6.2 mg/mL
40 µL	N,N,N',N' - TEMED 20% v/v
40 µL	$K_2S_2O_8$ at 25 mg/mL

As the solution began to polymerize, small aliquots, 2 -5 µL were applied to the organic salt electrodes. After polymerization, electrodes were left to stand for 1 hour in DDW, to remove any toxic precursors, before being assayed in the conventional manner.

2.5 Apparatus

Two different set-ups were used, one for pre- and post-*in vivo* probe calibrations and one for 'test' electrode calibrations. Probes designed for *in vivo* work had inbuilt reference and counter electrodes, see diagrams in section three of this chapter. The three or four wires that came out of the probe, one or two working electrodes, a reference and an auxiliary electrode, were then glued into a threaded contact holder from Plastics One (Roanoke, USA). This is described in more detail in chapter four. A screened multi-core coaxial cable, connected to the contact block, then led off to the potentiostat.

The dry probe was then filled with enzyme solution or buffer using the polythene/ vitreous silica tubing, using a Carnegie microdialysis pump. A 25 µL Hamilton syringe was filled with buffer or concentrated enzyme solution and connected to the polythene inflow by means of a short, wider length of polythene tubing. Once filling had finished, the inflow and outflow tubes were connected

together using the wider tubing, to prevent the probes drying out. Before use, probes were calibrated *in vitro* by holding the probe in buffer in a 2 mL container, which also held a 2x7 mm magnetic flea (BDH) used to stir the bulk solution. The whole configuration was mounted on an Orme magnetic stirrer. This set-up is shown in figure 2.2. The electrodes were connected to a potentiostat, set at a fixed potential. The current was allowed to settle down to a steady level, typically requiring 20 min to 1 hour, before any measurements were made.

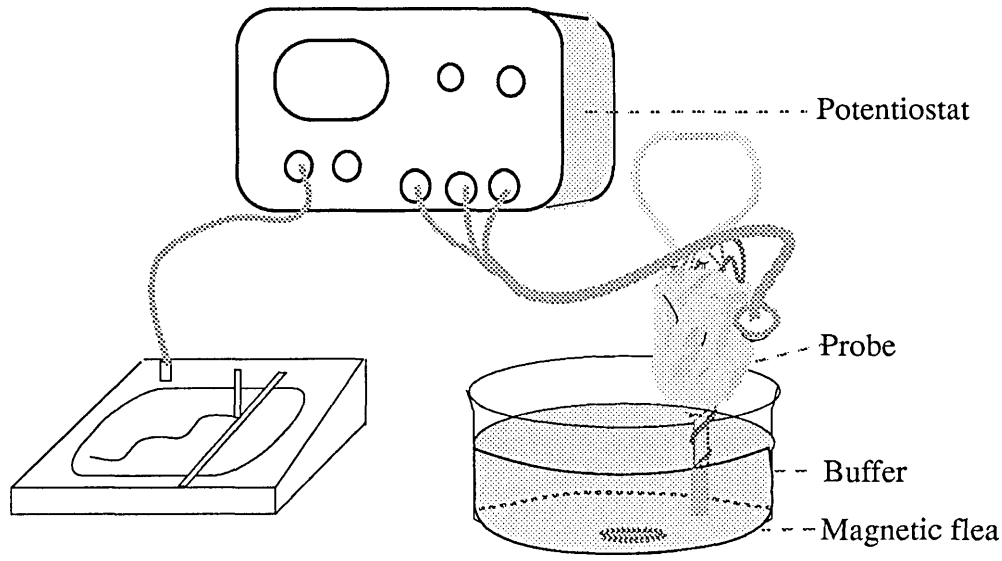


Figure 2.2 The set-up for the calibration of an *in vivo* probe

Calibrations were performed by addition of small aliquots, 2 to 20 μL, of a concentrated solution of analyte to the bulk solution in the 2mL container. Any increase in current, measured on a Gould 6000 XY or YT chart recorder was read off once steady-state had been reached.

'Test' electrodes, which were not designed for *in vivo* use, were either plain teflon coated wires, soldered to gold contact pins and held free in solution or they

were large, 5 - 20 mm diameter, membrane electrodes described in section 2.7. Both of these types had external counter and reference electrodes, which were made from 254 μm silver wire. They were housed in together in a block, from which shielded cable led off to the electronics. The working electrode was connected to the electronics by its own length of screened co-axial cable. The three electrodes were held in buffer and calibrated in a similar manner to the *in vivo* probes, figure 2.3

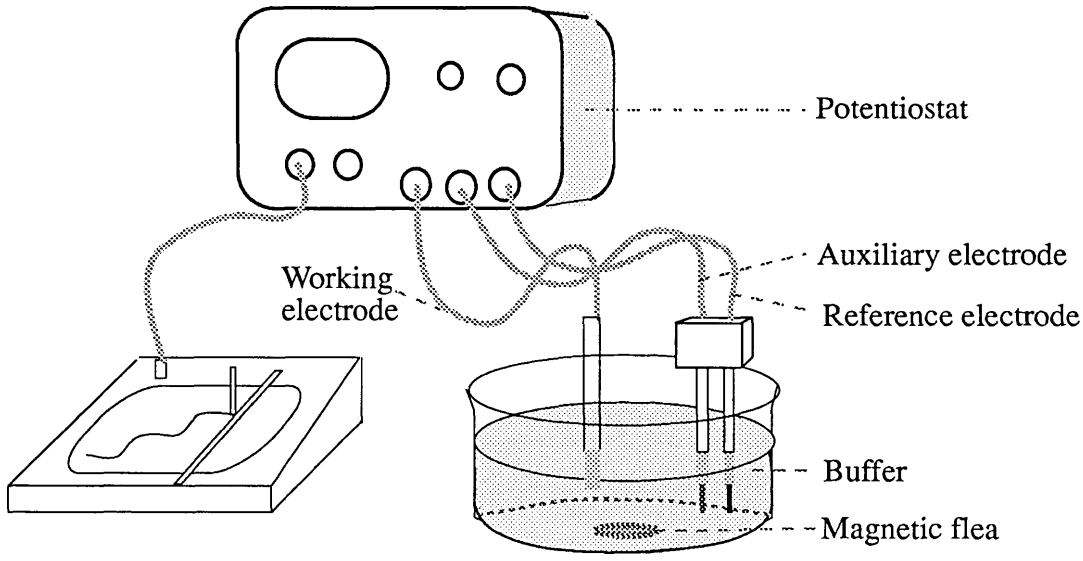


Figure 2.3 The set-up for the calibration of large test electrodes

2.6 Electronics

Two different potentiostats were used for *in vivo* and 'test' electrode work, the first type was designed and built by Dr Martyn Boutelle at Oxford and had the capability of measuring pA currents with low noise. The second included a Sallen and Key filter set at 0.1Hz, a 1 Volt offset and 100-fold amplifier; the circuit is shown in figure 2.4 and was purpose built using the designs kindly supplied by John

Hooper at Imperial College. The galvanostats and potentiostats used for electrode construction (deposition and plating) were built by John Hooper.

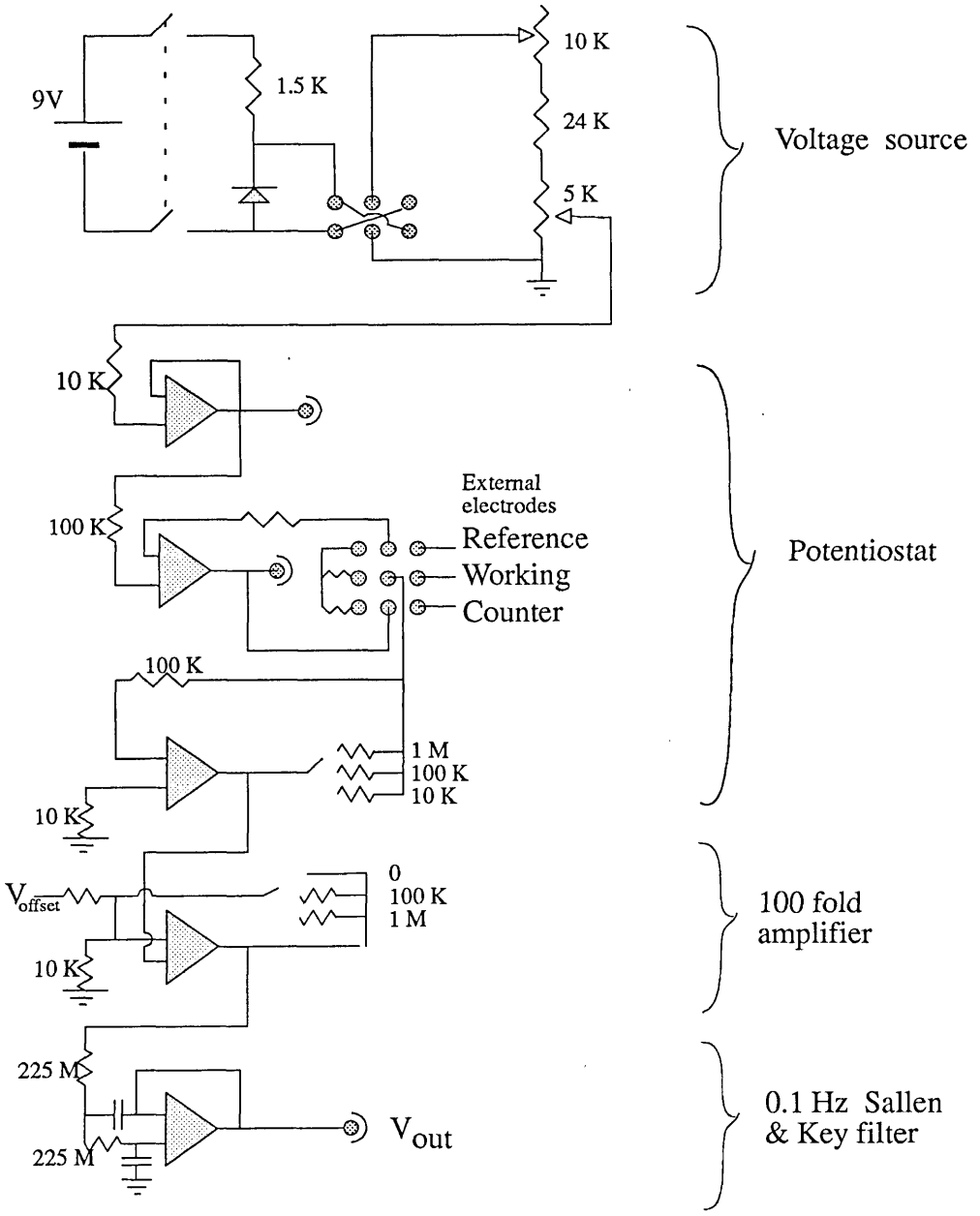


Figure 2.4 The potentiostat built using designs supplied by John Hopper. All the components were standard quality from RS Ltd. The operational amplifiers were powered by a +/- 15 V supply (RS).

Section 2: Working Electrode Synthesis

2.7 Large electrodes

The working electrodes used in these studies comprised of two radically different types. As discussed in the introduction, measurement of the NADH and reduced flavo-enzyme can be done either by using a chemical mediator (for NADH and $FADH_2$ enzymes) or by monitoring the production of H_2O_2 on a bare platinum electrode ($FADH_2$ enzymes alone). The latter type electrode was easy to construct as a small length teflon was removed from 50 μm teflon-coated platinum wire (Clark Electromedical Instruments). The exposed platinum was then coated with Nafion, which acted as an ascorbate barrier. The former type, the chemically mediated electrodes, are more complicated and the organic salt electrodes were made using several methods described below.

Some of the initial work involved the use of larger platinum cavity electrodes figure 2,5 a & d, where the organic salt could be packed in over the electrode (figure 2.5c) either bound in by silicone oil, as a paste, or drop coated in a polymer solution. The two polymers that were routinely used were polystyrene and acetylated cellulose and they were packed in the following way.

For silicone oil bound electrodes, the organic salt was mixed in with a droplet of oil in the ratio 1:9 (weight : volume). The paste was homogenized using a small pestle and mortar, and stored in a foil-covered sample tube. When required, small amounts of paste could be lifted out with a scalpel and worked into the cavity until the paste was level with the teflon (2.5c). Polymer-bound organic salt was prepared by dissolving the polymer in dichloro methane and adding organic salt to give a ratio of 9:1 (salt to polymer). The organic salt did not dissolve but formed a slurry in the polymer solution. Small droplets of this slurry were then applied to the electrode gradually building up the layers until the cavity had been filled. The binders were

essential as the organic salts otherwise became waterlogged and ceased to conduct. These large cavity electrodes had a grove near the top of the electrode, which served as a locater for a rubber "O" ring that held the semi-permeable membrane over the the electrode, trapping a solution of enzyme that had already been placed on the electrode, figure 2.5b.

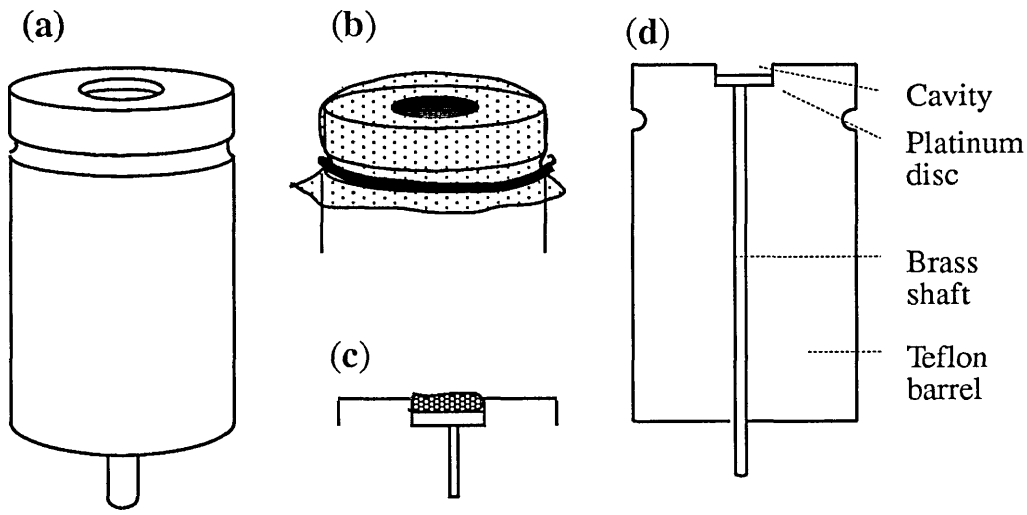


Figure 2.5 Large cavity electrodes (a) teflon-housed platinum electrode with empty cavity, (b) organic salt-filled electrode covered with a membrane secured with an 'O' ring, (c) cross-section showing packed cavity and (d) cross-section of a cavity electrode

The second method for preparing electrodes was as follows:

The cavity electrodes were made by extruding the teflon insulation over the metal, figure 2.6, making it possible to pack 250 μm teflon-coated silver wire with organic salt on its own, as shown by Boutelle *et al* (1986); however when packing organic salt into sizes of wire under 125 μm (5T), the teflon forming the cavity was too elastic and in most cases tended to lift the salt off the surface of the metal. Unlike

the large electrodes, no binder was required for the 250 μm electrodes, which was probably because they were the optimum size with a small diameter but with stiffer teflon.

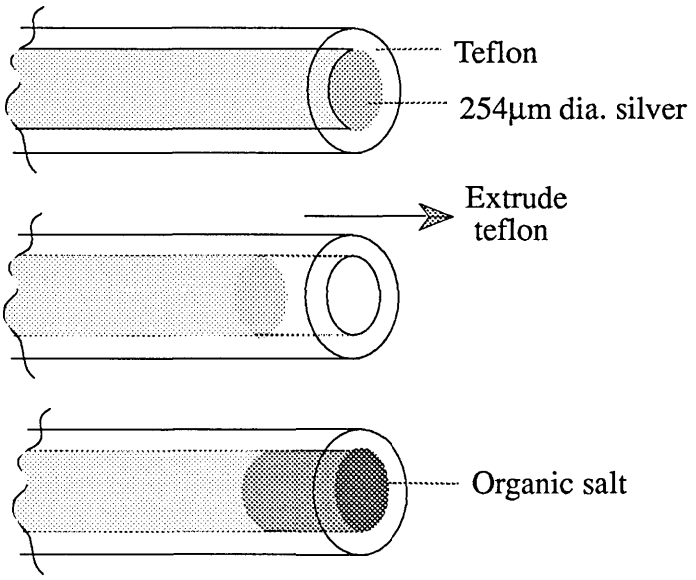


Figure 2.6 The technique of packing 254 μm teflon-coated electrodes. The teflon sheath is extruded over the silver and the resulting cavity is packed with organic salt

These cavity-packed electrodes were suitable for enzymes such as glucose oxidase, which adsorb strongly onto organic salts and therefore require no membrane to retain them. Boutelle's glucose electrode was used successfully *in vivo* to monitor real-time glucose levels. However, enzymes that require entrapment have to be incorporated in the probe system described in section three of this chapter.

As the technique of filling the teflon cavity could not be used successfully with the fine wires, 25 to 75 μm diameter, used for the *in vivo* probes, the polymer binding method was tried. However, coating the metal with the organic salt suspended in a polymer solution often produced insulating electrodes. This may have been due to surface tension properties, associated with such small wires, drawing the polymer to the surface as it evaporated. Drop-coating the binder and the

salt into 1mm cavities also did not produce satisfactory results. As indicated above, this was probably due to the elasticity of the finer teflon.

The two most reliable methods for coating the electrodes were firstly direct electrochemical synthesis of the organic salt on the electrode and secondly drop coating a slurry of organic salt, graphite and silicone oil, an adaptation of the method used for the larger electrodes.

2.8 Electrosynthesis of Organic salts

The electroplating technique was developed from the work of Driscoll (1988) and involves a two stage electrosynthesis of the organic salt from its constituent aqueous ions. The advantage of this technique is that the process can be controlled electrochemically, so that exact amounts of each ion can be deposited.

Several different techniques for electroplating NMP^+TCNQ^- and TTF^+ $TCNQ^-$ were tried by Driscoll and the recipe used here is a modification of the most effective one. Electrosynthesis has to occur in the aqueous phase otherwise both the intermediate and the final electrode surfaces will dissolve.

The apparatus used was similar to that described for 'test' electrodes, figure 2.3. Electrodes constructed out of copper, silver or platinum were held in a small (0.5 mL) sample pot with a 250µm Ag/AgCl reference and a silver counter and a magnetic flea. With everything set up, the sample pot was filled with 'O_2' purged plating solution and electroplating was begun. Plating lasted no longer than 5 minutes, because by this time the organic components began to oxidize.

Step 1

$$TCNQ^- + e^- \text{ ---> } TCNQ^\circ$$

$TCNQ^\circ$ was deposited on the metal surface, copper, silver or platinum/iridium, potentiostatically using an oxidizing potential of +100 mV or

+200 mV (vs Ag/AgCl)for 3 min. The plating solution comprised of 0.5 mg/mL LiTCNQ in 100 mM lithium acetate and was saturated with argon prior to plating to remove oxygen. The lithium acetate was used as a background electrolyte.

The output from the potentiostat was put through an integrator, which then measured the charge passed and hence the number of moles of $TCNQ^{\circ}$ deposited. As demonstrated in the equations below:

$$V_{out} = -\int \frac{1}{\tau} V_{in} \partial t \qquad (2.1)$$

Where τ is the time constant (τ =RC)

$$\frac{V_{out}}{R_M} = -\frac{1}{\tau}\int \frac{V_{in}}{R_M} \partial t \qquad (2.2)$$

$$Q = \frac{-V_{out}}{R_M} \tau \qquad (2.3)$$

Under slight magnification, crystals of $TCNQ^{\circ}$ could be seen covering the electrode and gave a pale to dark green colour depending on their coverage.

Step 2

$$NMP^{+} + TCNQ^{o} + e^{-} \text{----> } NMP^{+}TCNQ^{-}$$

$$TTF^{+} + TCNQ^{o} + e^{-} \text{----> } TTF^{+}TCNQ^{-}$$

Either aqueous NMP^{+} or TTF^{+} was then electroplated galvanostatically forming $NMP^{+}TCNQ^{-}$ or $TTF^{+}TCNQ^{-}$. For NMP^{+}, the plating solution used was 30 mg/mL $NMP^{+}SO_3^{-}$ in DDW; no background electrolyte was needed as NMP^{+} SO_3^{-} is quite soluble. As TTFCl is fairly insoluble in aqueous solutions, plating solutions containing 2 mg/mL TTFCl in 100 mM potassium acetate were used. As LiTCNQ is soluble and KTCNQ is not, potassium ions were used to prevent $TCNQ^{-}$

dissolving off the electrode and acetate ions used to prevent TTF^+ dissolution. The solutions were purged with argon and covered in silver foil to prevent attack from oxygen and light respectively.

Controlling the current galvanostatically meant that equal amounts of cation and anion could be plated on the electrode. For example, if 200 μC of charge was passed electrosynthesizing TCNQ°, then a reducing current of 2 μA would be applied for 100 seconds to form either TTF^+TCNQ^- or NMP^+TCNQ^-. The resulting crystals of both organic salts were black on inspection, and gave the electrode a very rough surface.

2.9 Organic salt paste coating

This method appeared as a modification of the silicone oil technique used for the larger electrodes, where the oily paste was packed into a recess using a fine scalpel blade. The only way to cover the micro electrode was to apply the paste as a solution. This technique appeared to have a much higher success rate than drop coating organic salt in cellulose acetate and this is probably because a conducting layer is formed on the surface of the paste electrodes, where as a layer of insulating polymer may form when only polymer is added. The correct ratio of NMP^+TCNQ^- : graphite: oil was vital to insure a lifetime of days rather than hours. The first micro electrode to be made in this way was a plain carbon paste electrode, consisting of 2.9mg graphite per ml silicone oil (as used by Boutelle *et al* 1989).

Two to four mm of metal was exposed at the tip of the electrode, a 250 μm silver wire, by rolling a sharp scalpel blade through the teflon and it was then coated in layers of paste by touching a droplet of the paste solution onto the metal, allowing the solvent to evaporate and then repeating the coating. As this electrode oxidized ascorbate over a period of days, similar electrodes were made with

NMP^+TCNQ^- added to the carbon paste coating solution. These gave excellent currents on addition of NADH and retained 100% activity over a three day period.

Initially it was assumed that the silicone oil was, by itself, conferring the stability, but electrodes made from NMP^+ $TCNQ^-$ and silicone oil only, failed to give activities lasting more than a few hours. Changing the concentrations of oil and organic salt still failed to give any longevity. It was only on the addition of graphite back into the electrode composition that suddenly increased the lifetime from hours to days. An explanation for this may lie in the conducting organic salts requiring a 'conducting filling', which will both retain conductivity if there is any water adsorption and also add a finer 'grade' of binder. Once the electrode coating had been optimized, probes were made using the needle design, **4** (described in the next section), filled with enzyme and tested.

2.10 Platinum electrodes

These electrodes were by far the simplest to prepare, as no delicate mediator or support had to be added to the surface. Short lengths (1,2 & 4mm) of 25 and 50 μm teflon-coated platinum were exposed by carefully removing the teflon. The exposed metal was then repeatedly dipped in Nafion™ solution (nafion dissolved in 95% alcohol (Du Pont)). Successive dipping, a 2 second immersion followed by 5 seconds of air drying, gradually built up layers of the negatively charged polymer on the surface of the electrode, with 40 coats reducing ascorbate oxidation by about 90%. After being left for 5 minutes to dry completely, the electrodes were ready for testing or incorporation into probes.

Section three: Probe Construction

2.11 Immobilized and entrapped enzymes

Initial work on making an in vivo sensor focused on an open-ended enzyme electrode with enzyme immobilized or entrapped on the electrode surface, which would have been similar to the glucose oxidase enzyme electrode used by Boutelle for *in vivo* glucose measurements in the rat brain (Boutelle *et al* 1986). These electrodes consisted of 250 μm teflon-coated silver wire with organic salt ($TTF^{+}TCNQ^{-}$), packed into the teflon cavity, see section 2.7. Glucose oxidase binds very strongly to organic salt electrodes needing no entrapment, but other enzymes, such as choline oxidase and glutamate dehydrogenase, had to be retained near to the electrode. Covering a micro electrode with a semi-permeable membrane, immobilizing the enzyme onto an electrode-bound polymer and restraining the enzyme inside a gel were three of the methods tried. None of these three techniques gave much success. Immobilization of glutamate dehydrogenase in a solution of poly-acrylamide which was cast onto the electrode was the most successful. The electrode gave good reproducibility, however it had a short life-time because the gel was unable to bind to the teflon and would easily break away from the electrode surface.

Coating the electrode in a polymer, nafion for example, did little to retain the enzyme; and binding enzyme with $PDP^{+}PSA^{-}$, see section 2.4, did not produce an electrode with a suitably long lifetime. These results showed that a membrane was required and this is where a solution was found.

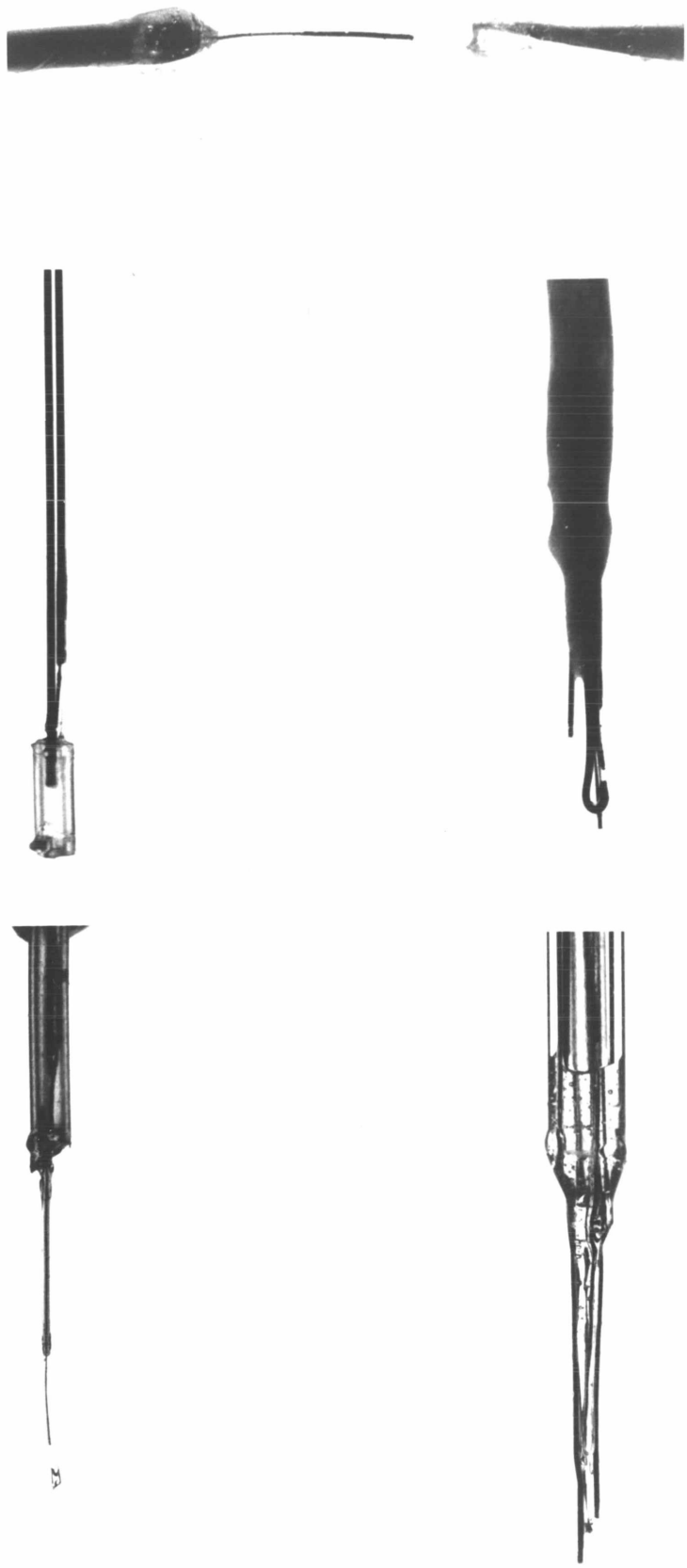


Plate 2.1 The five designs used in this work

2.12 Designing an implantable micro probe

Designing and producing an *in vivo* probe was a challenging and lengthy process and the final design only appeared after 18 months of progressive modifications. This section describes the evolution of the probe and how the design has become progressively more refined. The five designs are pictured in plate 2.1

Design 1

The very first design, design **1** figure 2.7, consisted of 0.5mm stainless steel (SS) cannulae (Goodfellow Metals) separated by a short length of dialysis fibre (Gambro). An electroplated 75 μm silver / organic salt electrode, see section 2.8 for details, was inserted inside the dialysis fibre prior to glueing inside the steel cannulae. A copper brace was attached to prevent the dialysis tubing from bending once wet, which may have damaged the electrode. Plate 2.2 shows the central electrode area in detail.

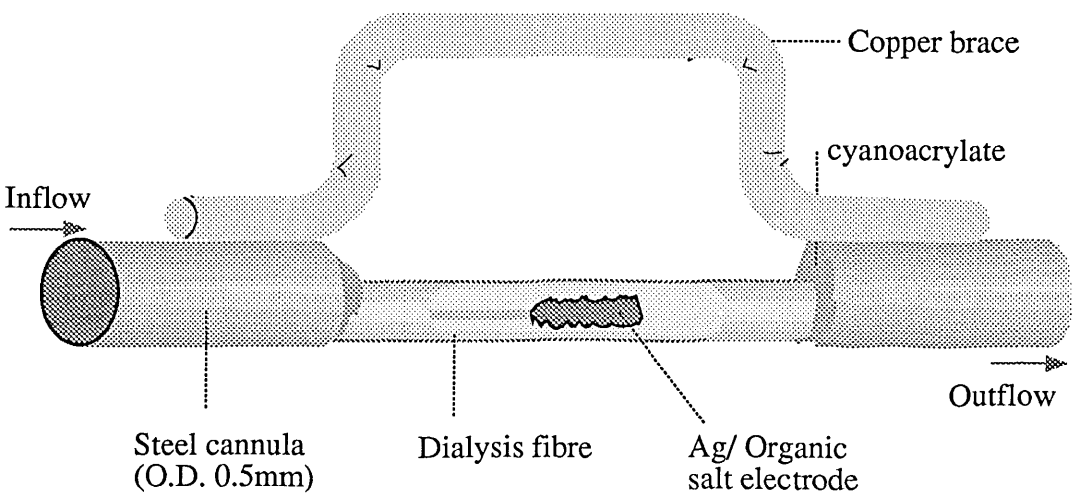


Figure 2.7 Design **1**, the first dialysis electrode



Plate 2.2 The active region of a design **1** probe. The photograph is magnified 10 times.

Design 2

This very crude design was used to test the principle of the dialysis probe and was quickly superceded by design **2**, as the long straight probe, **1**, was cumbersome when immersed in buffer during calibrations owing to its length and need for rigidity. Design **2**, being pointed, was far easier to dip into a stirred pot of buffer and used finer steel (0.2mm) with a finer working electrode, 50 μm silver. The probe was becoming small enough to be considered for *in vivo* work, except for the bulbous tip, which was a wider bore polythene tubing used to complete the flow at the bottom of the probe. Such a large tip made this design impractical for *in vivo* work, as the 1mm tip would act as a 'bulldozer' if implanted into nervous tissue. Design **2** is illustrated below in figure 28 and plate 2.3, overleaf, shows a ten fold magnification of the 'active end'.

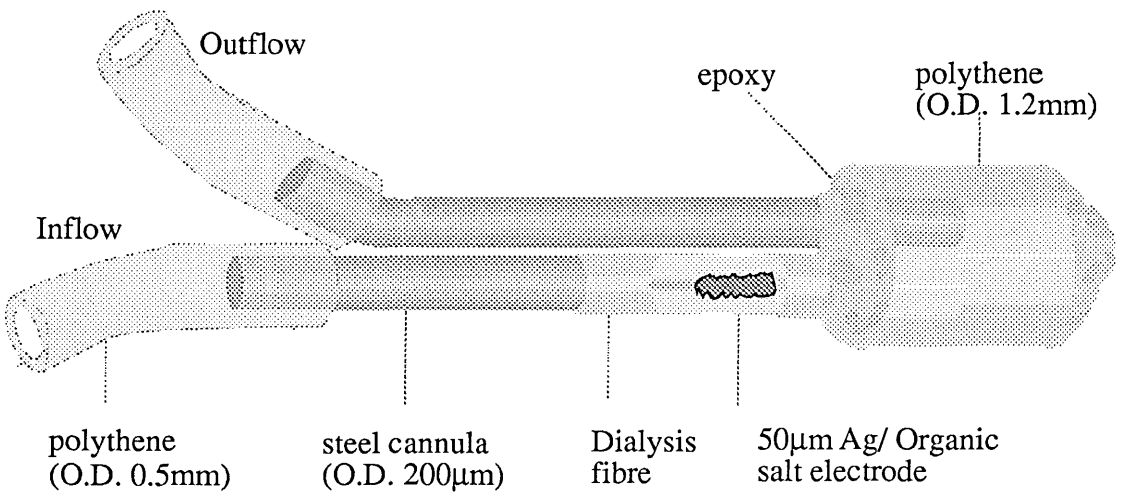


Figure 2.8 Design **2**, showing the fine steel tubes but with a bulbous tip



Plate 2.3 A design **2** probe seen at 10 fold magnification

Design 3

The removal of this polythene tubing was of fundamental importance and figure 2.9 shows the next probe design that was produced, (not drawn to scale). Design **3**, the first improvement on **2** consisted of the fine steel cannulae (200 μm) separated by 4mm of dialysis fibre. One of the steel tubes was bent into a 'J' shape, giving a more compact end to the probe (overall width ≈ 700 μm. Before joining the fibre to the steel, a short length (50mm) of insulated wire, either 50 μm silver or copper, was stripped of its insulation, usually teflon or polyamide, coated with organic salt, see section 2.7, and inserted inside the dialysis fibre. All the joints were then sealed with cyanoacrylate glue.

This design was used in some of the initial *in vivo* work, however it was superceded by the designs **4** & **5** after only a few experiments. The probe in plate 2.4, has been sealed up ready for implantation and has two 125 μm teflon-coated stainless steel recording electrodes near the active dialysis area as well as another partially-hidden 200 μm hollow stainless steel tube, used for infusion of ascorbate oxidase as described by (Brazell & Marsden 1982)

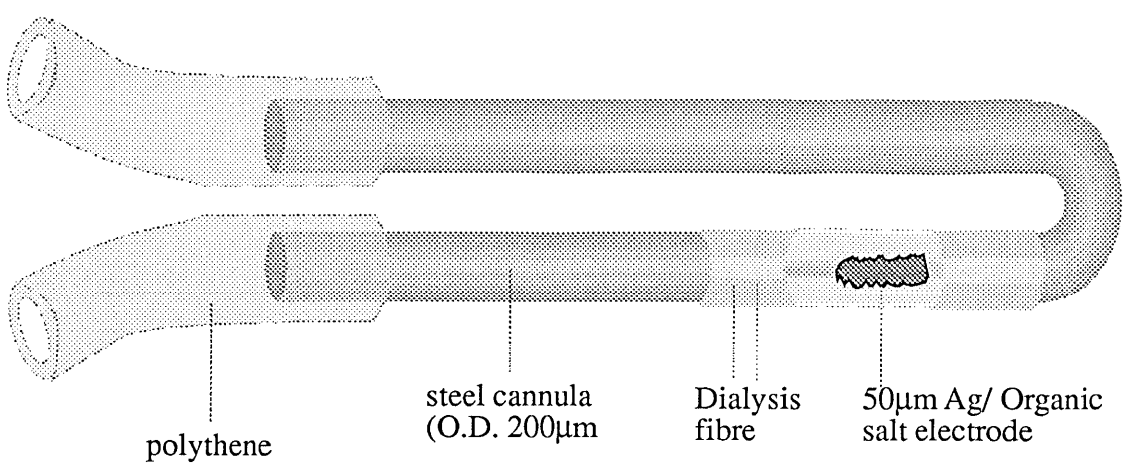


Figure 2.9 Design **3**, The 'U'- shaped steel made the probe small enough for *in vivo*, however the design was superceded by the **4** & **5**



Plate 2.4 A design **3** probe, ready for implantation, sealed in acrylate with two stainless steel electrodes and a hollow infusion tube

Design 4

The probe shown in the figure 2.10, design **4**, has an active sampling area which is smaller than design **3** by about 30%, making it a suitable size for implantation. This design is a needle shape and consists of two concentric tubes, an outer polythene tube (O.D. 1.2mm, Portex Tubing ltd) ending in a variable length of dialysis fibre (typically 8.5mm), the first half of which was covered in glue (typically 4.5mm) leaving the final 4mm exposed and the inner a vitreous silica tube (O.D. 140 µm, SCE ltd). The working electrode, a 25 µm polyimide-insulated copper wire, was inserted down the inner tube (140 µm silica tubing). The tip of the working electrode was bared and coated with organic salt paste, section 2.9, before being withdrawn into the dialysis fibre. The open end of the dialysis fibre was then sealed using cyano-acrylate or epoxy resin. For these *in vivo* probes, both the counter and the reference were inserted inside the polythene outflow tubing. This protected the electrodes from damage during implantation and gave the probe more versatility as all three electrodes were permanently in electrical contact.

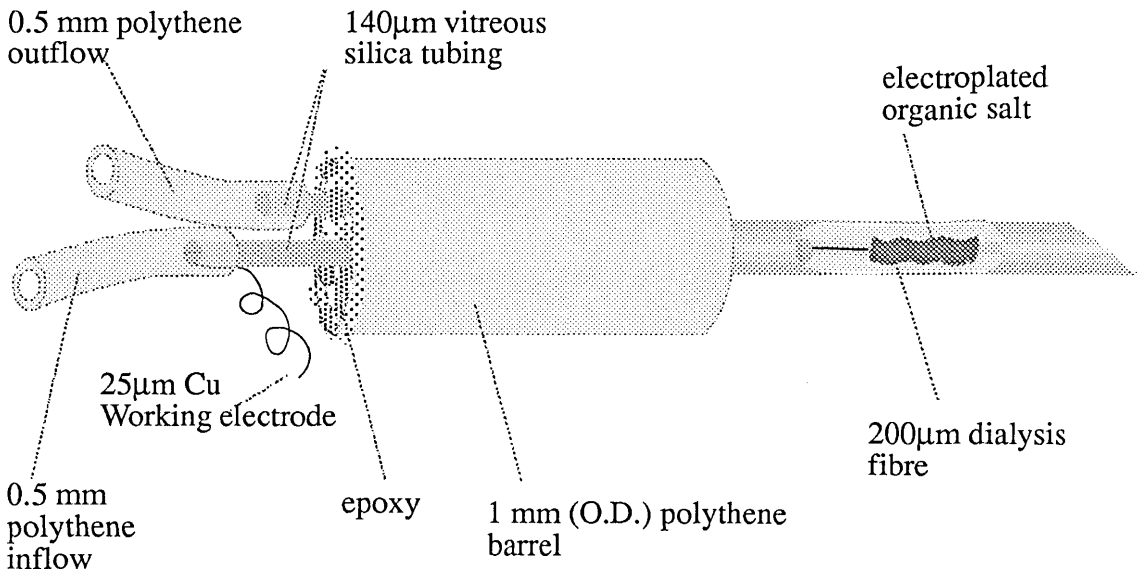


Figure 2.10 The design **4** probe, with the fine tip, making it equivalent to the commercial dialysis probes.

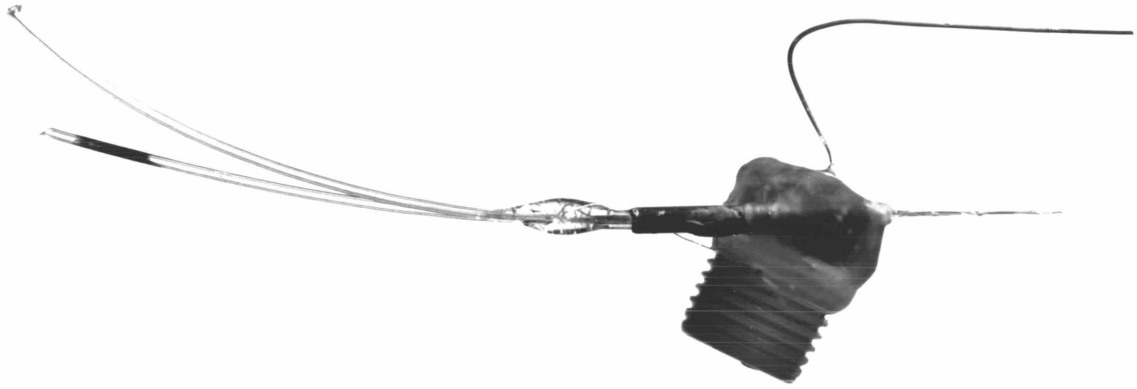


Plate 2.5 A design **4** probe,

This meant that probe was now a single needle rather than three individual electrodes. Polythene tubing (O.D. 0.5mm) was connected to the central silica glass tube and was used as the inflow for buffer and enzyme perfusions. A second shorter silica tube, again connected to a short length of polythene tubing, was inserted into the top of the probe and acted as the outflow.

Design ***5***

The final design, **5**, used nafion-coated platinum electrodes as opposed to organic salt paste electrodes. The teflon-insulated 50 μm platinum wire (Clark Electromedical) was inserted down the outer polythene tube and ran down inside the dialysis fibre parallel to the vitreous silica tubing. The exposed end of the platinum, usually 4mm, was coated with nafion before assembly and the probe was sealed with cyanoacrylic glue (Loctite) and covered with epoxy. The epoxy coat was added as there is evidence of cyanoacrylate breaking up if kept wet for long periods (Boutelle 1991). One final modification was made for the electrodes used for striatal work, chapter 4, and that was addition of an external 25 μm platinum electrode, wrapped around the outside of the dialysis fibre, its purpose to monitor ascorbate concentrations outside the probe. This probe is shown in figure 1.20 (page 49) and overleaf plates 2.6 & 2.7. The probes used to study the hippocampus had no such external electrode, instead they had 2 125 μm teflon-coated stainless steel recording electrodes, glued to the dialysis fibre approximately 0.7mm apart, figure 2.11 and plates 2.8 & 2.9. Two of the five probes described here, designs **3** and **5**, were used for *in vivo* work, **5** being the preferred choice as it was smaller.



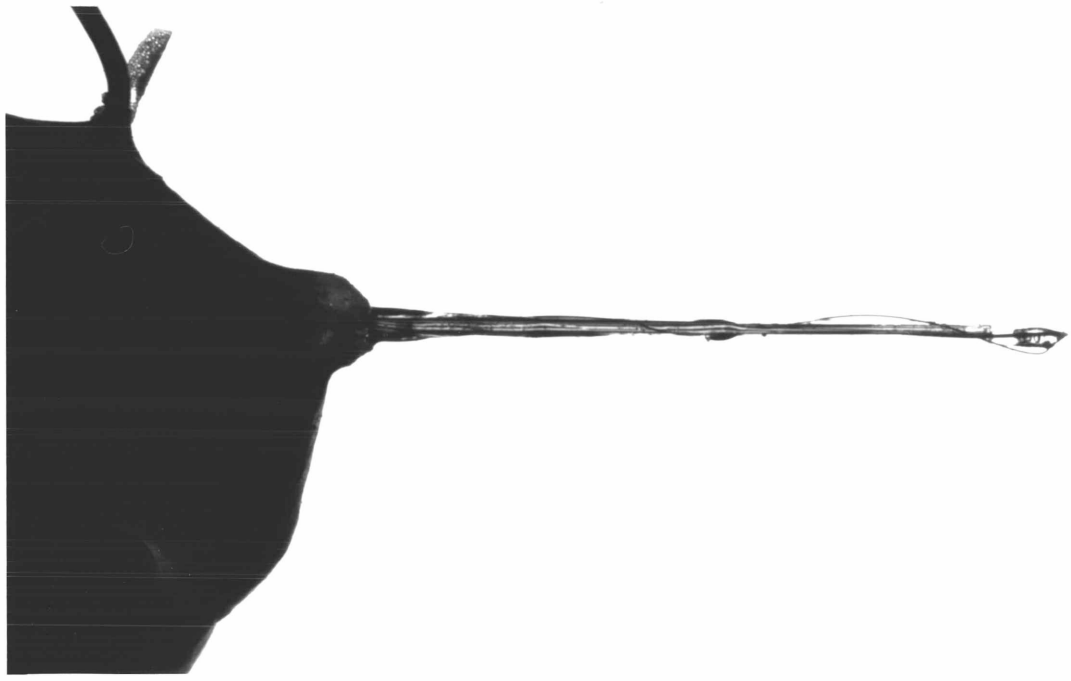


Plate 2.6 & 2.7 A life-size photo of the probe used for striatal implantation is shown above (2.6). The photograph below (2.7) shows the active area in more detail, in particular the external electrode and the line of epoxy sealing the upper 5 mm of dialysis fibre.

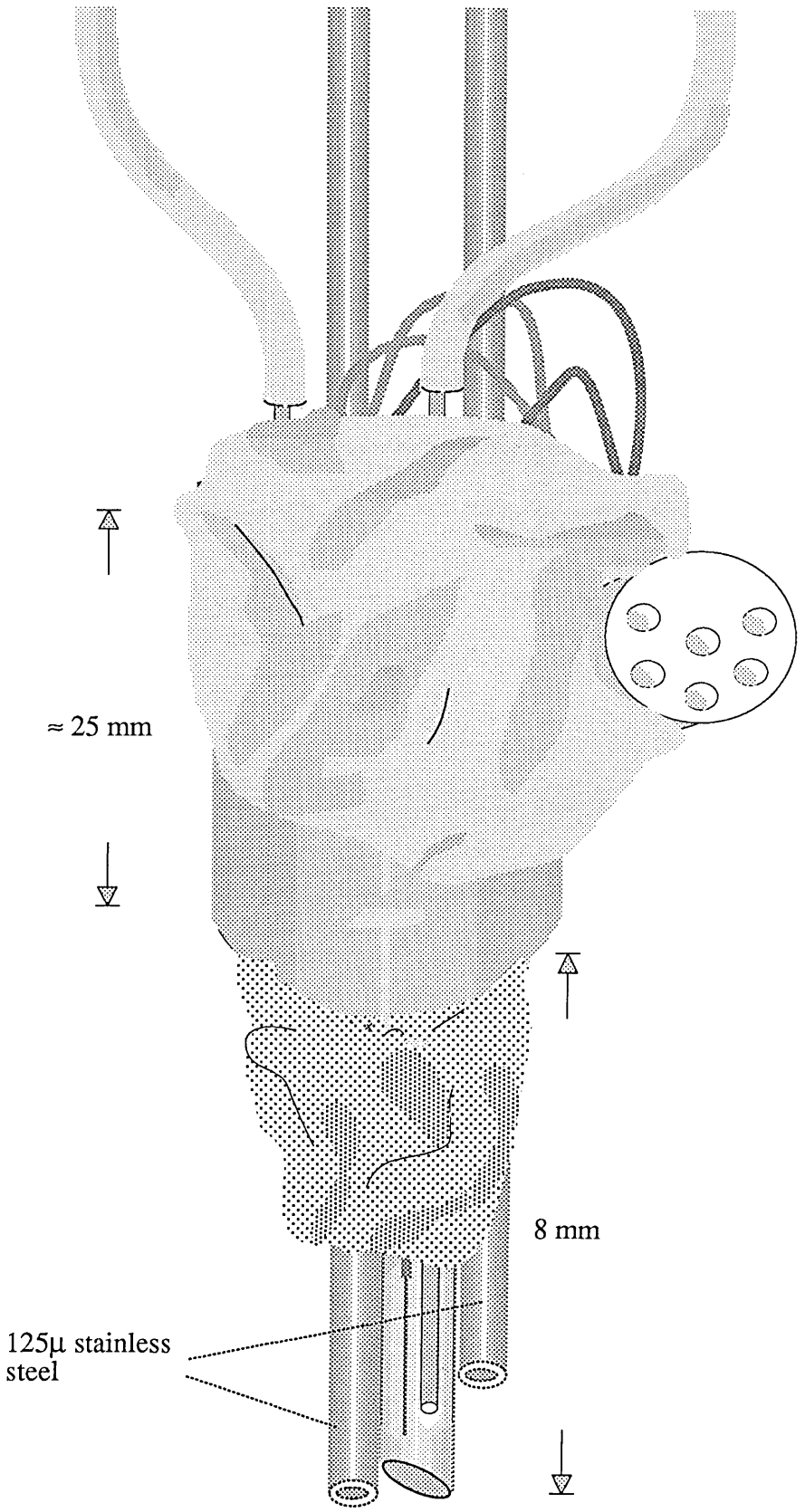


Figure 2.11 The design **5** probe, sealed and ready for implantation with the two 125 μm stainless steel recording electrodes.

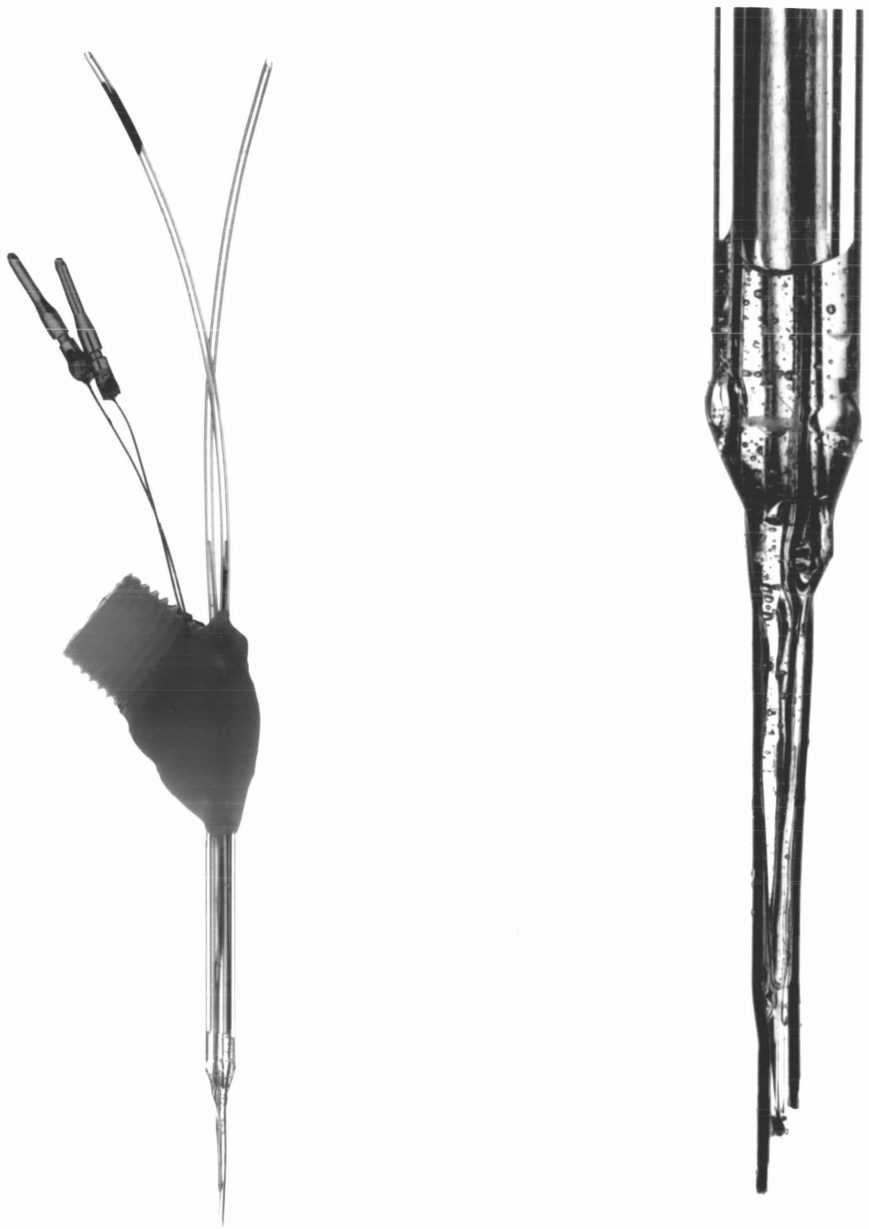


Plate 2.8 & 2.9 The photograph on the left (2.8) shows a lifesize probe ready for implantation. The photograph on the right (2.9) shows the active region with the lower stainless steel electrode yet to be cut down to size.

Chapter Three

The properties and lifetimes of the electrodes and probes

Section 2 of the previous chapter describes the four main methods used for synthesizing and fabricating the different electrode surfaces:

(1) tightly-packed, oil and polymer-bound organic salt
(2) electrochemically synthesized organic salt
(3) graphite paste organic salt
(4) nafion coated platinum electrodes

These surfaces were tested with one or more of the following, ascorbate, NADH, glutamate and glucose oxidase. The results are presented in the next sections.

3.1 Tightly-packed, oil and polymer bound organic salt

Tightly-packed electrodes

These techniques were only useful for the large 254 μm electrodes, although the problems of insulation by the binder, see section 2.6, were still encountered. The lifetime of a tightly-packed $TTF^{+}TCNQ^{-}$ choline oxidase electrode is shown in figure 3.1. The response time was fast, typically >90% in 5 seconds. In between runs, the electrodes were left in phosphate buffer and the drop-off in current after day 2 is caused by the enzyme desorbing from the surface. This was verified by testing an electrode that has been placed back into the same concentrated solution of choline oxidase that was used for the initial adsorption. If kept in enzyme solution this electrode retained the activity for over a week and an example of this recovery is shown in figure 3.2. However the response began to fall off after this time and this

may be attributed to the salt becoming water-logged as well as the enzyme becoming denatured. The organic salt had to be packed very tightly into the teflon cavity otherwise excess water absorption deactivated the electrode.

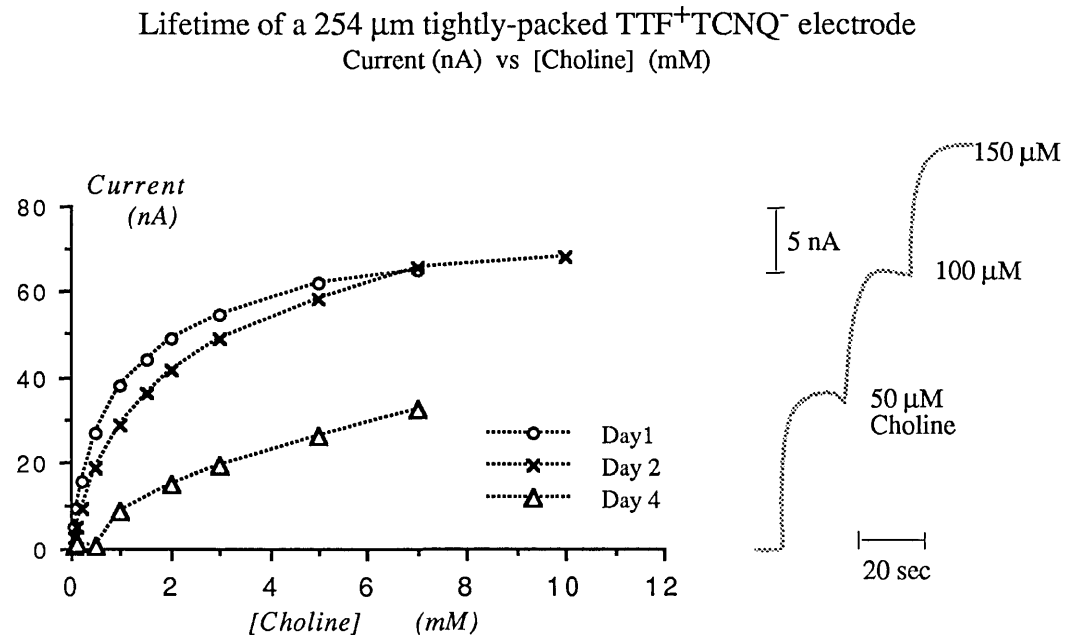


Figure 3.1a Graph showing the lifetime of a tightly packed $TTF^{+}TCNQ^{-}$ choline oxidase electrode at 0 mV (vs Ag/AgCl). The electrode set-up used is described in section 2.5.
Figure 3.1b, shows the response time

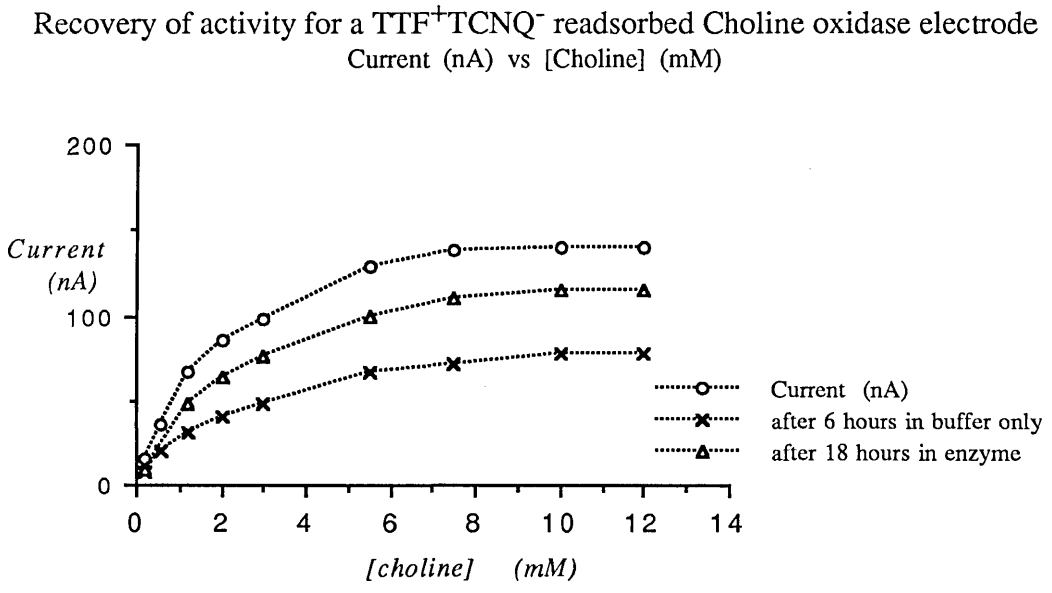


Figure 3.2 Graph showing the recovery of a tightly-packed $TTF^{+}TCNQ^{-}$ choline oxidase electrode, firstly after 18 hours soaking in (0.15U/μL), then following 6 hours in phosphate buffer and finally tested after being replaced back into the same enzyme solution. The electrode was held at 0 mV (vs Ag/AgCl). The electrode set-up used is described in section 2.5

Polymer-bound electrodes

Binding the electrodes with polystyrene appeared to do little to increase their lifetime. Figure 3.3 shows a plot for a polystyrene-bound NMP^+TCNQ^- electrode. It was tested with NADH as enzyme did not readily adsorb to its surface. This was probably because the hydrophobic aromatic groups of the polymer repel the hydrophilic surface groups of the enzyme. The response to NADH was good, but began to drop of after 24 hours. Both of these factors made this technique unsuitable.

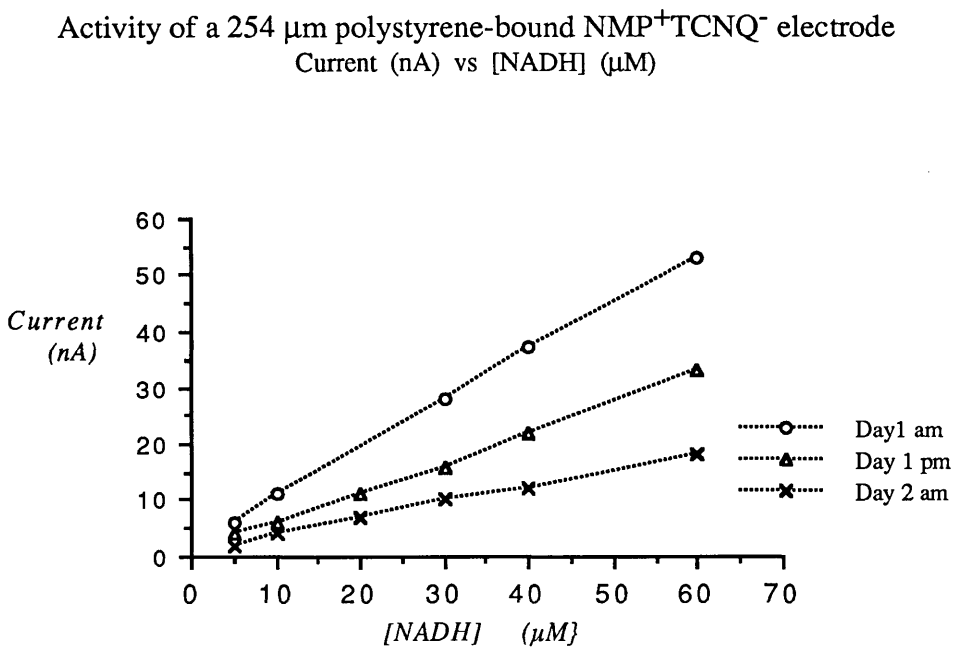


Figure 3.3 Graph showing the lifetime of a polystyrene-bound NMP^+TCNQ^- electrode. The electrode was held at 0 mV (vs Ag/AgCl). The electrode set-up used is described in section 2.5

Silicone oil-bound electrodes

Silicone oil-bound organic salt electrodes were also made and choline oxidase was adsorbed onto them. Their response was similar to the tightly-packed electrodes, namely the activity dropped off over a period of three days. The

properties of oil bound electrodes were examined further with micro electrodes, section 3.3 Figure 3.4 shows the activity of a 254 μm silicone oil-packed electrode.

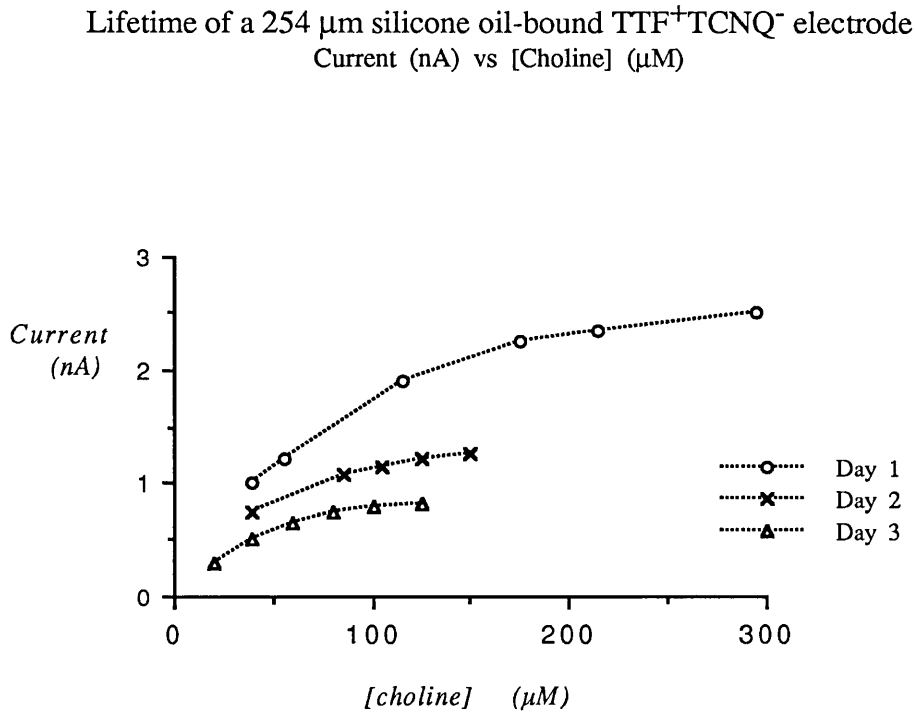


Figure 3.4 Graph showing the lifetime of a silicone oil-bound $TTF^{+}TCNQ^{-}$ electrode. The electrode was held at 0 mV (vs Ag/AgCl). The electrode set-up used is described in section 2.5

As well as there being a constant decrease in activity after the electrodes were removed from their enzyme solutions, the three techniques were not suitable for miniaturization because of the flexibility of the very fine 50 &75 μm teflon electrodes. It was therefore necessary to modify these techniques before they could be applied to micro-electrodes.

3.2 Electrochemically synthesized organic salt electrodes

Untreated electrochemically grown NMP^+TCNQ^- and TTF^+TCNQ^- had activities that lasted for 2 days at 100% but which slowly decayed over the next three days. Figure 3.5 shows the range of a 254 μm electroplated NMP^+TCNQ^- electrode tested with NADH at 0 mV. This technique was easily applied to 50 and 75 μm silver electrodes, as the fine wire could be placed in plating solution without problem and no cavity packing was required. However electroplated micro-electrodes had much shorter lifetimes than their larger brothers. Typically, the response for an electrosynthesized NMP^+TCNQ^- silver electrode was fast, but an untreated electroplated organic salt would only last for a few hours after which total activity was lost. (The bare metal electrodes were always roughened with a scalpel blade and then cleaned in acetone before use. Platinum electrodes were pre-washed in aqua regia) .

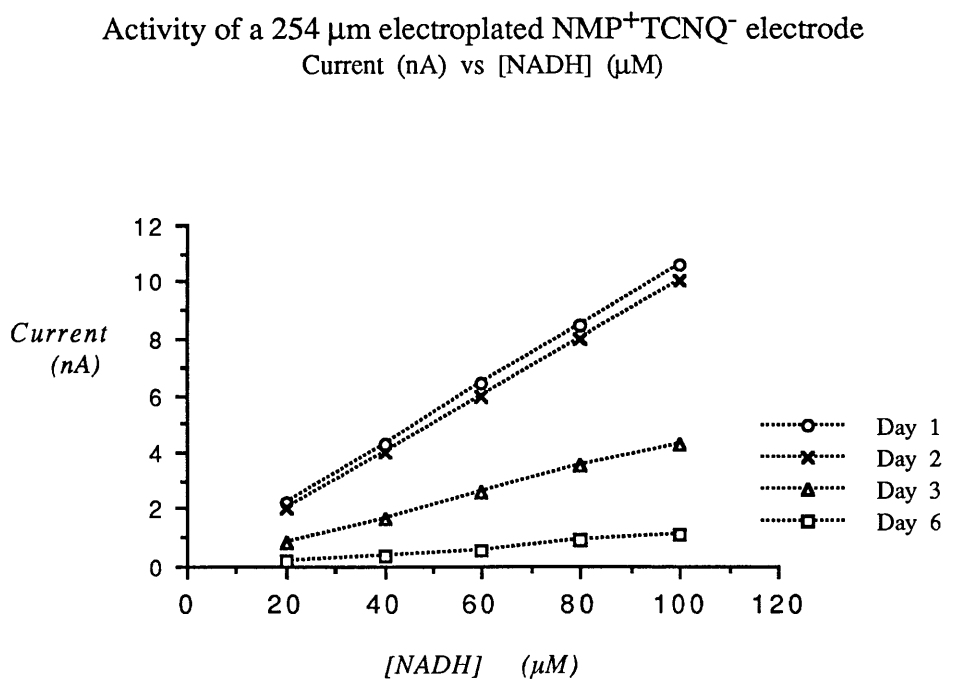


Figure 3.5 Graph showing the lifetime of an electroplated NMP^+TCNQ^- electrode responding to NADH at 0 mV (vs Ag/AgCl). The electrode set-up used is described in section 2.5

Varying the type of metal electrode was attempted to see if the electrode/ organic salt interface increased in resistance, due to, for example, the formation of metal oxides. Silver and copper both gave short-lived responses (4 hours), however electroplated 50 μm platinum wires gave longer activities, figure 3.6. This was probably due to a better organic salt/ Pt interaction that promoted smoother electroplating and hence less water absorption. Both cations (TTF^+ and NMP^+) had similar life-times on platinum and so it was obviously not the metal ion interaction that was the main problem.

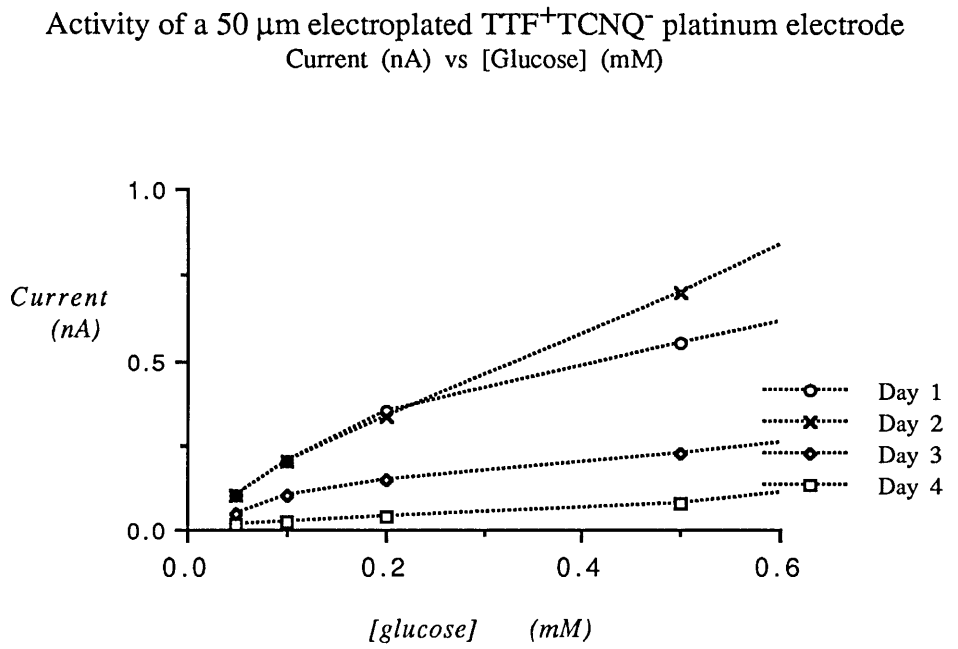


Figure 3.6 Graph showing the lifetime of a 50 μm electroplated NMP^+TCNQ^- Platinum electrode responding to glucose at 0mV (vs Ag/AgCl) over 4 days.. The electrode was made into a design 3 probe and filled with glucose oxidase. The set-up used is described in section 2.5

Inspection of the electrodes after the calibrations run showed the black crystals to be heavily water-logged and in some places patches of organic salt had lifted off the electrode. This was obviously the main reason for the deterioration in the electrode activity. It was assumed that during the electro-deposition of the

organic salt especially the first stage of $TCNQ^{o}$ formation, the crystals grew in a random and irregular manner, which left fine gaps that could take up water or electrolyte, causing the electrode to swell up like a sponge. As similar potentials were used for the different sized electrodes, the crystals grew at similar rates, leaving relatively bigger gaps on the smaller electrodes, reducing their activity faster.

If the deposition could be controlled to give a much more even organic salt layer, then a more stable electrode would probably result. The oxidation of $TCNQ^{-}$ may become more reproducible at lower LiTCNQ concentrations and by using lower voltages or linear sweeping. The 'pressed pellet' organic salt electrode, which is made by compressing organic salt at high pressures of 500 N/cm^2 forming a 3-4mm diameter pellet that can be housed inside an large electrode, lasts for long periods probably because no water can disrupt the very tightly compressed mediator.

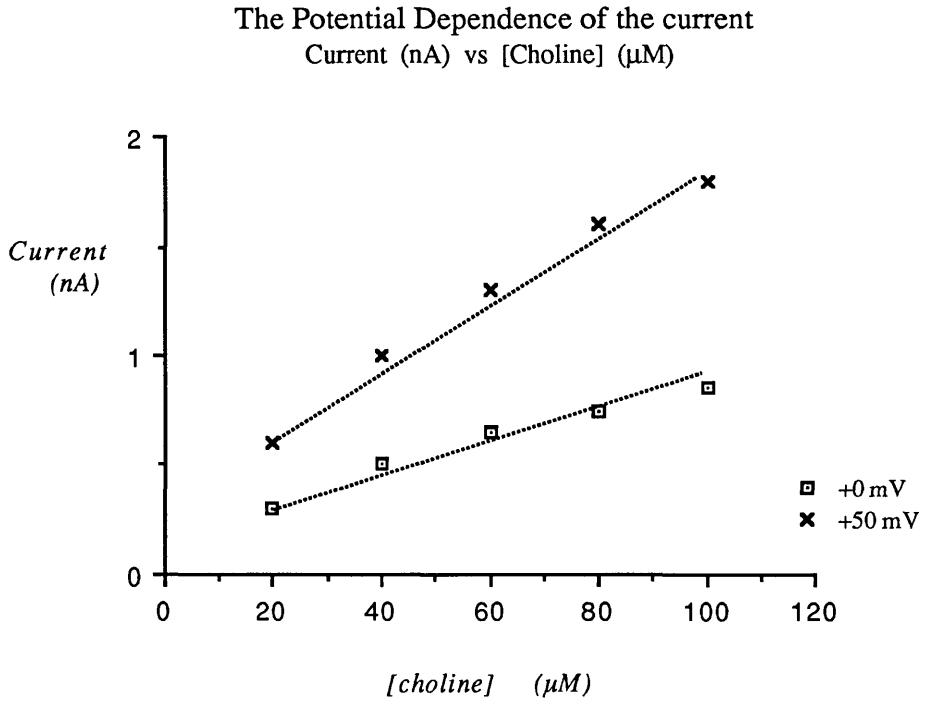


Figure 3.7 Graph showing the potential dependence of a 254 µm silicone oil-bound $TTF^{+}TCNQ^{-}$ electrode responding to choline. Choline oxidase was adsorbed onto the surface and the electrode was tested at 0 mV and +50 mV (vs Ag/AgCl).. The set-up used is described in section 2.5

The response of electroplated electrodes as a function of potential was investigated to see whether an increased potential would promote better sensitivity and longevity. Two runs were performed with the same electrode, one at +0mV and the other at +50mV (vs Ag/AgCl). As figure 3.7 shows, the raised potential increases the current output, however the background 'noise' was larger at the higher potential, and there was no overall improvement in longevity either.

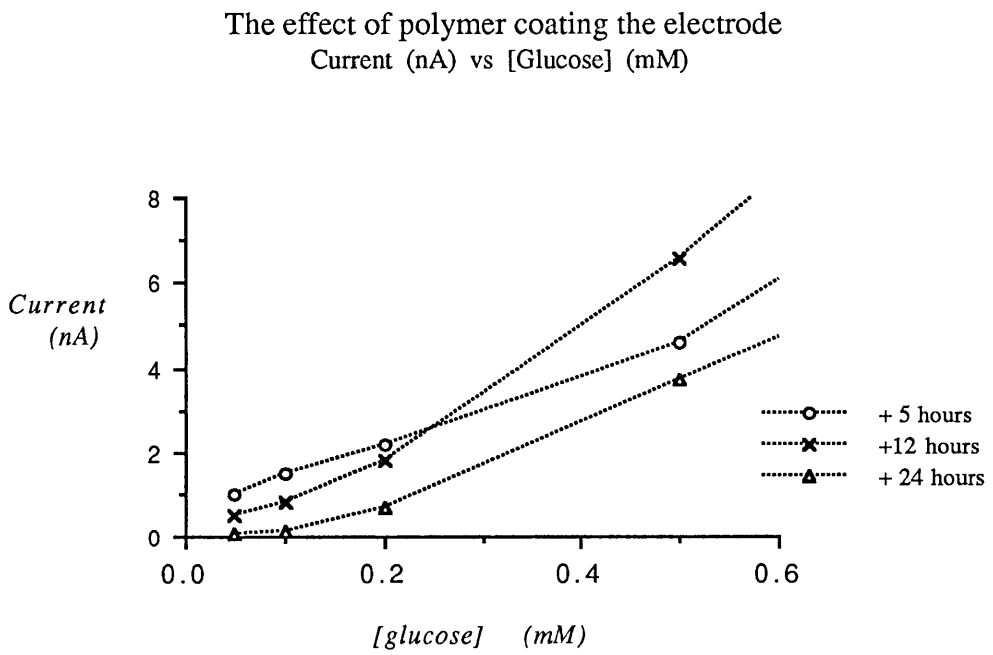


Figure 3.8 Graph showing the lifetime of a 50 μm electroplated $NMP^{+}TCNQ^{-}$ silver electrode coated in acetylated cellulose and organic salt, responding to glucose at 0mV (vs Ag/AgCl) . The electrode was made into a design 3 probe and filled with glucose oxidase. The set-up used is described in section 2.5

Modifying the electroplated electrodes, to confer extra stability on the probes was tried, but with little success: after electrosynthesis, the rough crystals were coated with either 5% cellulose acetate in acetone or 2mg/mL organic salt and 5% cellulose acetate in acetone. Figure 3.8 shows the response of one such probe and the effect of the polymer. Although bigger currents were seen due to more organic

salt being deposited on the surface, the polymer did not appear to stabilize the electrode. It is curious as to why polymer binding is a successful method with the larger electrodes, but has a detrimental effect on the micro electrodes. One explanation may lie in the surface tension properties of the fine electrodes during coating, which may force an insulating layer of polymer to the surface, giving less polymer-bound salt inside the coat and hence less stability.

Although the electrosynthesis is a reproducible way of coating electrodes, figures 3.6, 3.7 & 3.8 show that both the lifetime and the sensitivity required improvement before the technique of electroplating can be used for *in vivo* work. Had other techniques not proved more successful, then the electrodeposition could have been studied further.

3.3 Organic salt paste coating

This method appeared as a modification of the silicone oil technique used for the larger electrodes, where the oily paste was packed into a recess using a fine scalpel blade. The only way to cover the micro electrode was to apply the paste as a solution. This technique appeared to have a much higher success rate than drop coating organic salt in cellulose acetate. Both 254 μm and 50 μm electrodes could be coated in this manner. The first micro electrode to be made in this way was a plain carbon paste electrode, consisting of 2.9mg graphite per ml silicone oil (used by Boutelle *et al* 1989). As this electrode oxidized ascorbate over a period of days, similar electrodes were made with $NMP^{+}TCNQ^{-}$ added into the coating solution. The first electrode used to establish this technique was a 254 μm silver wire, which was coated in paste containing $NMP^{+}TCNQ^{-}$. It was tested with NADH and responded well over a week, with 100% activity over a three day period figure 3.9.

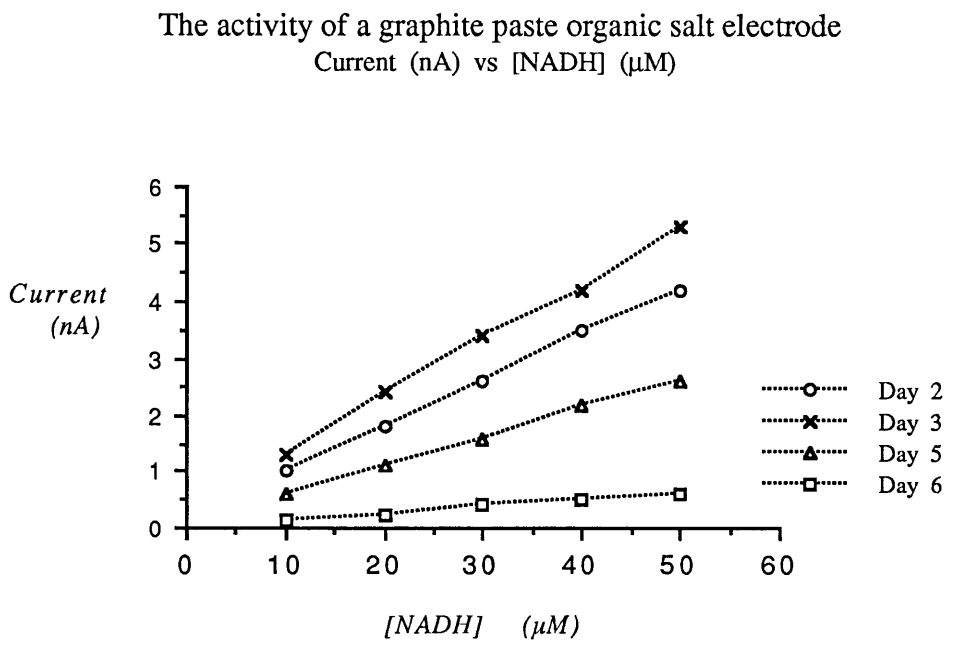


Figure 3.9 Graph showing the lifetime of a 254 μm graphite paste NMP^+TCNQ^- silver electrode responding to NADH at 0mV (vs Ag/AgCl) over 6 days. The set-up used is described in section 2.5

The right ratio of NMP^+TCNQ^-: graphite: oil was vital to insure a lifetime of days rather than hours. Initially it was assumed that the silicone oil was, by itself, conferring the stability, but just NMP^+TCNQ^- and silicone oil alone failed to give activities lasting more than a few hours. Changing the concentrations of oil and organic salt still failed to give any longevity. It was only on the addition of graphite back into the electrode composition that suddenly increased the lifetime from hours to days. Figures 3.10 a & b compare the currents and the lifetimes of electrodes with and without graphite in the binder. Once the electrode coating had been optimized, design **4** probes were made using this design.

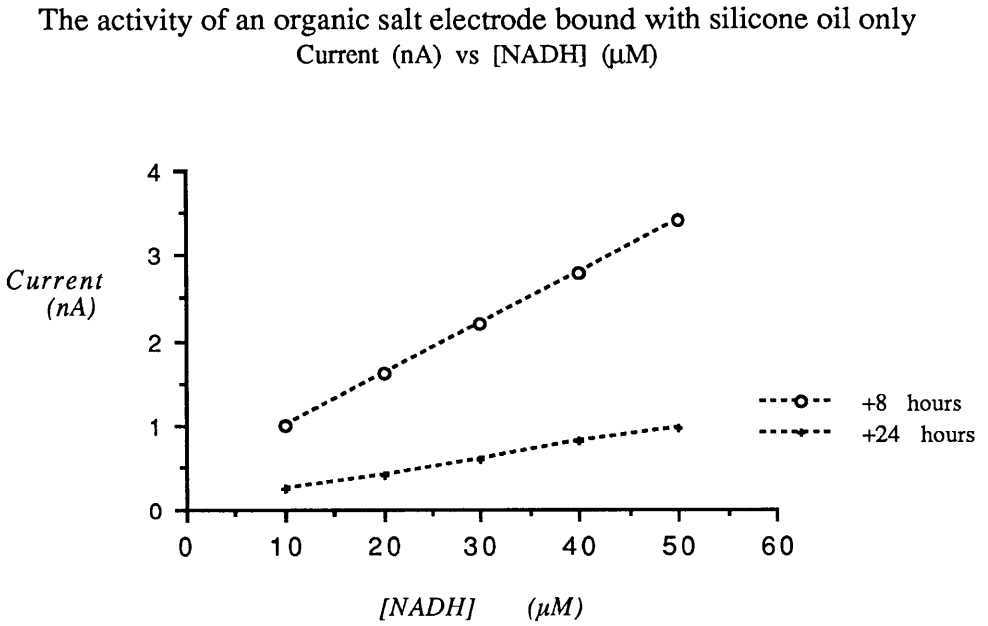


Figure 3.10.a Graph showing the lifetime of a 50 μm NMP^+TCNQ^- silver electrode bound with silicone oil only, responding to NADH at 0 mV (vs Ag/AgCl). The set-up used is described in section 2.5

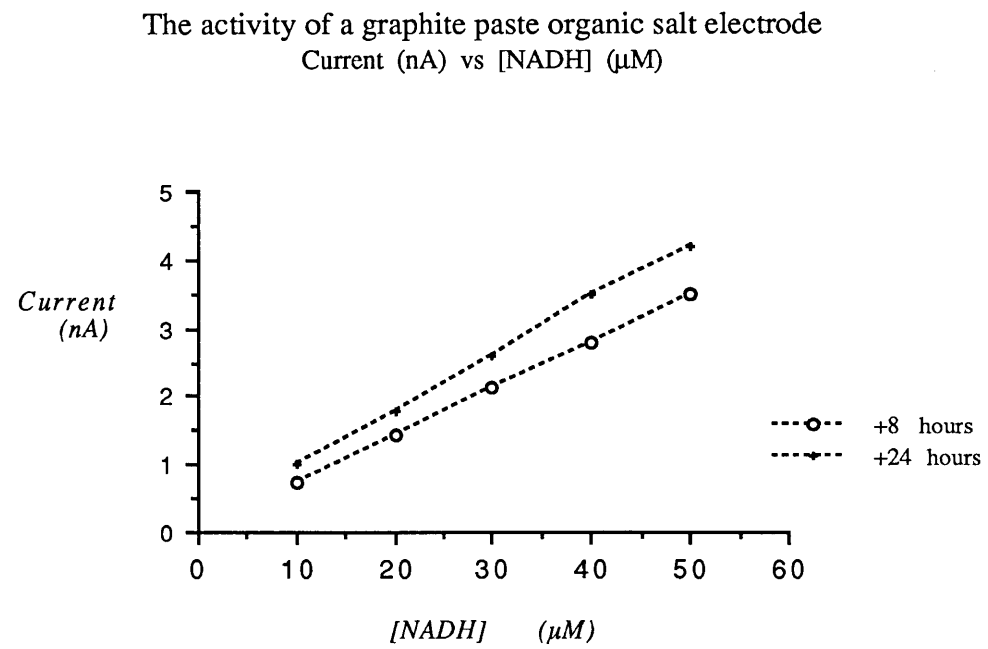


Figure 3.10.b Graph showing the lifetime of a 50 μm NMP^+TCNQ^- silver electrode bound with silicone oil and graphite, responding to NADH at 0 mV (vs Ag/AgCl). The set-up used is described in section 2.5

3.4 The Platinum / peroxide system

As stated earlier in section 1, the main difference in this system is the mediator used. Rather than having an insoluble mediator on the electrode, oxygen is used as the electron shuttle, forming hydrogen peroxide, which is electroactive.

In solution, $\text{Enz-FADH}_2 + O_2 \text{ ----> Enz-FAD} + H_2O_2$

at the electrode +650 mV. $H_2O_2 \text{ ----> } O_2 + 2H^+ + 2e^-$

The advantage of this system is that no delicate mediator has to be applied onto the electrode, and being ubiquitous, oxygen does not have to be added to the system. A bare platinum wire, stripped of its insulation, oxidized peroxide for 3 days at 100% recycling efficiency, and with much greater sensitivity than the TTF^+TCNQ^- system. The electrodes needed no pretreatment, only coating in Nafion™ to repel ascorbate, when used *in vivo*. Their response is demonstrated in figures 3.11 and 3.12, which show both sensitivity and activity respectively.

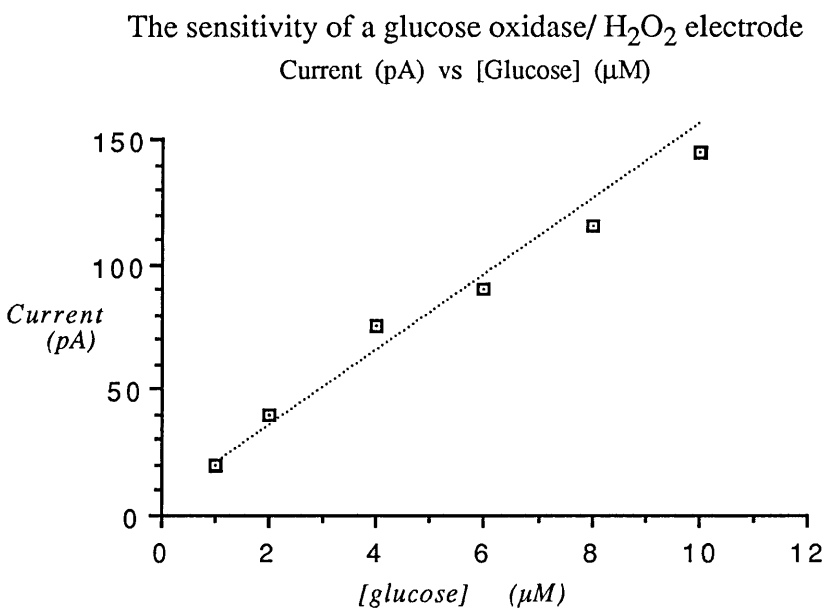


Figure 3.11 Graph showing the sensitivity of a bare 50 µm platinum electrode, responding to glucose at +650 mV (vs Ag/AgCl). The electrode was incorporated into a design **5** probe and filled with glucose oxidase (2 U/µL). The set-up used is described in section 2.5

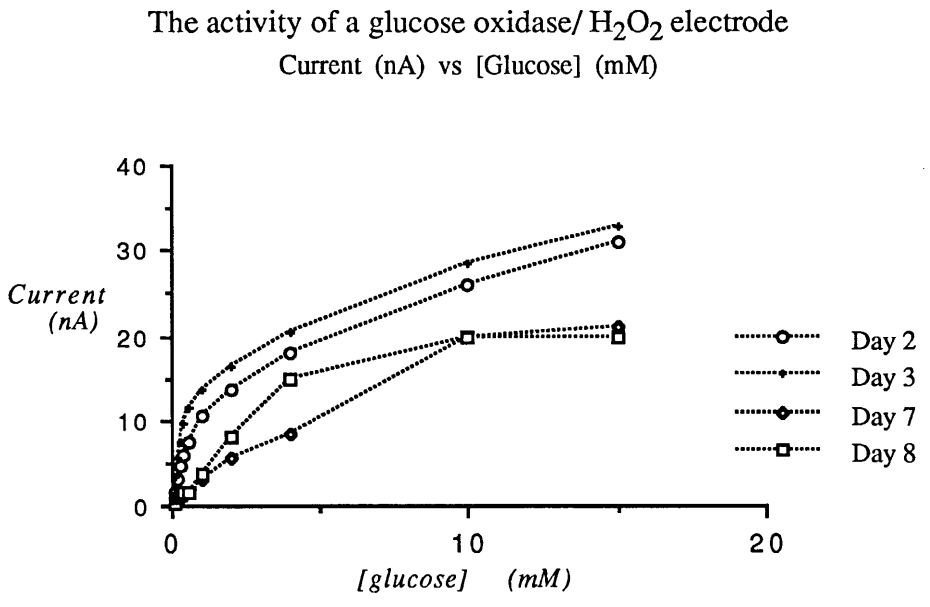


Figure 3.12 Graph showing the activity of a bare 50 µm platinum electrode, responding to glucose at +650 mV (vs Ag/AgCl) over 8 days. The electrode was incorporated into a design **5** probe and filled with glucose oxidase (2U/µL). The set-up used is described in section 2.5

The potential and the size of the platinum electrode were investigated as the high potentials used for the oxidation of H_2O_2 in physiological tissue also oxidize other electroactive moieties present. It would of course be beneficial if the potential of the electrode could be lowered without reducing the sensitivity.

Catalysed systems

The reaction mechanism for mediated enzyme electrodes produces a characteristic pattern when studied with cyclic voltammetry. When a reversible mediator, such as ferrocyanate, is cycled in the absence of enzyme, two peaks are seen as oxidation and reduction of the mediator occurs, figure 3.13a. At low substrate concentrations there is very little turnover of the mediator by the enzyme and consequently a cyclic voltammogram shows only a small change in the anodic current (as the mediator adsorbs to the electrode and is no longer truly reversible, the peaks shift apart). At high substrate concentrations there is a greater turnover of the mediator, which ensures that any mediator oxidized by the electrode is immediately

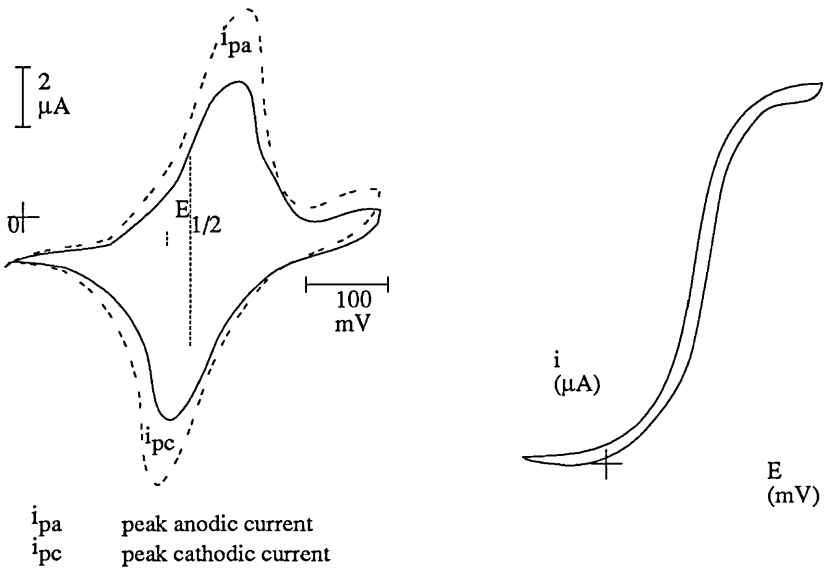


Figure 3.13a & b (**a**, left) cyclic voltammogram for a reversible mediator ferrocyanate on a Nickel electrode, produced by cycling in buffer (——) and NADH (- - -), (**b**, right) a theoretical catalytic curve for an enzyme mediated system

reduced by the enzyme, producing the characteristic 'catalytic current', figure 3.13b. Thus the catalytic wave, for a reversible mediator, has no cathodic peak as the concentration of oxidized mediator is very small. Examples of this are shown below in figures 3.14 & 3.15.

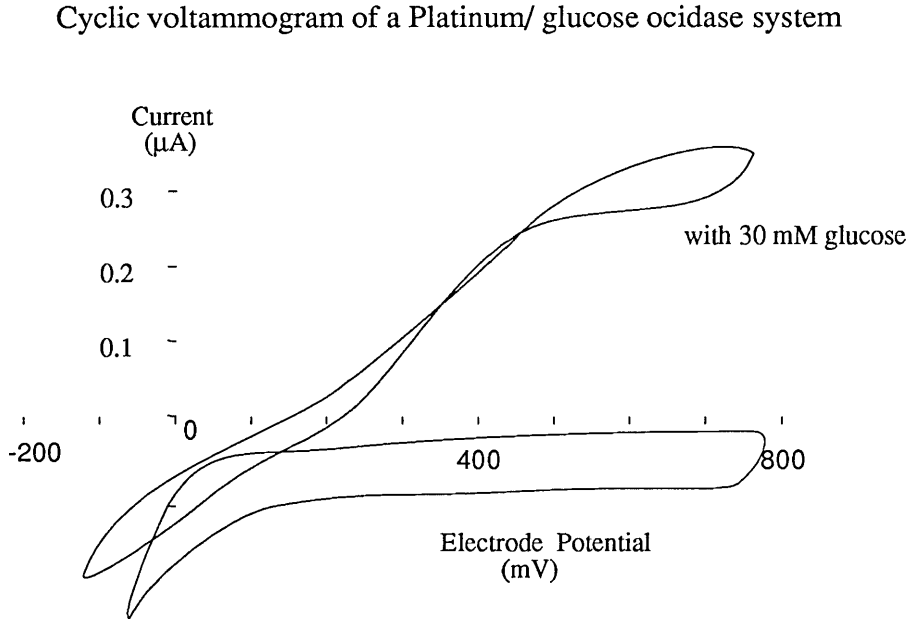


Figure 3.14 A cyclic voltammogram showing a plot of current (nA) vs electrode potential (mV) for probe design **5**, perfused with 0.8 U/µL glucose oxidase and cycled at 20 mV/sec with and without 30 mM glucose. The electrode set-up is described in section 2.5

Cyclic voltammogram of a Platinum/ glutamate oxidase system

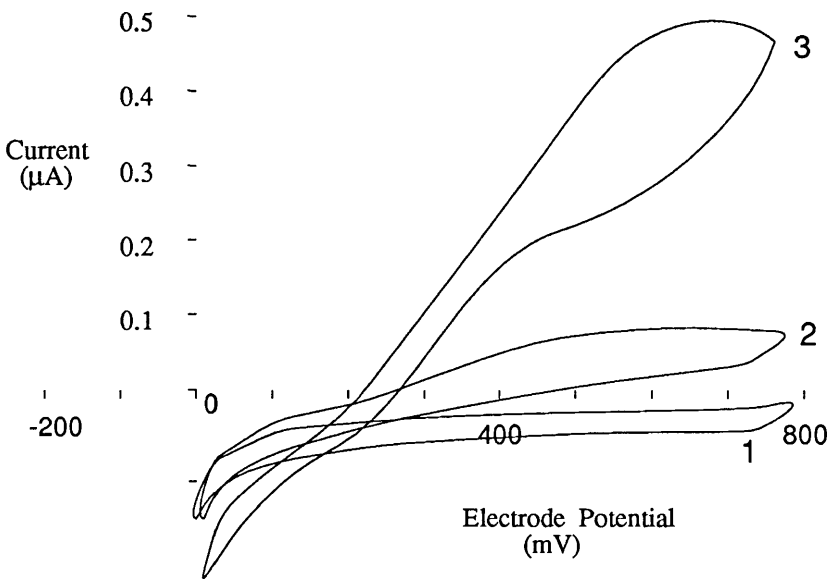


Figure 3.15 A cyclic voltammogram showing a plot of current (nA) vs electrode potential (mV) for probe design **5**, perfused with 0.5 U/μL glutamate oxidase and cycled at 20 mV/sec in (1) buffer, (2) 100μM glutamate and (3) 10 mM glutamate. The electrode set-up is described in section 2.5

The two examples shown above use an irreversible mediator (H_2O_2) and so no reduction peak is seen even without substrate. Figure 3.15 illustrates the difference between low and high substrate. The current (i_L) can be described by equation 3.1 (Nicholson & Shain 1964)

$$\text{Enz-FADH}_2 + O_2 \longrightarrow \text{Enz-FAD} + H_2O_2$$

$$H_2O_2 \xrightarrow{k_{cat}} O_2 + 2H^+ + 2e^-$$

$$i_L = \frac{nFAC_o (D_o k_{cat})^{1/2}}{1 + e^{nF/RT (E - E_{1/2})}} \qquad (3.1)$$

Where k_{cat} is the pseudo first order rate constant, D_o the diffusion coefficient of O_2 ,C_o the concentration of O_2, A the area of the electrode, E & $E_{1/2}$ the electrode potential and the standard reduction potential and n,F,R and T the Faradaic constants. The theory assumes that [O_2] >> [Enzyme]

Electrode potential

Calibrations of the electrode at six potentials, from 150 mV to 650 mV were performed with 4 1 μM aliquots of glutamate to ascertain whether lower potentials could be used for glutamate measurement. The results over an eight day period, shown in figure 3.16, confirm the linear sweep plot and show that the potential could be lowered, reducing the interference and still keeping the sensitivity.

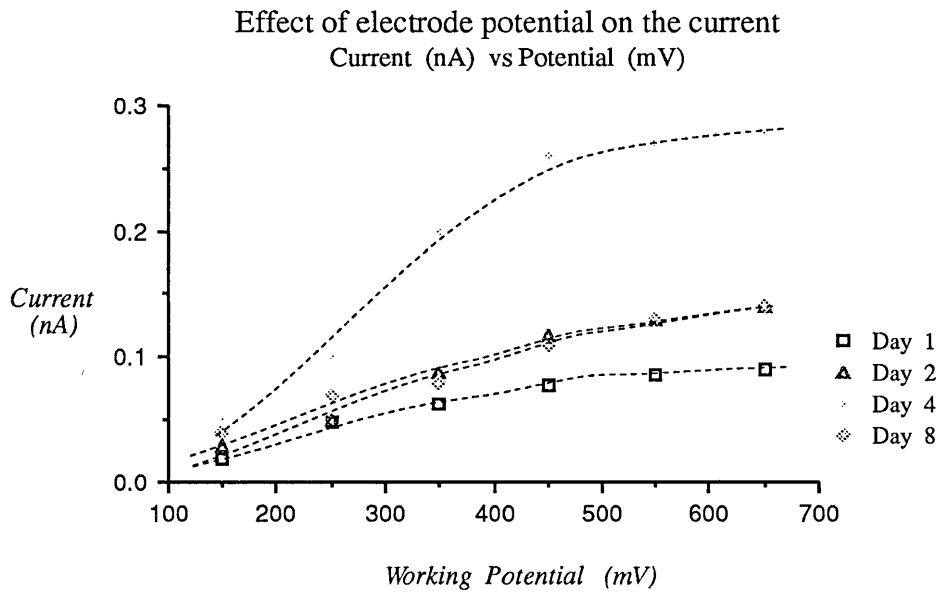


Figure 3.16 Graph showing the dependence of potential on the current for a 50 μm platinum electrode over an 8 day period. The electrode was made into a design 3 probe and filled with 0.5 U/μL glutamate oxidase. The current values are averages for four 1μM glutamate additions. The electrode set-up is described in section 2.5

Electrode size

The electrode size was studied to measure the effect of surface area on the current measured. Equation 3.1 predicts that the current is proportional to the surface area of the electrode and this was investigated using a 'three-in-one' probe. This was a design **3** probe ('U' shaped), which contained three 50 μm platinum electrodes each with different surface areas as well as a silver auxiliary and an Ag/AgCl reference electrode. The smallest, a disk of platinum, had an area of 0.008

mm^2; the second was 2mm of exposed metal with an area of 0.6 mm^2 and the largest had an area of 1.2 mm^2. The platinum electrodes were arranged together in the dialysis tubing, so that all three could be used for calibrations. The probe was filled with 0.5 U/μL of glutamate oxidase and each electrode was calibrated with four 10 μM aliquots of glutamate. The advantages of having three electrodes inside the one probe were that each measurement was done under identical conditions and within a short time of each other . Figure 3.17 shows how the electrode surface area affects the current measured. Table 3.1 shows the ratios averaged for three runs:

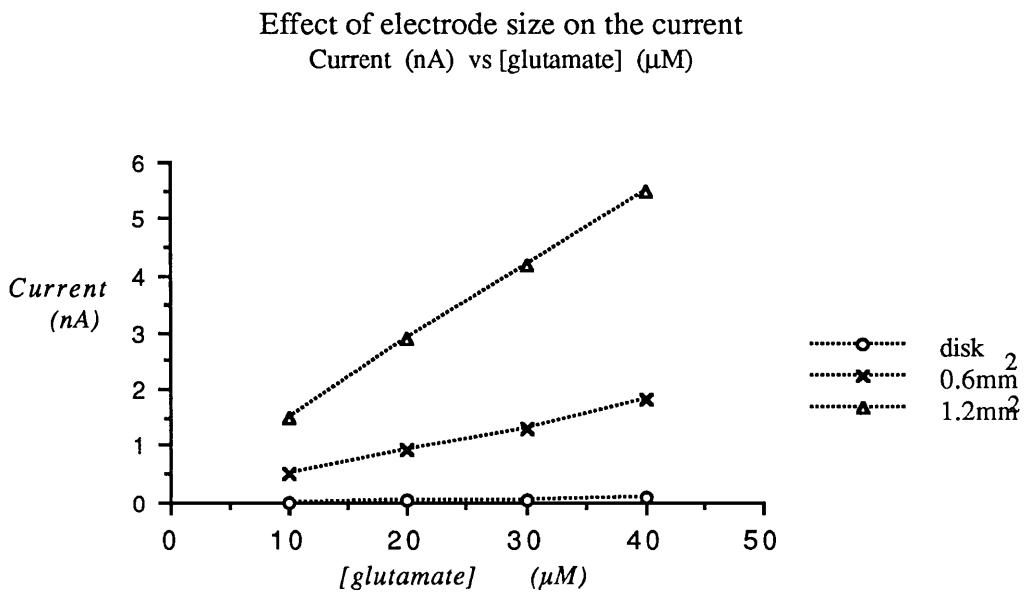


Figure 3.17 Graph showing the dependence of size on the current for a three 50 μm platinum electrodes all of different sizes The electrodes were made into a design 3 probe and filled with 0.5 U/μL glutamate oxidase. The electrode set-up is described in section 2.5

Table 3.1 Comparison of electrode sizes and currents

Surface area mm^2	Current nA	Relative area -	Relative current -
0 .008	0.059	1	1
0.68	2.11	80	35
1.2	8.85	160	150

The graph and the table confirm that the linear relationship (equation 3.1) holds for the platinum peroxide system. The value for the intermediate electrode size is low and this was probably due to reduced surface area, either caused by an air bubble or expansion of the teflon coat once the probe had been assembled. As the currents vary with electrode area and potential, these two experiments suggest the process is 'electrode controlled'.

3.5 Enzyme entrapment

An ideal sensor would have no membrane retaining the enzyme, but have just enzyme adsorbed or immobilized onto the electrode surface. However, with the exception of glucose oxidase, this is rarely possible. Attempts to immobilize glutamate dehydrogenase proved, in the main, unsuccessful, not only because some of the enzyme's active groups have to be well protected during immobilization (Havekes *et al* 1974), but also because the immobilization supports proved unstable and hard to attach on organic salt-based micro-electrodes (the enzyme has been immobilized on carbon fibres, Kuhr 1991). Having external teflon sides gave no possible means of attachment for the polymer and cross-linker. Thus any support used must either be mixed in with the organic salt or coated on the electrode surface.

Three different supports, which could be mixed in with the organic salt were considered: oxidized graphite, amino methyl polystyrene and a 50-50 co-polymer of polystyrene and maleate. It was planned that these could act as both organic salt binders and immobilization supports (Cass *et al* 1984 immobilized glucose oxidase to the carbonyl groups of oxidized graphite). However, as polystyrene was found to be a poor binder, as previously shown in section 3.1, the two hydrophobic polymers were not tried. Glutamate dehydrogenase was immobilized on oxidized graphite, using the method described by Cass and his colleagues, but the process was not successful probably because of inadequate protection.

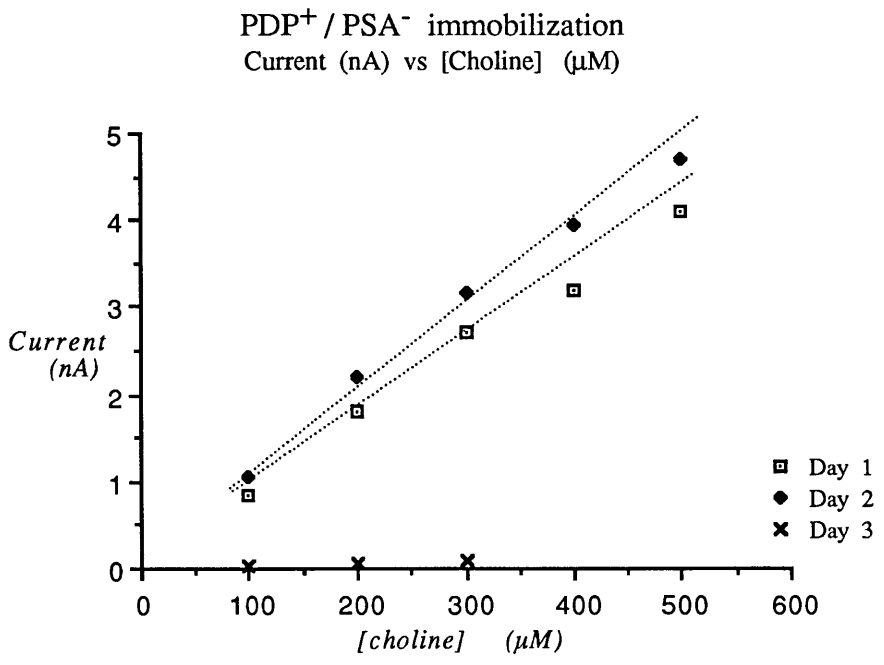


Figure 3.18 Graph showing the activity of a tightly-packed $TTF^{+}TCNQ^{-}$ electrode with choline oxidase immobilized by $PDP^{+}PSA^{-}$ polymerization, section 2.4. The electrode was held at +0 mV (vs Ag/AgCl). The set-up used is described in section 2.5

Only limited success was achieved by coating enzyme-bound polymer on the organic salt surface. Using PDP^{+} / PSA^{-} and polyacrylamide, electrodes were built that were active for a couple of days. Figures 3.18 & 3.19 show the activies of PDP^{+}/PSA^{-} and polyacrylamide immobilized glutamate dehydrogenase respectively.

As these figures show, the reproducibility is good but the life-time is fairly short, about one day. In both cases the problem that effected these electrodes was that the immobilized films lifted off the electrode surface after 24 hours of testing. The teflon sides of the electrode provide no rough edges for the film to seal onto and the electrode surface was obviously too smooth and fragile as well.

It can be seen that the immobilization of enzymes using polymer films was unsuitable for *in vivo* electrodes and meant some type of membrane was required to entrap the enzyme or enzymes. This led to the production of the probes, described in section three of chapter two.

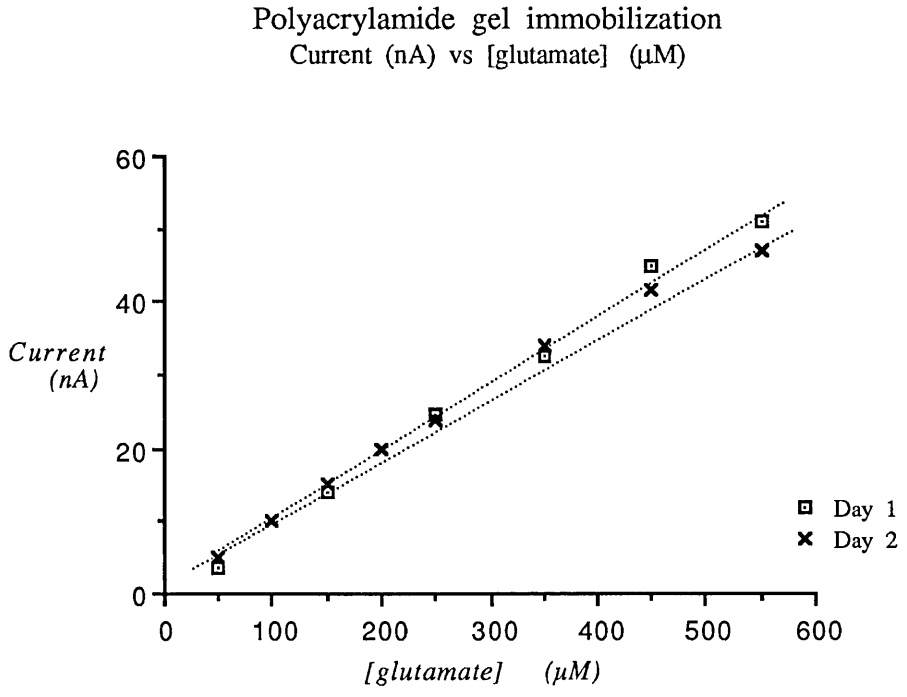


Figure 3.19 Graph showing the activity of a tightly-packed $TTF^{+}TCNQ^{-}$ electrode with glutamate dehydrogenase immobilized by polyacrylamide gel polymerization, section 2.4. The electrode was held at +0mV (vs Ag/AgCl). The set-up used is described in section 2.5

3.6 The measurement of glutamate with the microprobes

The first of this study's *in vivo* probes used glutamate dehydrogenase with NMP^{+} $TCNQ^{-}$ electroplated onto the electrode. As this technique was unsuitable for experimental use, due to the short lifetimes of these electrodes, the *in vivo* work was stopped until a better system was found. The progression through organic salt paste to platinum electrodes and the accompanying changes in probe design are set out below.

The first probe (design **1**), shown on pages 74 & 75, was designed as a test for the suitability of dialysis fibre as a membrane and was obviously too cumbersome for much use. Figure 3.20 illustrates the reproducibility achieved for the probe using glutamate dehydrogenase, 10 mM NAD^{+} and 0.5mM ADP. The

sensitivity was good, reaching as low as 20 μM resolution. However the life-time of the electrode was very short and this was once again assumed to be due to the absorption of water by the electroplated organic salt.

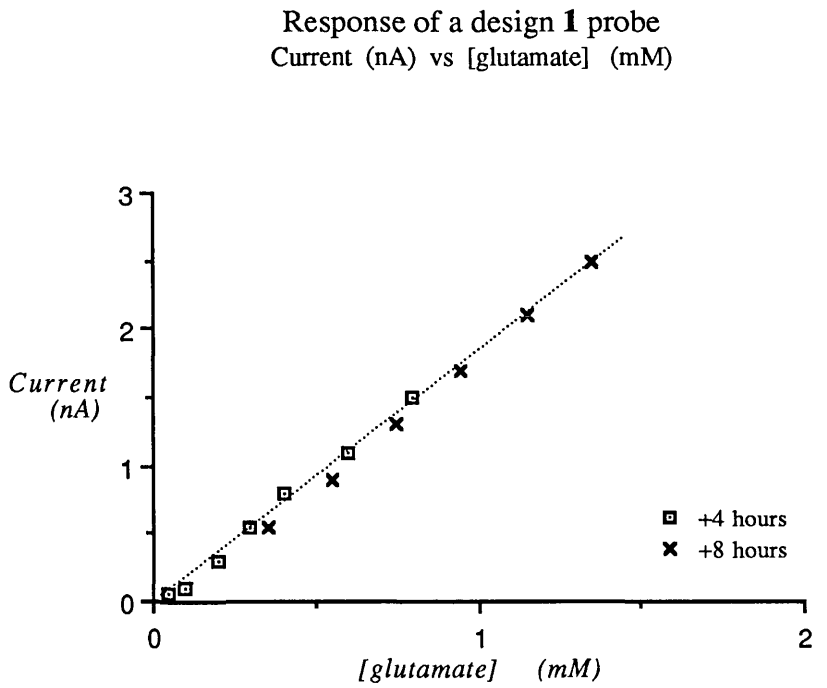


Figure 3.20 Graph showing the lifetime of a design 1 probe with an electroplated NMP^+TCNQ^- electrode perfused with glutamate dehydrogenase, 10mM NAD^+ and 0.5mM ADP. The electrode was held at +0 mV (vs Ag/AgCl). The set-up used is described in section 2.5

The second design (**2**), shown on pages 75 &76, was more practical for handling and testing as it was a pointed probe rather than a long bulky one. The response for this design is shown in figure 3.21, where it can be seen that the response is very poor, probably because the electroplated NMP^+TCNQ^- is already deteriorating. The reason for this poor performance compared with the electrode in design **1**, figure 3.20, is that the metal used was 50 μm silver wire, 33% thinner than the wire used in probe **1** , which appears to decrease the activity. (There was a similar drop in activity going from 254 μm to 75 μm silver wire, figures 3.5 & 3.6)

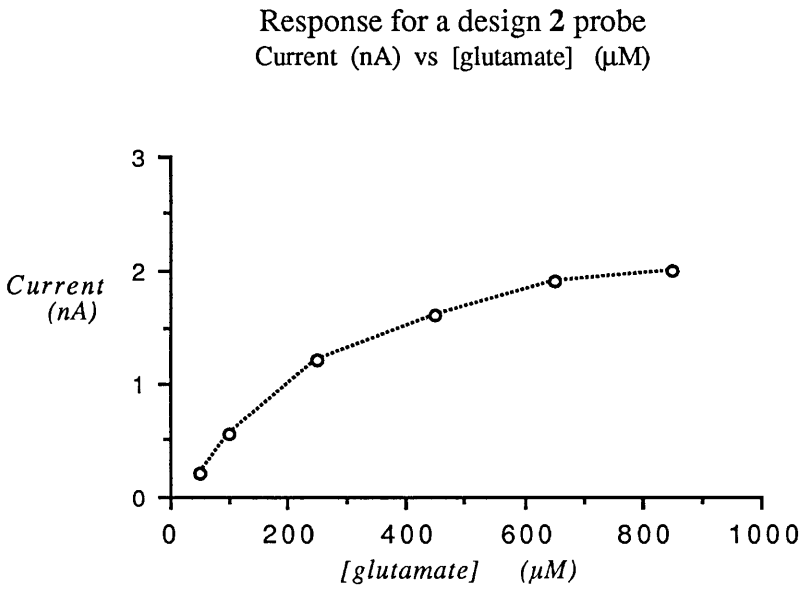


Figure 3.21 Graph showing the response of a design **2** probe with an electroplated NMP^+TCNQ^- electrode perfused with glutamate dehydrogenase, 10mM NAD^+ and 0.5mM ADP. The electrode was held at +0 mV (vs Ag/AgCl). The set-up used is described in section 2.5

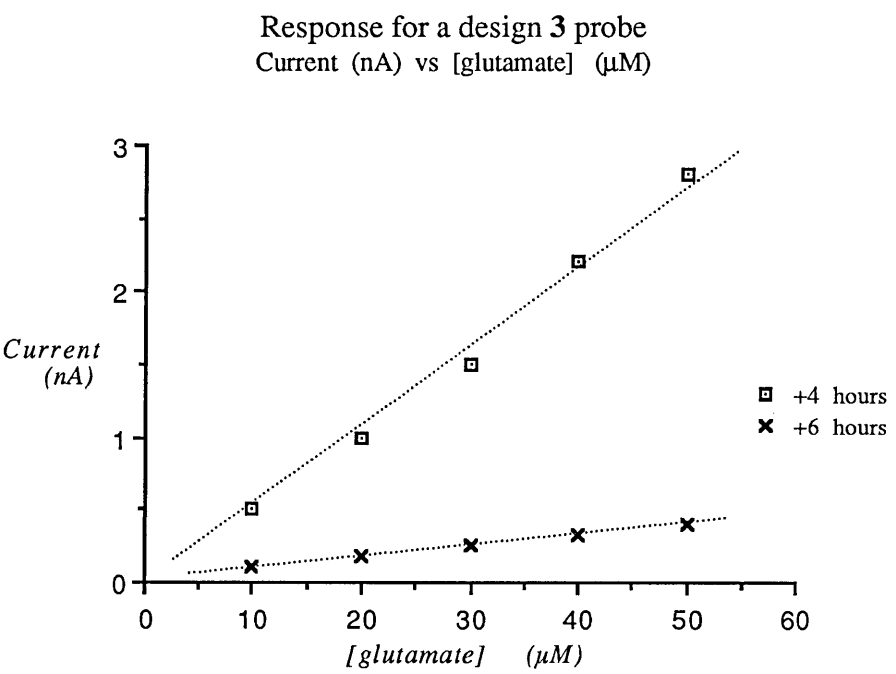


Figure 3.22 Graph showing the lifetime of a design **3** probe with an electroplated NMP^+TCNQ^- electrode perfused with glutamate dehydrogenase, 10mM NAD^+ and 0.5mM ADP. The electrode was held at +0 mV (vs Ag/AgCl). The set-up used is described in section 2.5

Design **3**, shown on pages 78 & 79, had similar difficulties as the wire used was 50 μm silver. The response is shown in figure 3.22, with the response to glutamate dying off after the first few hours of testing. An attempt to increase the electrode life-time was made using a coat of nafion to try and repel the electrolyte. Figure 3.23 shows that this technique had limited success, improving the activity for 6 hours or so. The current was also reduced due to repulsion of glutamate by the nafion.

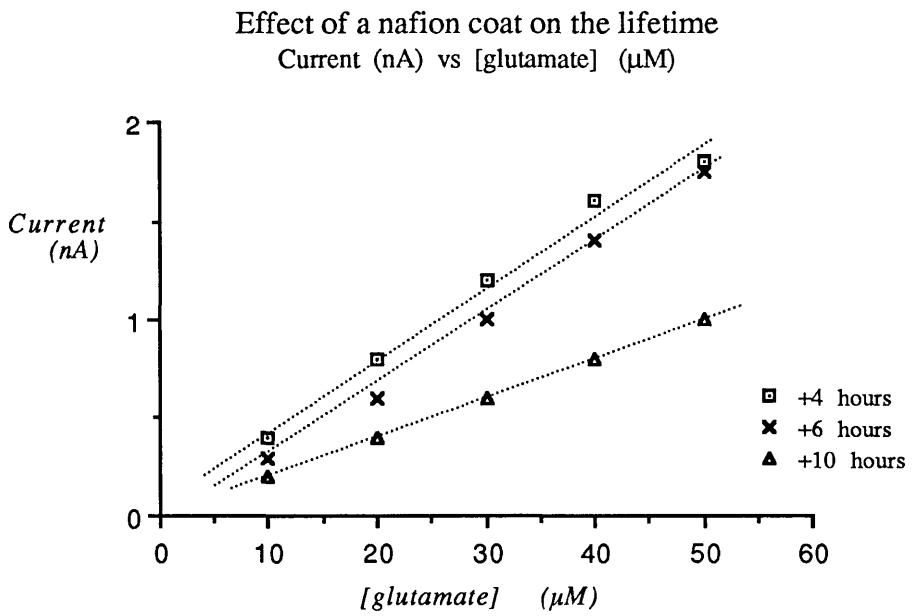


Figure 3.23 Graph showing the lifetime of a design **3** probe with an electroplated NMP^+TCNQ^- electrode, with one coat of nafion, perfused with glutamate dehydrogenase, 10mM NAD^+ and 0.5mM ADP. The electrode was held at +0 mV (vs Ag/AgCl). The set-up used is described in section 2.5

As the electroplating would not work over a sufficient period, organic salt paste electrodes were used next. Also, in order to overcome some of the problems encountered with the dehydrogenase enzyme, in particular the diffusion of NAD^+ into the surrounding environment, glutamate oxidase was tried in its place. Figure 3.24 shows a profile of a design **4** probe, shown on pages 80 & 81, with a 25 μm copper electrode coated in NMP^+TCNQ^- paste (graphite and silicone oil) perfused with glutamate oxidase.

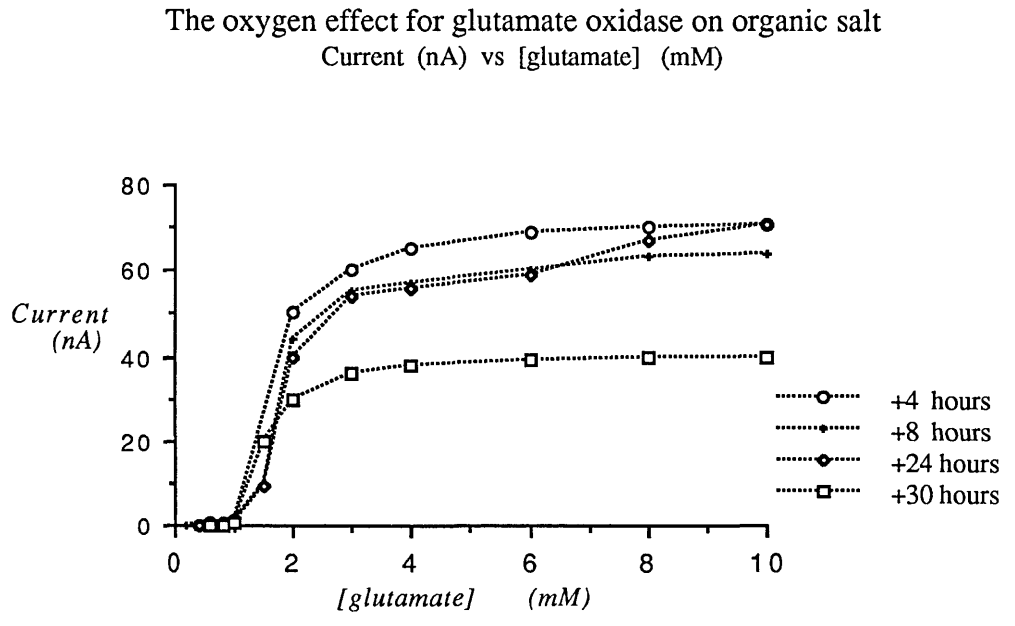


Figure 3.24 Graph showing the lifetime of a design **4** probe with an organic paste NMP^+TCNQ^- electrode, perfused with 2U/μL glutamate dehydrogenase. The electrode was held at +0 mV (vs Ag/AgCl). The set-up used is described in section 2.5

A large 'O_2' effect can be seen with this arrangement. The effect is not seen with glucose oxidase indicating that the problem probably lies in the position of the prosthetic flavin group within the enzyme. A deeply burried $FADH_2$ would be oxidized more easily by oxygen than a bulky organic mediator. Figure 3.25 shows the sensitivity achieved with the probe. The resolution of the system reached the 10μM glutamate level, however this was still not low enough for the 1-2 μM changes expected under physiological conditions. The lifetime of the sensor was lower than that expected for an organic salt paste electrode, as the activity began to drop off after 30 hours use. This may be due to the diameter of the electrode. It was seen in the electroplated systems that as the electrode size decreased so did the life-time. The same may be applied here. The problems encountered with the organic paste/ oxidase probes meant another mediated electrode pathway was required.

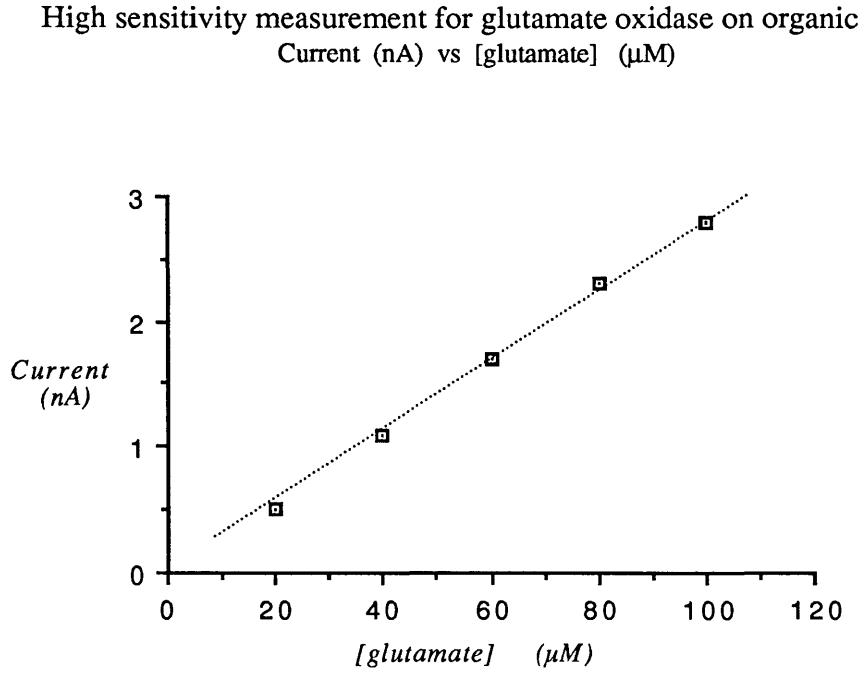


Figure 3.25 Graph showing the lifetime of a design **4** probe with an organic paste NMP^+TCNQ^- electrode, perfused with 2 U/μL glutamate oxidase. The electrode was held at +0 mV (vs Ag/AgCl). The set-up used is described in section 2.5

The use of platinum to measure H_2O_2 produced by glutamate oxidase was very encouraging and a 100-fold increase in the detection limit was achieved, figure 3.26. The activity was also improved with probes lasting for a week. The response time was very fast, even for a membrane electrode, typically 90% in 5 sec. This was achieved because the electrode was pushed close to the edge of the membrane by the 140 μm silica tubing, reducing the diffusion distance.

The work done in the section, 3.4, showed that with 0.5 U/μL of glutamate oxidase in the probe, the current was controlled by the size and potential of the electrode. The dependence of the enzyme concentration was studied to see if that became rate controlling at low concentrations. With a design **5** probe, three different enzyme concentrations 1, 0.1 and 0.01 U/μL of glutamate oxidase were tested and the results are shown in figure 3.27. There was a small drop in the activity of the 0.01U/μL electrode, suggesting that the enzyme becomes rate limiting below 0.1 U/μL.

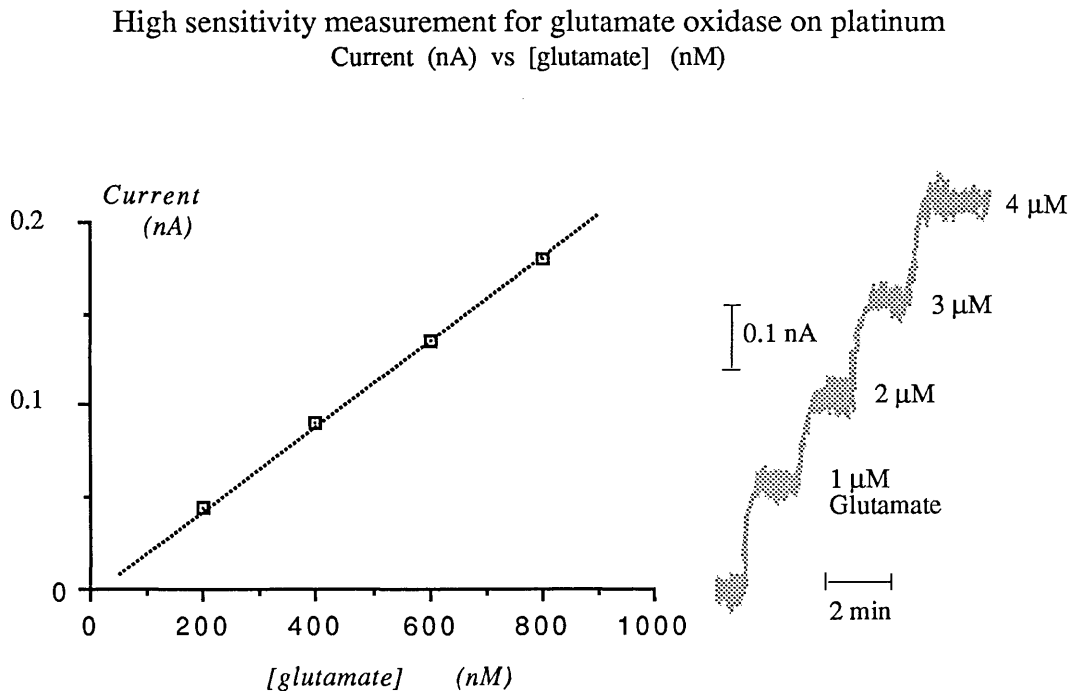


Figure 3.26a Graph showing the sensitivity of a design **5** probe with a 50 µm platinum electrode, perfused with 2U/µL glutamate oxidase. The electrode was held at +650 mV (vs Ag/AgCl). The set-up used is described in section 2.5
Figure 3.26b Response curve showing current (nA) vs time (min)

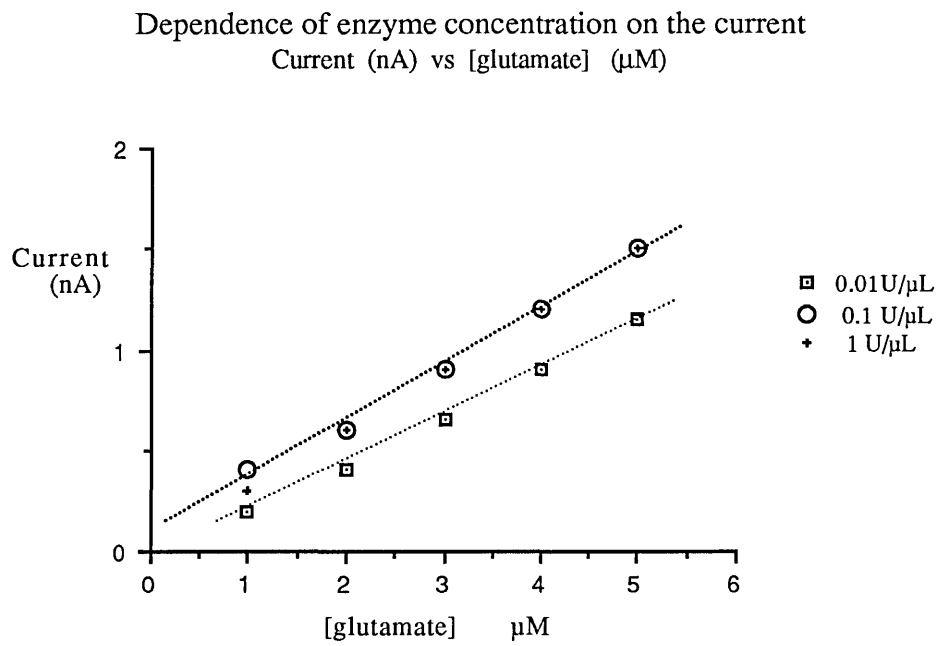


Figure 3.27 Graph showing the dependence of enzyme concentration on the current for a design **5** probe with a 50 µm platinum electrode, perfused with three glutamate oxidase concentrations. The electrode was held at +650 mV (vs Ag/AgCl). The set-up used is described in section 2.5

This was checked by calibrating a glutamate electrode with a low enzyme concentration (0.005U/μL) over its full range and analysing the data with both a 'Hanes' and a 'rho' plot. The 'Hanes' plot, (used by Albery *et al* 1986), ([S]/j) vs [S], figure 3.28, shows a flat region at low substrate concentration, implying membrane control.

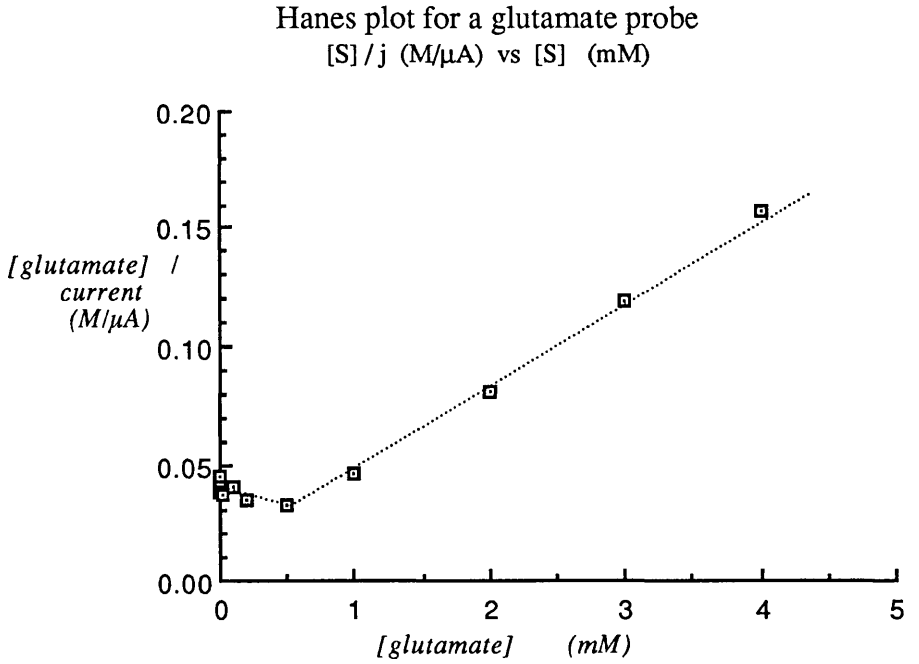


Figure 3.28 Graph showing the Hanes plot for a design **5** probe with a 50 μm platinum electrode, perfused with 0.005 U/μL glutamate oxidase. The electrode was held at +650 mV (vs Ag/AgCl). The set-up used is described in section 2.5

The 'rho' plot, described by Albery and Bartlett (1985), is a complex equation for analysing the rate controlling processes. From the Hanes plot the reciprocal of the 'y' intercept, $[S_\infty/i]_0$, gives a value for k_{ME}', the heterogeneous rate constant for the electrochemical reaction. The value 'ρ' can be calculated as:

$$\rho = (s_\infty / i)^{-1} / k'_{ME} \quad .$$

The rho plot is then obtained by plotting:

$$(\rho^{-1} - 1) / S_{\infty} \quad \text{against} \quad \rho$$

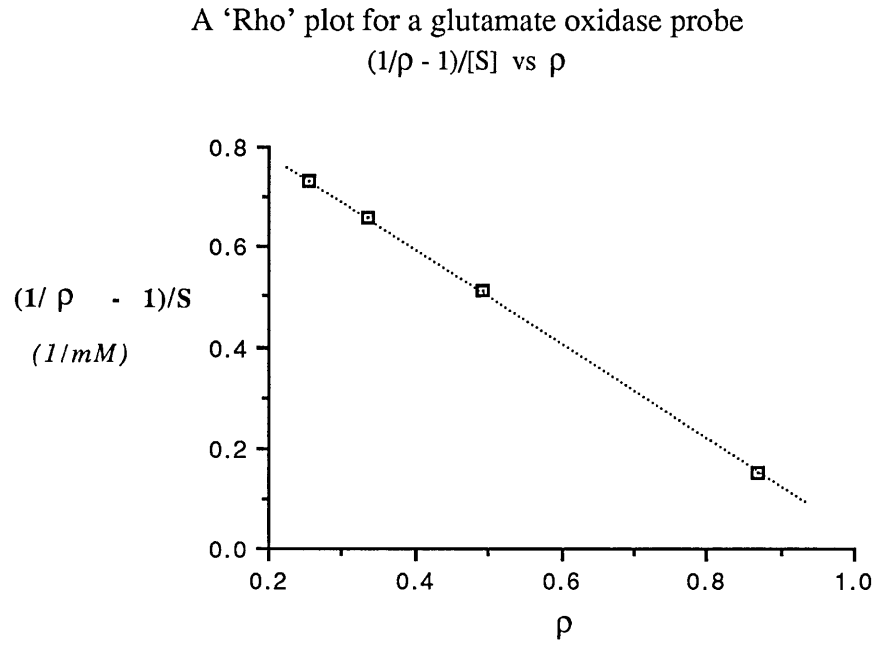


Figure 3.29 Graph showing a'rho' plot for a design **5** probe with a 50 μm platinum electrode, perfused with 0.005 U/μL glutamate oxidase. The electrode was held at +650 mV (vs Ag/AgCl). The set-up used is described in section 2.5. The numerical values for the y intercept ($1/K_{ME}$) and the x intercept (k_S'/k_{ME}') are 0.98 and 1.03 respectively.

K_{ME} can be calculated from the reciprocal of the y intercept and k'_S/k'_{ME} from the ρ intercept. The plot above, figure3.29, gives:

K_{ME} as 1.02 mM and k'_S/k'_{ME} as 1.03.

As $k'_S \approx k'_{ME}$, it confirms the Hanes plot in that the process is membrane controlled. This contradicts the electrode size and potential results on pages 102 & 103, which support oxidation at the electrode as the rate limiting step and these two plots suggest that electrode area lies very close to boundary between membrane and electrode control, giving this anomaly.

Substrate Specificity

The selectivity of the probe is very important for physiological sampling and the enzyme is obviously the key controller of this. Glutamate oxidase is quoted by Kusakabe *et al* (1983) to be highly specific, reacting poorly with aspartate (0.6% of glutamate response). A design **5** glutamate probe was tested and found to be insensitive to the L-amino acids, except to glutamine and tyrosine and to a minor extent aspartate, as shown in table 3.2. Tyrosine is electroactive (Crespi 1990) and was oxidized by the electrode rather than by the enzyme. As physiological levels of tyrosine are very low it does not affect *in vivo* measurements.

It was the amino acid glutamine that presented a problem. When it was added to give a bulk concentration of 20 μM, a current was produced which was ≈ 60% of the glutamate response. Further additions showed this activity to be saturated at 60-80μM,suggesting that the enzyme preparation had a small glutamine oxidase impurity, figure 3.30. This glutamine activity would create serious problems for glutamate measurement in the brain, however the basal glutamine levels in the ECF have been measured at 195μM in the hippocampus (Lerma *et al* 1985) and 122 μM in the stratum (Young & Bradford 1986) which would saturate this putative glutamine enzyme, abolishing any effect it may have other than to increase the background current.

Table 3.2 Selectivity of the glutamate probe

Substrate	Activity (%)
L-glutamate	100
L-aspartate	1
L-glutamine (0-60μM)	60
L-tyrosine	50
arginine, isoleucine, histidine, phenyl alanine alanine, valine, , lysine, HO-proline, leucine methionine, serine, cysteine, cystine, asparagine threonine,glycine, proline, tryptophan,	0

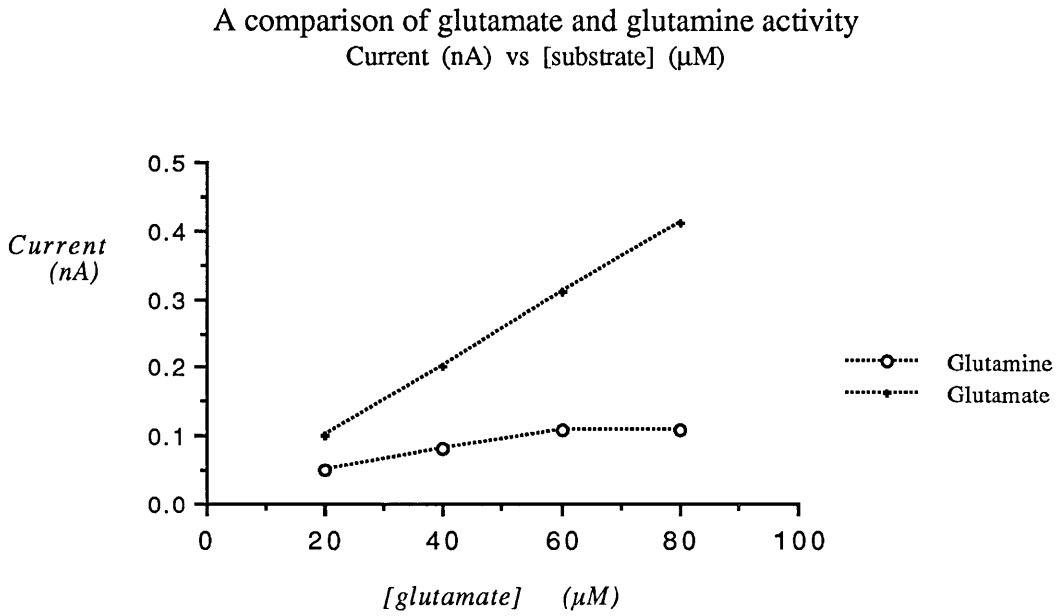


Figure 3.30 Graph comparing the sensitivity of the enzyme to glutamate and glutamine. The design **5** probe with a 50 µm platinum electrode was perfused with 0.5 U/µL glutamate oxidase. The electrode was held at +650 mV (vs Ag/AgCl). The set-up used is described in section 2.5

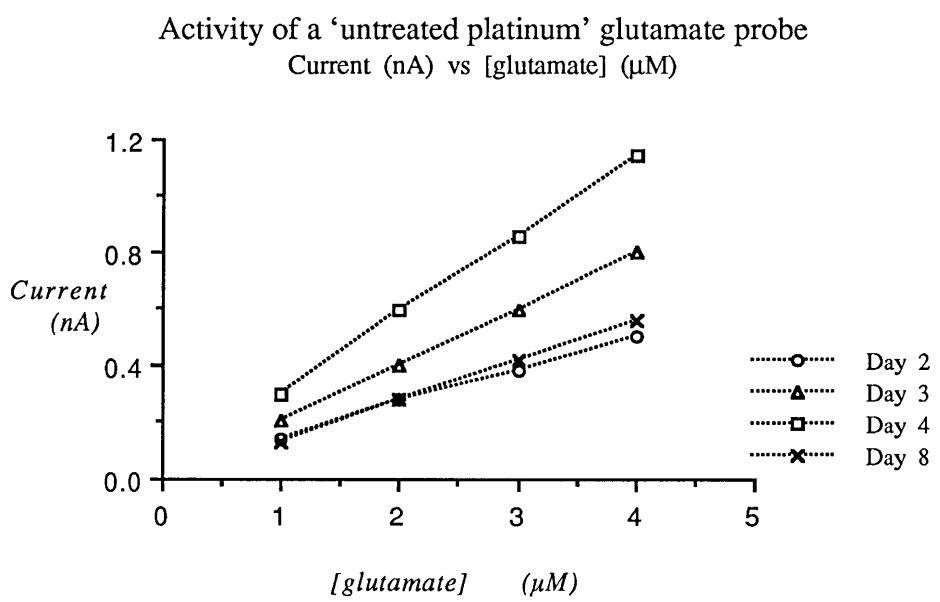


Figure 3.31 Graph showing the lifetime of a design **5** probe with a 50 µm untreated platinum electrode, perfused with 2 U/µL glutamate oxidase. The electrode was held at +650 mV (vs Ag/AgCl). The set-up used is described in section 2.5

The lifetime of bare platinum electrodes perfused with glutamate oxidase was similar to the glucose probes, lasting over a week with good activity., figure 3.31. However, when the electrode was treated with nafion both the sensitivity and the lifetime of the probe decreased; reasons for this are discussed in section 3.9. Typically a probe with 10 nafion coats would last 3 days at 100% activity.

3.8 The measurement of acetyl choline

Acetyl choline can be measured using two enzymes, acetyl choline esterase and choline oxidase with and without mediation. The best result was achieved with a bare platinum electrode, identical to the glutamate system. The sensitivity was excellent with 100nM ACh being measured, figure 3.32, and the lifetime was as good as the glutamate probes. The first ACh probe to be made was tested for three days and increased with activity on each successive day.

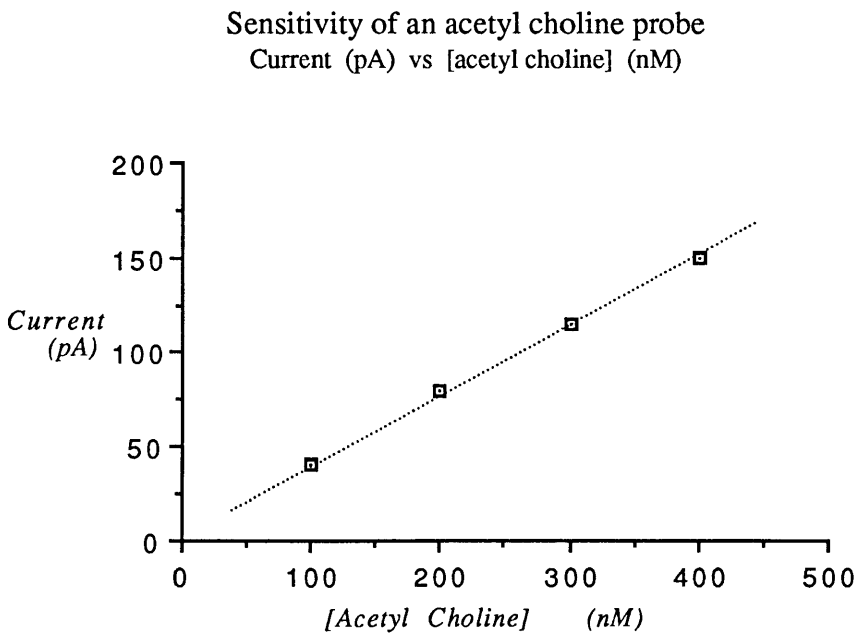


Figure 3.32 Graph showing the sensitivity of an acetyl choline. The design **5** probe with a 50 µm untreated platinum electrode was perfused with 100 U/µL acetyl choline esterase and 2 U/µL choline oxidase. The electrode was held at +650 mV (vs Ag/AgCl). The set-up used is described in section 2.5

3.9 Removal of Interference

Along with miniaturization, interference from other electroactive metabolites and neurotransmitters is the biggest problem affecting *in vivo* neurophysiological recording. The two main techniques used for removing interference were coating the electrode in nafion and the addition of ascorbate oxidase into the perfusion solution. Nafion repels negatively charged species from the working electrode, in principal removing interference from ascorbate, uric acid, DOPAC and HVA.

However to be effective, the nafion 'membrane' was too thick, reducing the glutamate generated signal, because it provided a physical barrier to the H_2O_2 as well as to the ascorbate. Figure 3.33 shows the response for an electrode with different coatings of nafion.

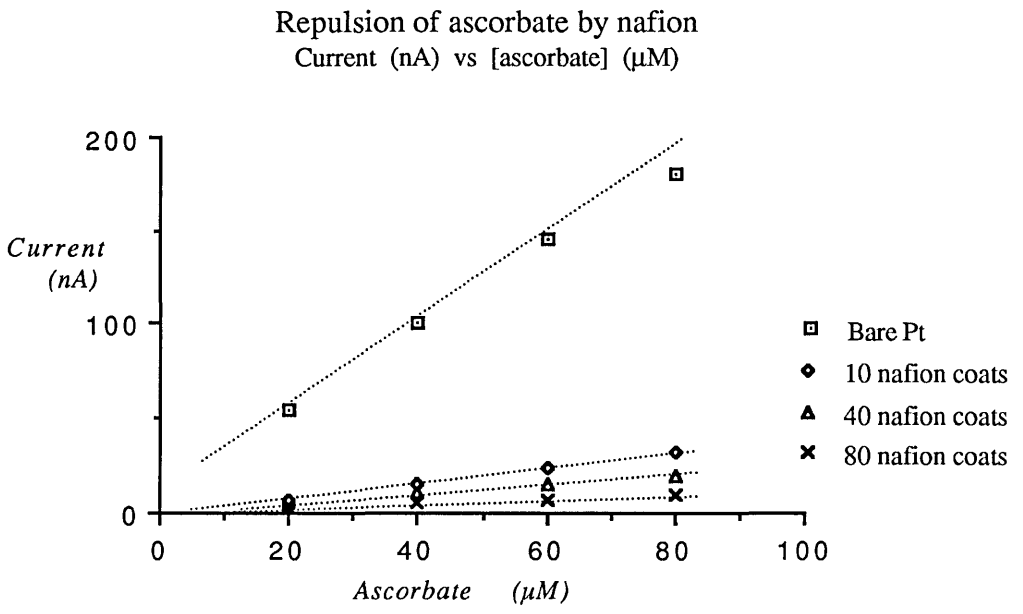


Figure 3.33 Graph showing the effect of coating a platinum wire in nafion. The electrode was held at +650 mV (vs Ag/AgCl). The set-up used is described in section 2.5

Figure 3.34 illustrates the effect 15 nafion coats has on the glutamate response. The current was reduced by a factor of 6, which became significant when the probes were required to measure glutamate concentration changes in the μM region, i.e. close to the highest sensitivity.

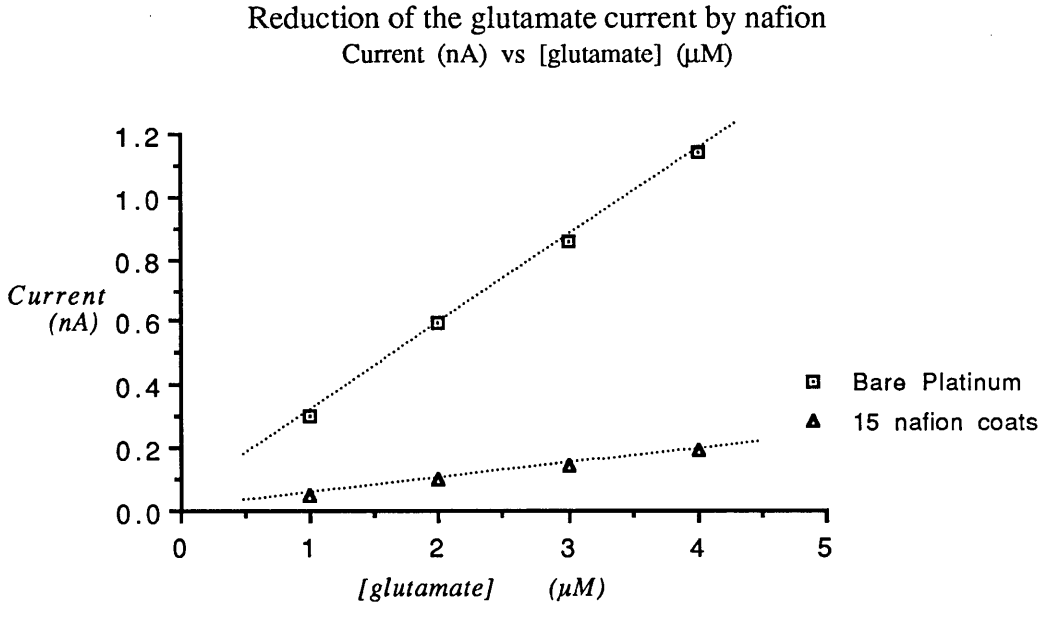


Figure 3.34 Graph showing the reduction in the glutamate current with nafion coating a platinum wire. The electrode was held at +650 mV (vs Ag/AgCl). A design 5 probe was used with 2 U/μL glutamate oxidase. The set-up used is described in section 2.5

The other problem with nafion was that it increased the 'background noise' of the electrode, reducing the apparent sensitivity. Nafion coated electrodes would begin to lose their high sensitivity after three days. This may have been due to positively charged proteinaceous matter adsorbing onto the nafion surface.

Ascorbate oxidase can be used for eliminating ascorbate as it produces H_2O rather than H_2O_2, because its electron accepting centre in the protein is a copper ion not a flavin, and so catalyses the reaction via a different mechanism. Had it produced H_2O_2 , it would obviously have defeated the purpose of using it to eliminate ascorbate. The enzyme's effect can be seen in figure 3.35.

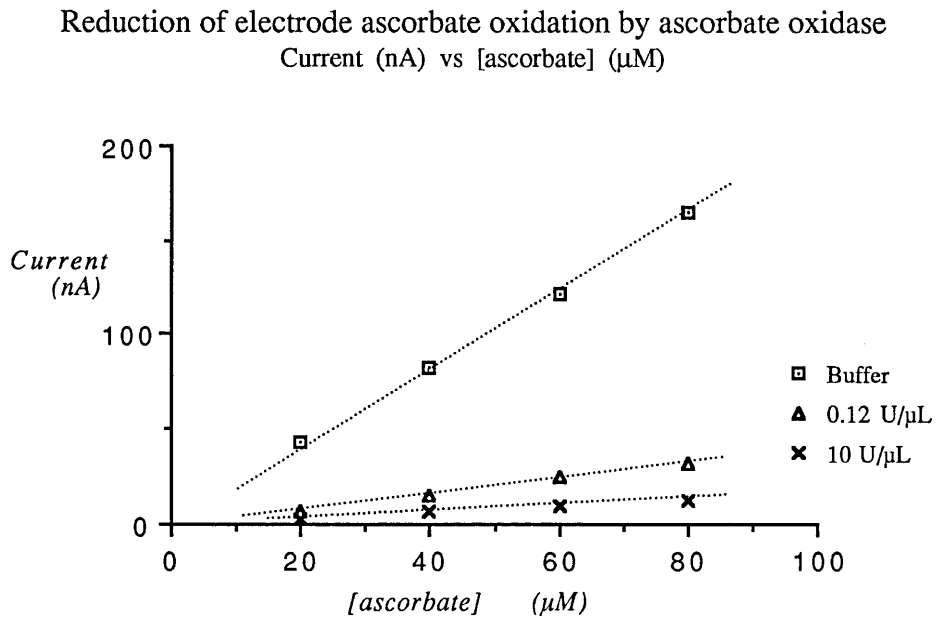


Figure 3.35 Graph showing the effect of ascorbate oxidase on the electrode interference. A design 3 probe was perfused with 0.12 and 10 U/µL ascorbate oxidase. The electrode was held at +650 mV (vs Ag/AgCl). The set-up used is described in section 2.5

The results for the two techniques, nafion coating and addition of ascorbate oxidase, show that together they can provide a very efficient interference trap. However the reduction in glutamate signal means that an optimum coating of nafion has to be reached, depending on the experiment performed.

Chapter Four

The measurement of glutamate in the striatum

4.1 Striatal neural pathways

The optimized probe (design **5**), described in chapters two and three, was used for measurements of *in vivo* levels of glutamate in the rat brain during behavioural responses. As the introduction states, the striatum is part of the basal ganglia, one of whose functions is the control and regulation of motor activity. The basal ganglia-thalamocortical pathways connecting the striatum and the other brain areas are depicted in figure 4.1. The figure shows the 'direct' pathway from the

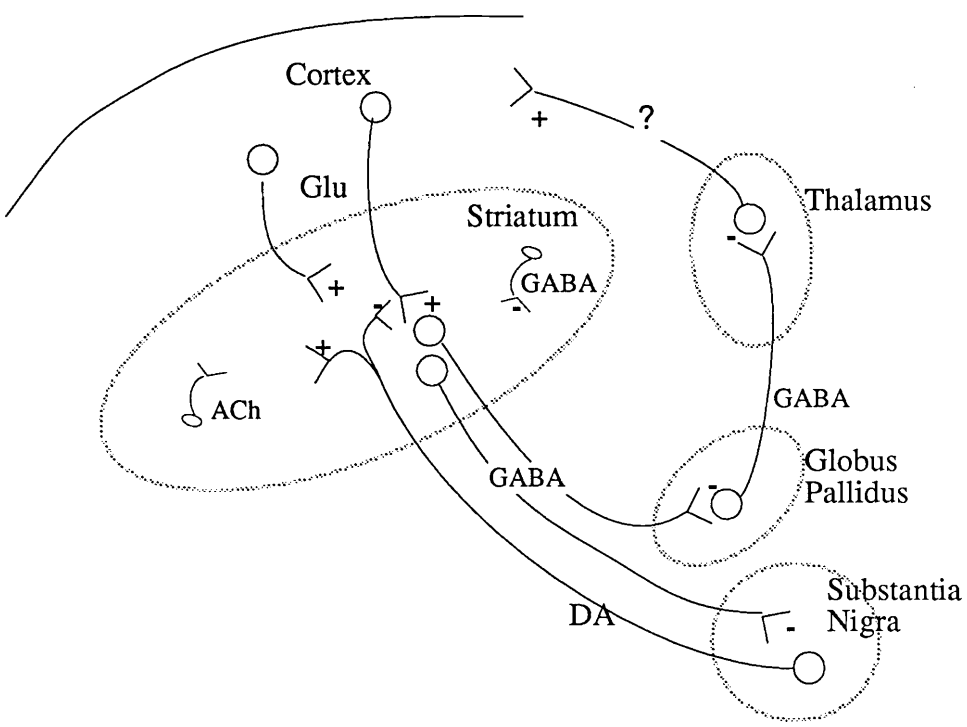


Figure 4.1 The basal ganglia-thalamocortical pathway (adapted from Angevine & Cotman1981, Alexander & Crutcher 1990 and Graybiel 1990)

striatum to the basal ganglia output nuclei (there is also an parallel 'indirect' path, not shown in figure 4.1, through the exterior globus pallidus and the subthalamic nucleus). Both the pathways receive a glutamatergic input from the cortex (Girault *et al* 1990) and the passage of information proceeds through the globus pallidus and substantia nigra to the thalamus via GABAergic (and substance P) neurons. The loop is completed by excitatory connections back into the cortex (Alexander & Crutcher 1990 and Graybiel 1990), providing a means of modulating the motor activity and preventing overload, before information is sent off to the brain stem and spinal chord.

In the striatum a lot of work has focussed on the relationship between glutamate and dopamine (reviewed by Carlsson & Carlsson 1990). As figure 4.1 shows dopamine has both an excitatory and inhibitory role in the striatum, with possible presynaptic mediation of glutamate release by dopamine D_2 receptors. Other work has examined the role of glutamate regulation of dopamine release by N-methyl D-aspartate receptors on the dopaminergic terminals (Fillenz *et al* 1991, Wheeler 1991 and Abercrombie & Keefe 1991)

With regard to motor activity, Fillenz and her colleagues have shown that behavioural motor activities such as chewing and sniffing releases dopamine (DA) (Wheeler 1991), ascorbate (Boutelle *et al* 1989) and 5-hydroxytryptamine (5-HT, Pei *et al* 1990) in the striatum. The new glutamate probe provided the next step forward in real-time analysis of the neurotransmitter relationships.

4.2 Probe implantation

For each experiment, a calibrated probe was implanted into the right dorsal striatum of the male rat, using the following method: a male Sprague/ Dawley rat, weighing between 275 and 325 g, was anaesthetized with 10% chloral hydrate. The

skull was exposed and two skull screws (Clark Electromedical) were fixed to the lower skull plates. A 2 mm hole was drilled through the skull and the dura carefully pierced. The probe was stereotactically implanted into the right striatum in the following position +1.0 mm Anterior-Posterior, +4.5 mm Lateral and -7.5 mm Dorsal-Ventrally to Bregma. Although the animal was earthed through the reference electrode, it was necessary to incorporate an additional earth, a 250 μm chloridized silver wire, which was implanted into the outer cortex just under the dura. This earth removed any electrical spikes that were caused by touching or handling the animal. Once implanted, the probe was secured to the skull and its screws by dental acrylate (Plastics One) and the rat was left to recover overnight. Figure 4.2 below shows a typical implantation.

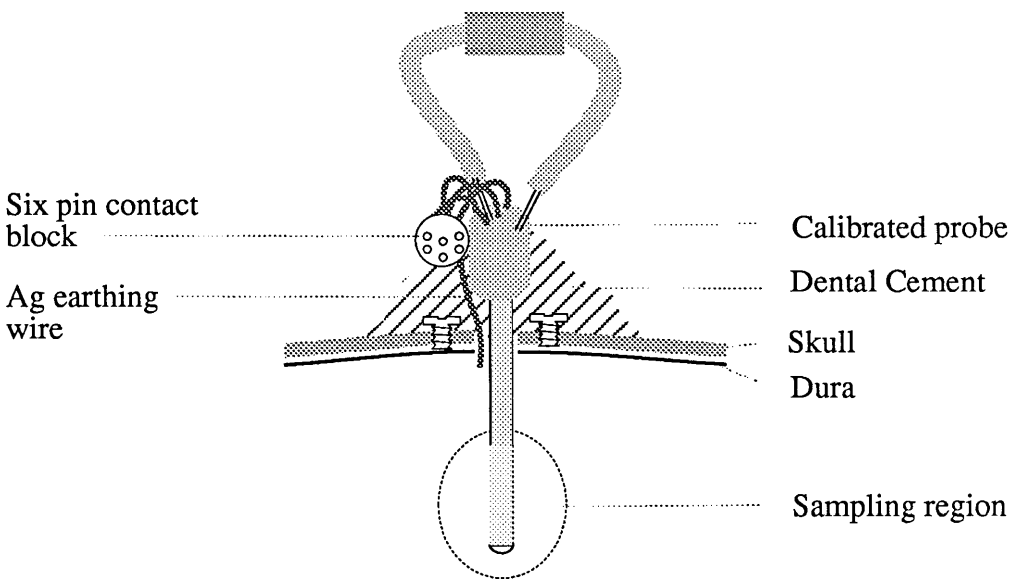


Figure 4.2 Diagram of an implanted probe showing skull screws and silver earthing wire

Prior to implantation, the probes were perfused either with Ringer's solution or with an enzyme solution consisting of either ascorbate oxidase (10 U/μL) or glutamate oxidase (0.5-2 U/μL) and ascorbate oxidase (10 U/μL) in Ringer's

solution and then calibrated either with ascorbate or with both ascorbate and glutamate. Chapter three showed the effects of nafion, ascorbate oxidase and glutamate oxidase on the currents measured on platinum electrodes. For the striatal work, an additional external platinum electrode, held at +350 mV (vs Ag/AgCl), was used to monitor the ascorbate concentration around the outside of the probe.

4.3 The 'tail pinch'

The main behavioural test used in this series of experiments was the 'tail pinch', first described by Antelman *et al* 1975. As the name suggests it involves placing a paper clip on the rat's tail about 30 mm from the tip for a period of five minutes. Normally the rat licks the paper clip, but if presented with a stick it sits still and gnaws at the stick and exhibits some vacuous chewing until the paper clip is removed. This pinch appears only to cause mild irritation to the rat and yet provides a very reproducible physiological response.

Fillenz and her colleagues have shown, using microdialysis and carbon paste electrodes implanted in the striatum, that a large increase in ascorbate, about 20% above basal levels, is observed during a tail pinch and that the increase begins immediately the paper clip is put on and falls sharply away once it is removed (Boutelle *et al* 1989). They have proposed that the increase in ascorbate is due to the uptake of neuronally released glutamate, through an exchange system, outlined in chapter one. Further support for this theory would be the confirmation of a possible parallel increase in glutamate with the ascorbate release during the tail pinch and this is where the dialysis electrode has been used.

The best results were achieved using the following procedure: Ringer-filled probes were calibrated with ascorbate before being implanted. Figure 4.3 illustrates the possible interference observed with no ascorbate oxidase in the probe and with

nafion repelling negative ions on the internal electrode only. A typical interference response is shown overleaf in figure 4.4, where the external current is larger due to the absence of a nafion protecting layer.

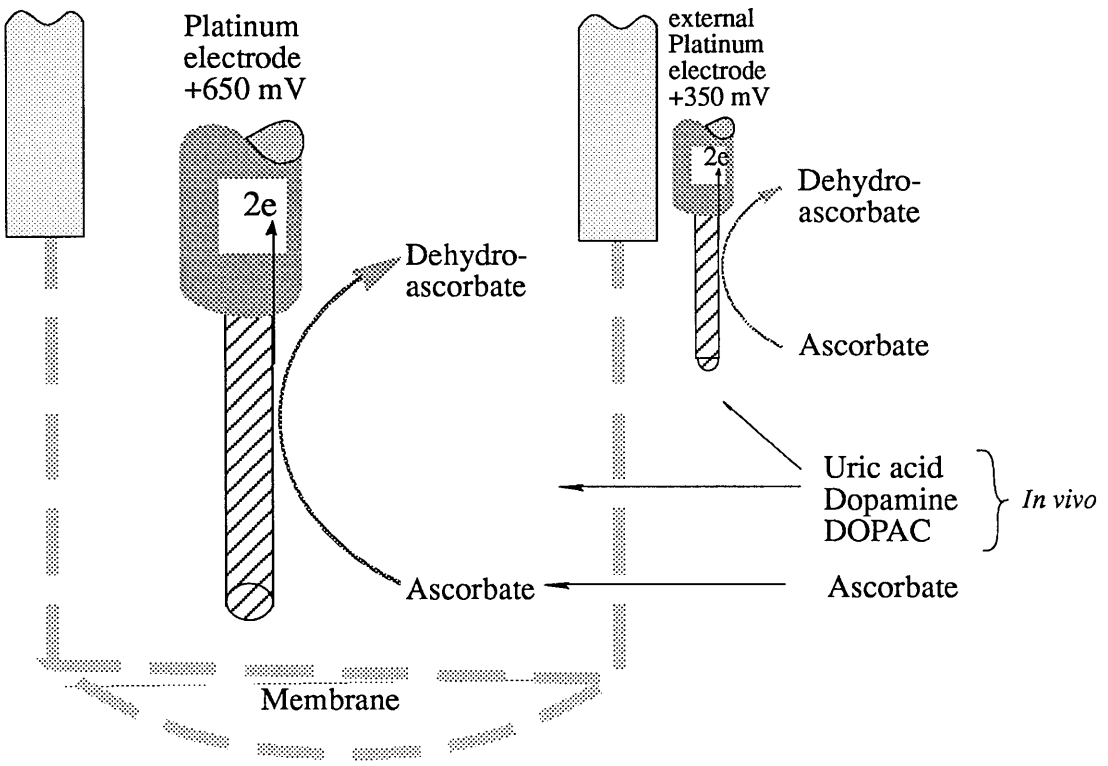


Figure 4.3 Schematic view of the interference measured on the internal and external electrodes for a pre-implantation calibration.

Once implanted, the Ringer-filled probes were perfused with different enzyme solutions and this allowed 'blank', 'control' and 'glutamate' runs to be performed on the same probe and in the same animal, providing a considerable advantage over implanted glutamate oxidase-filled probes, where no 'blank' and 'control' runs were possible.

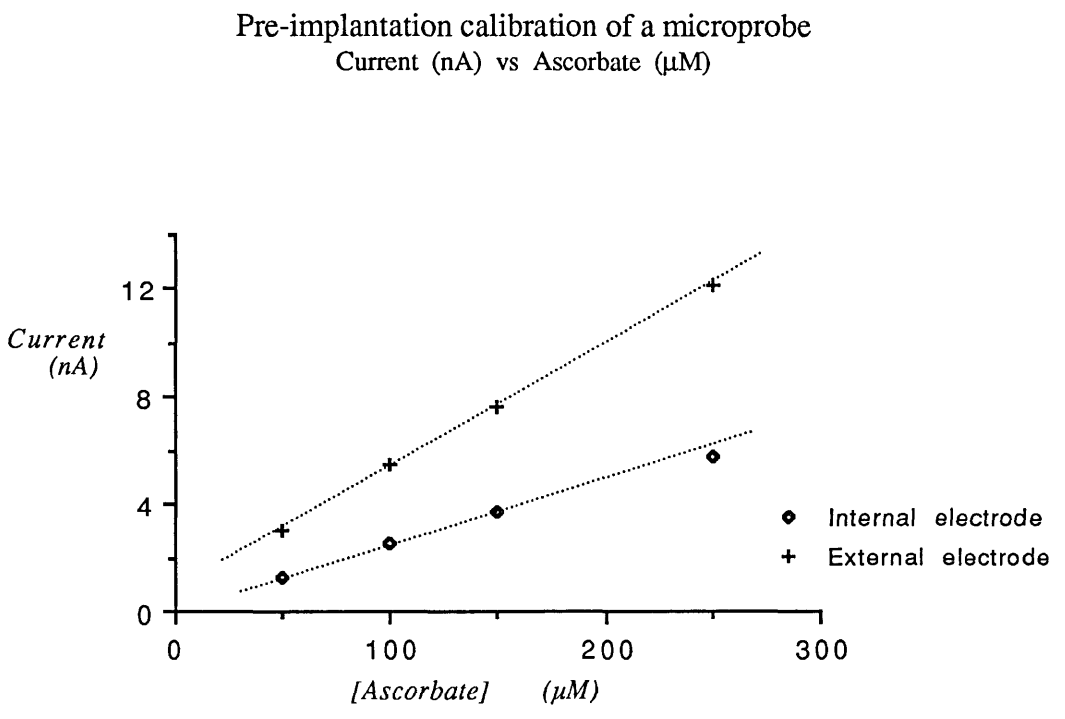


Figure 4.4 Pre-implantation ascorbate calibration of a probe prior to implantation into the striatum. The Internal electrode was held at +650 mV and the external at +350 mV. The set-up is described in section 2.4

The day after implantation, the contact block on the rat's head was connected to a two channel potentiostat, designed by Dr Boutelle, by means of a swivel contact and a 30 cm length of screened six-core cable (Plastics One, USA). This gave the rat full mobility and being light, gave no apparent discomfort. The currents in the two electrodes were allowed to decay to steady values, which normally took about an hour. After a 10 minute period of steady base-line current, a tail pinch was performed. Figure 4.5 shows a typical result. There is a sharp increase in current as soon as the pinch begins lasting for the duration of the test. As soon as the pinch is stopped, the current is seen to fall. The current on the internal electrode steadies at a higher value and this is probably due to an increase in the electrode's own background drift.

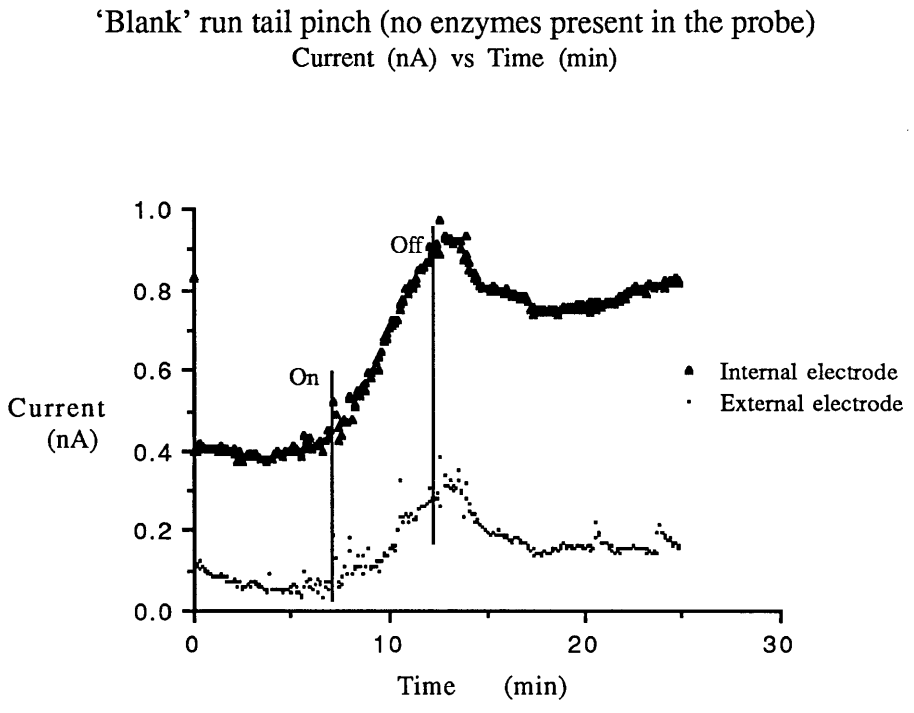


Figure 4.5 A typical 'blank' run for a probe with Ringer alone surrounding the electrode. The figure shows traces for oxidation of electroactive species on both the external and the internal electrodes at +350 and +650 mV respectively. The 'on' and 'off' marks indicate when the paper clip is attached and removed.

As the probe was filled with Ringer alone, both internal and external electrodes detected changes in electroactive species, which were most likely to be ascorbate, DOPAC, 5-HIAA and uric acid, based on their μM extracellular concentrations (Fillenz *et al* 1986, Benveniste 1989). Dopamine levels may have changed but these levels are near the 50nM region and so they unlikely to have much effect (Benveniste 1989 and Zetterström 1986). The presence of the nafion membrane on the internal electrode, repelling negatively charged species greatly reduces this interference, as shown in chapter three. The interfering species can be completely removed by addition of the relevant enzymes, such as uricase and ascorbate oxidase and the next part of this experiment does this.

4.4 The 'Control' run

Having performed a tail-pinch with just Ringer in the probe, a solution of ascorbate oxidase (10 U/μL) was perfused through the probe using a Carnegie microdialysis pump. Figure 4.6 sows the probe profile and figure 4.7 shows the current trace for perfusion of this solution.

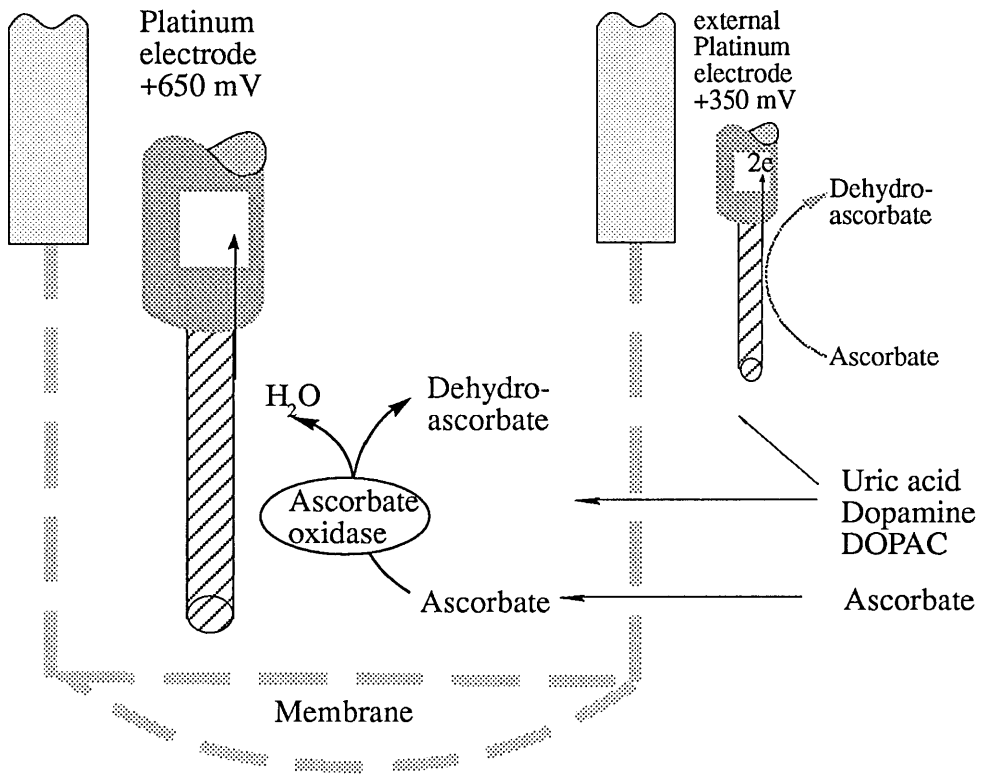


Figure 4.6 Schematic view of the removal of interference for the internal and external electrodes of an implanted probe.

As the flow begins, there is a sudden perturbation of the electrolyte around the electrode causing a sudden spike in the trace. This is then replaced with a gradual decay in both the internal and the external current as the interfering molecules are removed from the electrolyte around the working electrodes by the

flow before they are oxidized. The current then plateaus when the diffusion reaches steady-state and then a further drop is sometimes observed as the enyme penetrates the electrode area, at 16-17 minutes in figure 4.7. This drop corresponds to removal of any ascorbate that has not been removed by the flow, but is instead oxidized by the enzyme. The residual current is now due to the electrode background current and the other electroactive species present in the ECF. Their removal by enzymatic means was not required as the next tail-pinch shows.

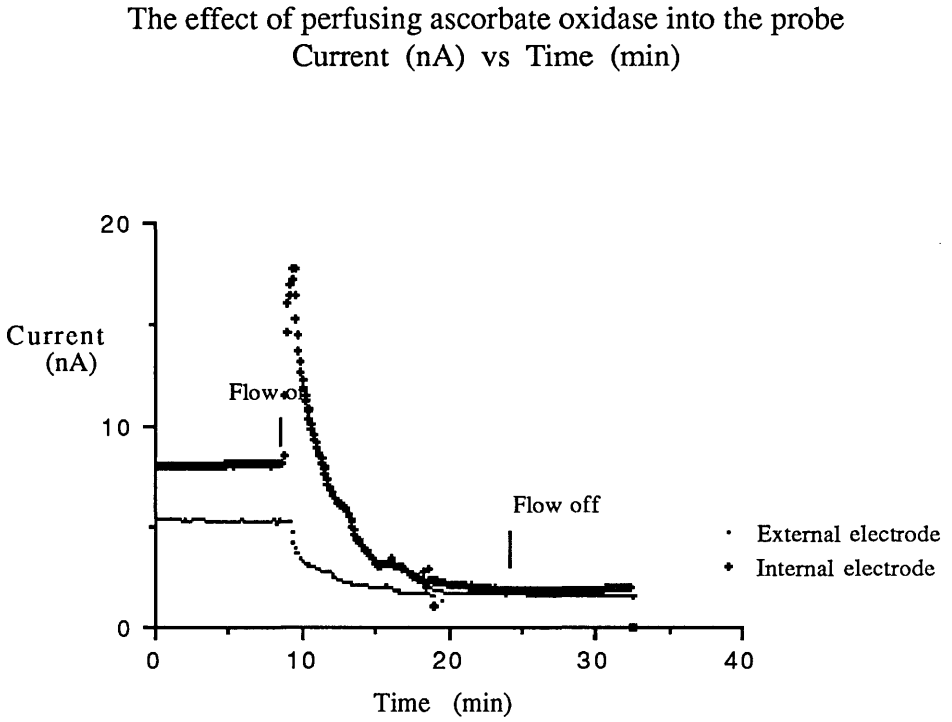


Figure 4.7 The effect of perfusing 10U/μL ascorbate oxidase through the probe at 0.5 μL/min, when implanted in the striatum. The current values are averaged over 5 second intervals. (When the flow is turned off the enzyme is present in the solution and is not flushed out)

The perfusion was stopped and the rat was left for an hour so that any changes in the striatum caused by either the perfusion or the enzymes could be allowed to settle down. Then, once steady-state had been reached, a second tail pinch, the 'control', was given. The introduction of the ascorbate oxidase should

remove the tail pinch peak seen on the internal electrode, whilst the peak seen on the external electrode should be retained. The result of this tail-pinch, shown below, was a profound reduction in the electroacitve species' signal that had previously been observed for the 'blank' run.

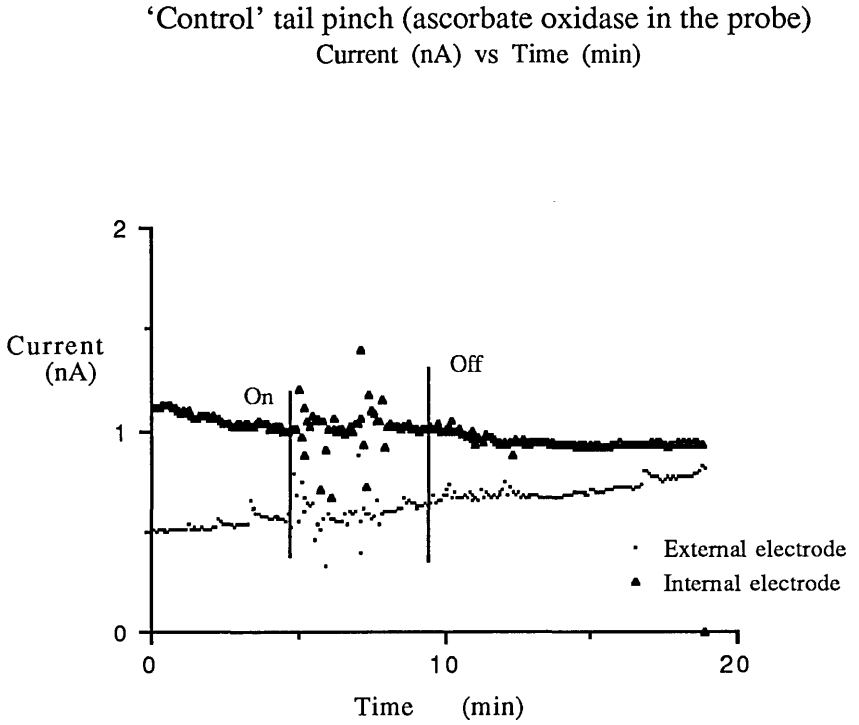


Figure 4.8 A typical 'control' tail pinch for a probe with10 U/μL ascorbate oxidase surrounding the electrode. The figure shows traces for oxidation of any remaining interferents on both the external and the internal electrodes, at +350 and +650 mV respectively, that have not been oxidized by the enzyme.

As figure 4.8 shows, the current barely increases with this control run, indicating that the presence of the oxidase is sufficient to remove the interference. Hence only the ascorbate is giving rise to the peak seen in the blank run. Levels of DA, DOPAC and uric acid may be changing, but obviously by insignificant amounts. One apparent anomaly in the control run is the loss of the peak on the

external electrode and this has been put down to the very efficient ascorbate oxidase, which not only clears ascorbate inside the dialysis tubing but also in the ECF immediately surrounding the probe. The control run provides an excellent base-line for the tail-pinches in the presence of glutamate oxidase.

4.5 Glutamate measurement during the tail pinch

As a drop in current was observed on addition of ascorbate oxidase, a corresponding increase in current was expected when a solution of glutamate oxidase and ascorbate oxidase in Ringer was perfused into the probe, caused by oxidation of the glutamate from the ECF producing H_2O_2, as illustrated in figure 4.9.

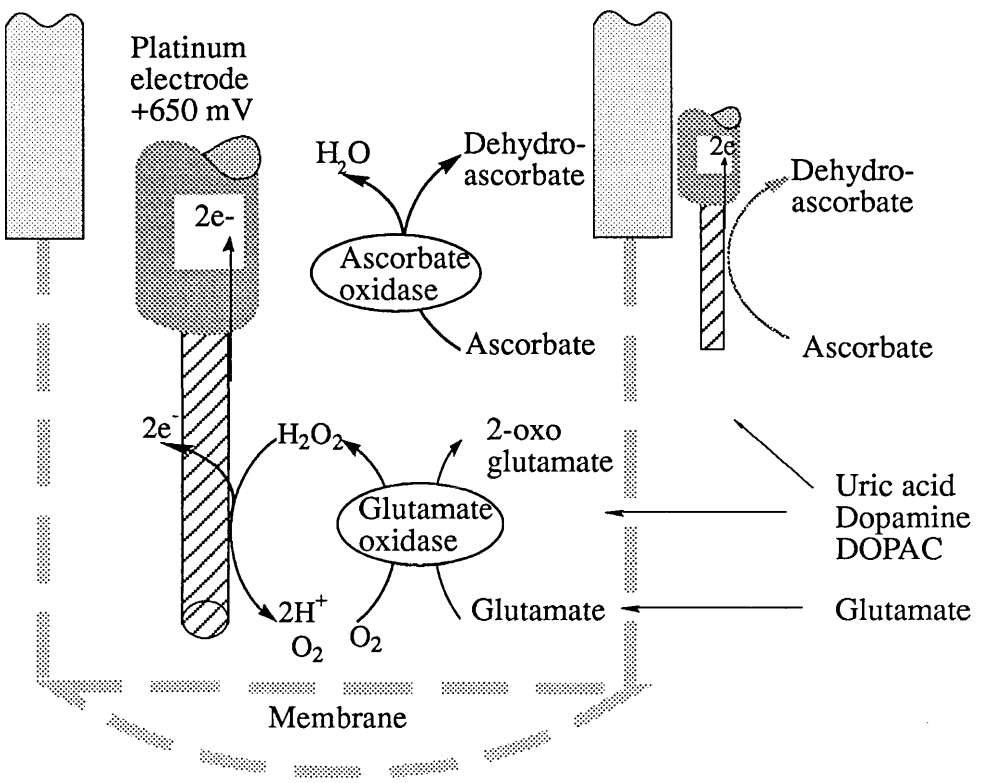


Figure 4.9 Schematic view of the measurement of glutamate on the internal electrode of an implanted probe.

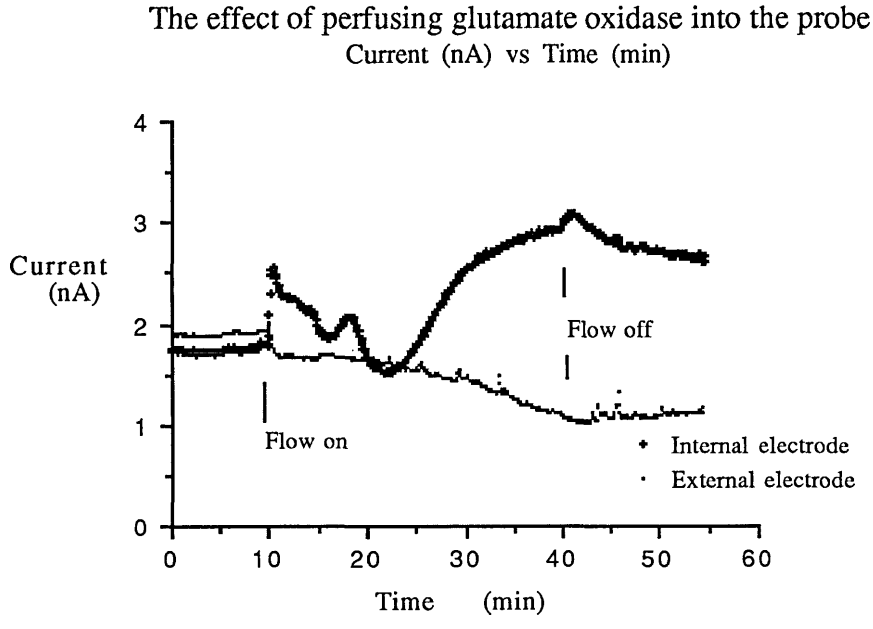


Figure 4.10 The effect of perfusing 10U/μL ascorbate oxidase and 2 U/μL glutamate oxidase through the probe at 0.5 μL/min, when implanted in the striatum. The current values are averaged over 5 second intervals. (When the flow was stopped both enzymes still remained in the probe)

An increase of approximately 1 nA was indeed seen and as figure 4.10 shows, it was only observed on the internal electrode. H_2O_2 can be measured at potentials of +350 mV (section 3.4) and so the external electrode indicates that little H_2O_2 is escaping into the brain (the potential of the external electrode may have been too low to pick up such small glutamate levels). As chapter three showed there to be a small glutamine activity, which saturated at ≈80μM, an estimation of the basal glutamate level can be made from this current increase, providing an assumption of the glutamine level is made. Estimations of the extracellular glutamine concentrations in the striatum have been quoted as ranging from 90 to 121 μM (Kopf & Venema 1985 (estimation from 1 μL/ min) and Young & Bradford 1986). This would produce a current of 100 pA at most, leaving approximately 0.9 nA that comes from glutamate oxidation. An estimation of the basal glutamate level can be read off an *in vitro* calibration for an identical probe, filled with ascorbate oxidase and glutamate oxidase, a plot of which is shown in figure 4.11.

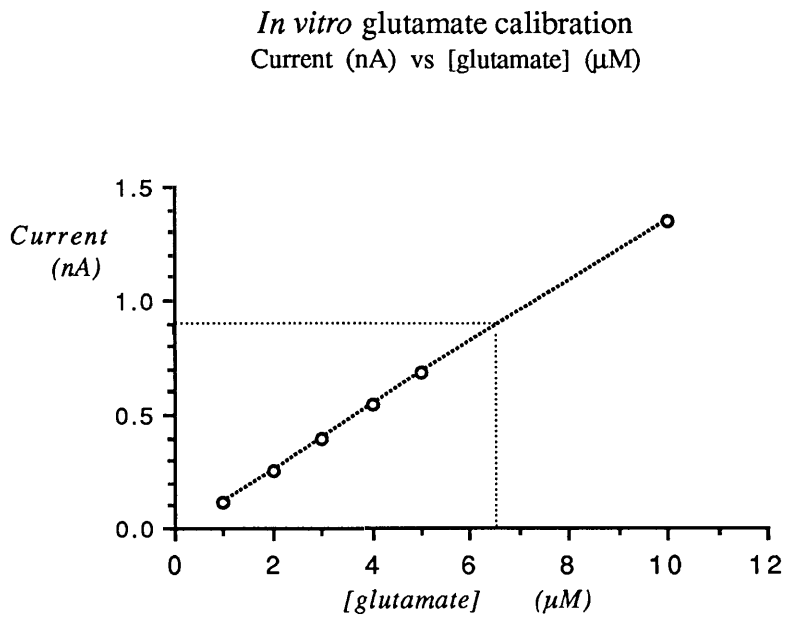


Figure 4.11 A calibration for a probe filled with 10 U/μL ascorbate oxidase and glutamate oxidase . The electrode was held at +650 mV (vs Ag/AgCl) . The set-up is described in section 2.4. The dotted line marks the estimation of basal glutamate levels in the striatum.

In a review of microdialysis, Benveniste (1989) quotes basal striatal glutamate levels ranging from 8 to 20 μM. Using the probes, a current of 0.9 nA corresponds to a glutamate concentration of ≈ 6.5 μM. This value is has not been corrected for any 'depletion' of the glutamate levels in the immediate vicinity of the probe, although this effect is not as pronounced for the non-flowing enzyme sensors as it is for the micodialysis probe, were the probe lies in a region of lower analyte concentration due to the perfusion. It must be stressed however, that this value comes from only one run and that at least five repetitions are required for a realistic figure.

Having left the rat for an hour to allow any perfusion effects to be eliminated and once a steady-state current had been reached, another tail-pinch was given to the rat and the rise in glutamate was measured, figure 4.12. The trace clearly shows a increase in current for the duration of the tail-pinch and a decay back to basal values

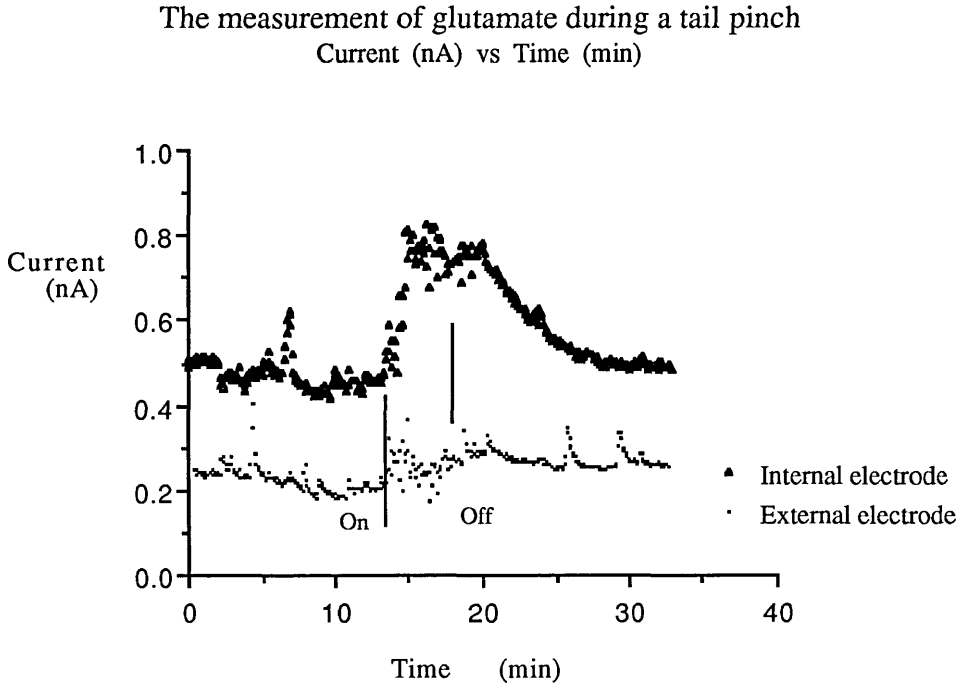


Figure 4.12 A typical 'glutamate measurement' run for a probe with 10 U/μL ascorbate oxidase and 2 U/μL glutamate oxidase surrounding the electrode. The figure shows traces for enzyme-linked oxidation of glutamate on the internal and interference on the external electrodes, at +650 and +350 mV respectively,

once the paper clip had been removed. Assuming the glutamine activity is already saturated, the increase must be due to glutamate. The rise in current of 0.35 nA corresponds to an increase in glutamate concentrations of ≈2.5 μM, i.e. a 40% increase on basal levels. Work by Girault and coworkers (Girault *et al* 1990) shows that as the striatal glutamate levels rise by 217% with increased neuronal activity, the glutamine levels fall 28% (the extracellular glutamine is taken up to provide intracellular glutamine for conversion to glutamate) A drop in glutamine levels by this amount would mean the putative activity may become unsaturated leading to a drop in the 'apparent' background current. If this is the case then the rise in current and thus glutamate concentration is larger than the 0.35nA estimated.

4.6 Catalase perfusion

Further confirmation of the increase being enzyme derived comes from the use of catalase in the perfusion medium. With a steady base-line, a solution of catalase (100 U/μL), glutamate oxidase (1U/μL) and ascorbate oxidase (10U/μL) in Ringer was perfused into the probe. The catalase acts as a scavenger, removing any H_2O_2 from the area close to the electrode. So as enzymatically produced H_2O_2 is not oxidized on the electrode, addition of catalase to the perfusate should suppress any tail-pinch response. Figure 4.13. shows the effect of perfusing the catalase,

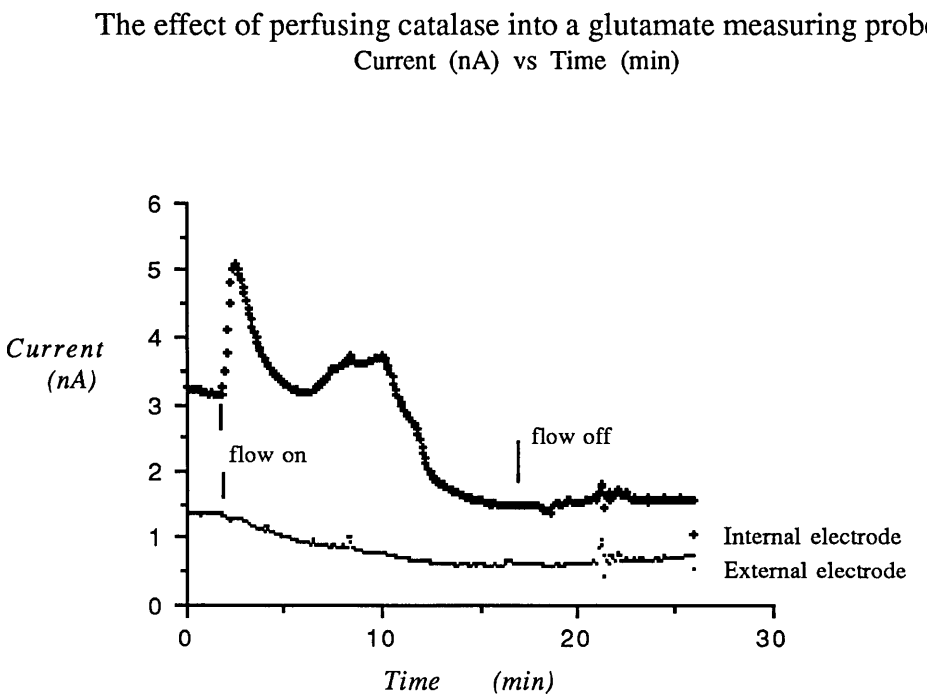


Figure 4.13 The effect of perfusing catalase (100 U/μL), 10U/μL ascorbate oxidase and 2 U/μL glutamate oxidase through the probe at 0.5 μL/min, when implanted in the striatum. The current values are averaged over 5 second intervals

where there was a dramatic reduction in the current seen on the internal electrode. Figure 4.14 shows the effect of tail pinch with the three enzymes present in the probe. The removal of the peak proves the previous tail-pinch was measuring glutamate, assuming the glutamine activity is still saturated.

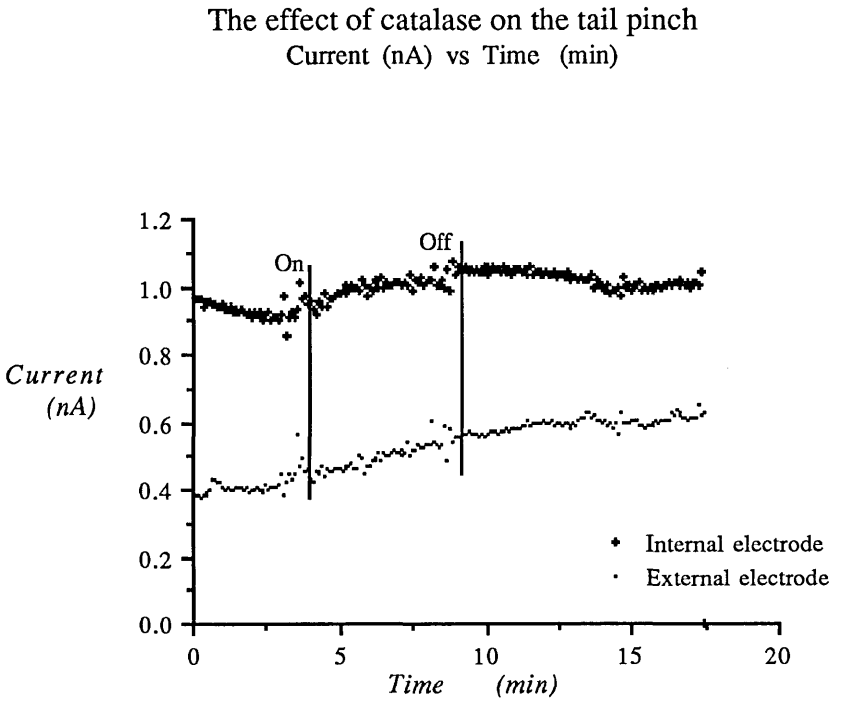


Figure 4.14 The effect of perfusing 10U/μL ascorbate oxidase and 2 U/μL glutamate oxidase through the probe at 0.5 μL/min, when implanted in the striatum. The current values are averaged over 5 second intervals

4.7 Pharmacological effects

Dopamine D_2 receptor agonists such as apomorphine have been shown to increase the motor activity and with this, rises in dopamine and ascorbate concentrations have been seen (Wheeler 1991 & Zetterström *et al* 1991). If the change in ascorbate is mirroring a glutamate rise then this should be measurable with the glutamate probe. The apomorphine is administered by a sub-cutaneous injection and the rise in ascorbate and dopamine is slow and long lasting. When implanted with a glutamate measuring probe, the rat was given an injection of apomorphine (0.5 mg/kg dissolved in boiled saline) and the rise in glutamate was measured in the normal manner. Figure 4.15 shows the effect. The trace mirrors the increases seen previously for ascorbate, providing further support to Fillenz's theory for the ascorbate / glutamate relationship.

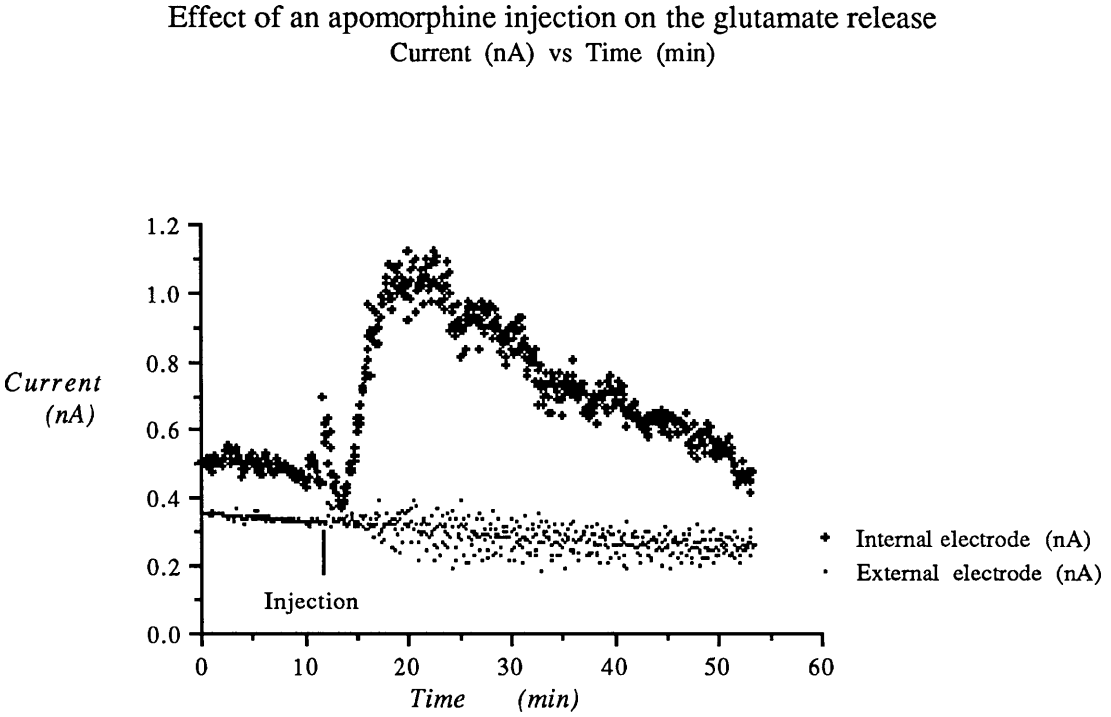


Figure 4.15 The effects of an apomorphine injection on the glutamate release. The induced motor activity began to decrease 15 minutes after the injection.

4.8 Conclusions

The results shown above illustrate the two main advantages of the probes, they have a fast time resolution and the ability to be characterized *in vivo*. Whilst further studies are required to characterize the *in vivo* response to the tail pinch, the probes provide a very important step towards understanding the nreurotransmitter relationships in the striatum.

Out of sixteen electrodes made during the period spent on the striatal work only six were implanted in the striatum and the reasons for this low success rate were usually mechanical problems with both the probes and the rotating electrical swivel contact, which allowed free movement of the animal. Air bubbles often appeared inside the dialysis fibre blocking up the flow during the 'priming' of the

probes and the currents were often too noisy probably due to poor contact to the six pin connectors. Out of the six implanted, three responded well giving some of the results shown above and the others gave little in the way of intelligible results and this was because of flow blockage during the experiments and noisy electrical interference and spiking. By the end of the set of experiments, the success rate was improving as these problems were overcome by careful electrical soldering and monitoring of the infused solutions for possible bubbles.

Chapter Five

Glutamate measurement in the Hippocampus

5.1 Long-term potentiation and previous glutamate measurements

Being an important excitatory amino acid, the role of glutamate in the hippocampus has been has been studied for a number of reasons, an example is its neurotoxicity in hypoxic-ischaemia (Benveniste *et al* 1984 and Choi & Rothman 1990). This chapter focuses on glutamate's role in long-term potentiation (LTP)

The cellular mechanisms responsible for the sustained enhancement observed in LTP remain unresolved, as the effect may be mediated by pre or post synaptic mechanisms. As stated in section 1.8, LTP requires both associativity and co-operativity for the induction and maintenance of the increased synaptic efficacy, (Teyler & DiScenna 1987). Triggering requires a near simultaneous presynaptic activation and post-synaptic depolarization, making the process associative. Studies in the dentate and CA1 have shown that this triggering requires a stimulation strength which activates a sufficient number of afferent fibres, giving the event its cooperativity. There is also a 'synaptic specificity', where only tetanized synapses show LTP (Madison *et al* 1991).

The pre-synaptic depolarization of the glutamatergic terminals results in an influx of calcium into the granule cells through the post synaptic, voltage dependent, excitatory amino acid linked receptors (NMDA type). This is shown by NMDA antagonists such as 2-amino-5-phosphonovalerate (APV), which block the induction

(Collingridge *et al* 1983 & Collingridge & Bliss 1987) The influx of calcium initiates the processes leading to potentiation of the excitatory post synaptic potential (EPSP) by activation of the NMDA receptor channels, whether it has a further role is unclear (Gustafsson & Wigström 1988). The role of post synaptic activity in LTP induction has also been shown by blocking the post synaptic inhibition, which greatly increases LTP induction.

A sustained increase in glutamate release in the dentate gyrus, has been measured before, during and after LTP by Bliss and his colleagues (Lynch *et al* 1989 and Errington *et al* 1987) by sampling perfused ACSF every few minutes using push-pull cannulae. Increased glutamate release with increased stimulus frequency has also been detected both *in vivo* and *in vitro* (Bliss *et al* 1990). However Ben-Ari and colleagues has shown that in the CA1, there is no LTP-dependent increase in glutamate (Aniksztejn *et al* 1989)

The glutamate probes were a possible technique for verifying Bliss's 'push-pull' data and examining the findings of Ben-Ari, giving a continuous response and cutting down on the laborious off-line HPLC/ fluorimetric assay.

5.2 Probe Construction

The glutamate probes used for the behavioural studies described in Chapter Four were modified slightly for the hippocampal measurements, and are shown in plates 2.8 & 2.9. Unlike the striatal probes, these had no external platinum electrodes as firstly they supplied little information in the striatum and secondly it was thought that they would interfere with the two 125 μm stainless steel recording electrodes that were positioned in the sampling region of the probe. The 'active area' of the probes, the length of dialysis fibre that was not sealed over with epoxy, was reduced from 4 mm to under 2 mm. The first stainless steel (SS) recording electrode was glued parallel to the dialysis fibre so that its end lay in the middle of

the sampling region and the second, again parallel, extended just below the tip of the probe. The arrangement of the recording electrodes was such that, when implanted in the dentate gyrus, the upper recorded from the molecular layer and the lower from the granule cell body layer. This is illustrated in figure 5.1. The probes replaced the 'push-pull' cannulae as a straight exchange and all the other conditions remained identical.

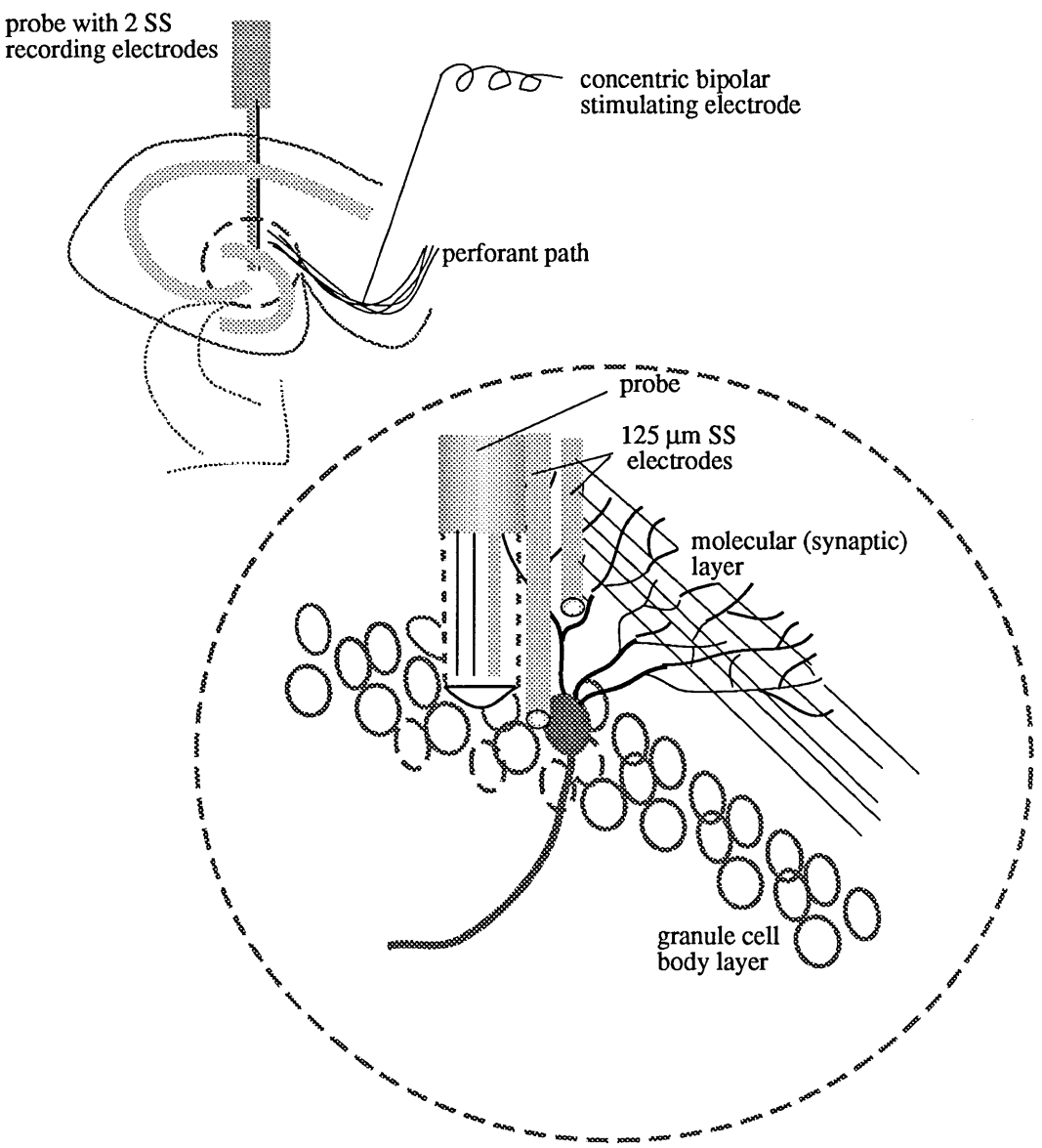


Figure 5.1 A saggital section through the rat hippocampus showing the site of implantation of the probe and recording electrodes in the dentate gyrus. (Adapted from Errington *et al* 1987)

Before implantation, the probes were perfused with 10 U/μL ascorbate oxidase with or without 0.5 U/μL glutamate oxidase in Krebs-Ringer and were left overnight at +4°C, which increased the probe's activity as enzyme adsorbed onto the electrode surface. The following morning, the probes were connected to a potentiostat via a six-core screened cable (Plastics One), calibrated in Krebs-Ringer with ascorbate and glutamate, if they contained glutamate oxidase, using the method described in section 2.5 and then implanted in the following manner.

5.3 Probe Implantation

Male Sprague/ Dawley rats, weighing between 300 - 400g, were anaesthetized with 1.5 mg/kg urethane (i.p.), and held by ear and mouth bars with lambda and bregma level (this injection was sufficient to anaesthetize the rat for the whole experiment). The skull was exposed with a drill and two small areas removed, one for insertion of the probe and the other for insertion of a concentric bipolar stimulating electrode (Rhodes Instruments). This was placed 4.4 mm laterally and 8 mm caudally (to bregma) and advanced into the brain to stimulate the medial perforant path.

The probe was held rigidly by the Plastics One contact block and the stainless steel electrodes were connected to the external circuit by means of two 2 mm gold contacts (A.W.P.). The probe was lowered into the dentate through the cortex and the CA1. Whilst inserting the probe, the evoked potentials were continuously monitored on a dual voltage oscilloscope after being amplified and filtered. The probe's position was adjusted to maximize the slope of the population excitatory post synaptic potential (EPSP) measured in the molecular layer (upper electrode). Once in position the stimulus frequency was set at 0.033 Hz and the hippocampus was left to recover from the implantation for six hours.

The glutamate derived current was measured continuously from the moment the probes were connected for the *in vitro* calibration. After implantation, high currents were seen as the probe was picking up high concentrations of both glutamate and interferents and probably pH changes caused by the rupturing of the cells. Over the six hour stabilization period, the current measured on the probe decreased steadily, as the cell damage was minimized. Once the base line had steadied a series of runs could be performed to study the effects of increased stimulus frequency on glutamate release. The current was continuously monitored in the form of a voltage on a Gould Y-T chart recorder running at a rate of 2 min /cm

5.4 Stimulus frequency procedures

The basal 0.033 Hz stimulus frequencies consisted of 50 μs monopolar pulses of ≈5 mA and these were given for the whole duration of the experiment. Increases in stimulus frequency took three different forms, table 5.1:

Table 5.1 Stimulus frequencies

(1) for reversible increases, the frequency was increased 60 fold to 2 Hz for 1 minute, before being taken back down to 0.033 Hz again,

(2) for LTP induction, three trains of 250 Hz for 200 msec (50 pulses) at 30 second intervals were given, followed by 0.033 Hz again, (the impulse strength was identical to the 0.033 Hz stimulations so that the same number of fibres were stimulated, but at a higher rate)

(3) for Epileptogenic tetani, 3 Hz stimuli were given for 3 to 5 minutes .

It was found that the short 2 Hz stimuli could be repeated at 5 minute intervals for 30 minutes or so without effecting the physiology of the granule cells. These developed as a good test for the probes as they produced a stimulus-dependent release of glutamate.

5.5 *In vivo* 'control' or 'perfusion' experiments

The first experiments that were required were the 'control' runs to show that the currents being measured were glutamate oxidase-derived and not due to interference. The experiments that was used were similar to those used in the previous chapter to show glutamate, and not interferents, was being measured in the striatum. Probes that had been perfused with 10 U/μL ascorbate oxidase only and calibrated *in vitro* with ascorbate , were implanted in the usual manner and left to stabilize. Figure 5.2 shows a typical pre-implantation calibration plot for a probe.

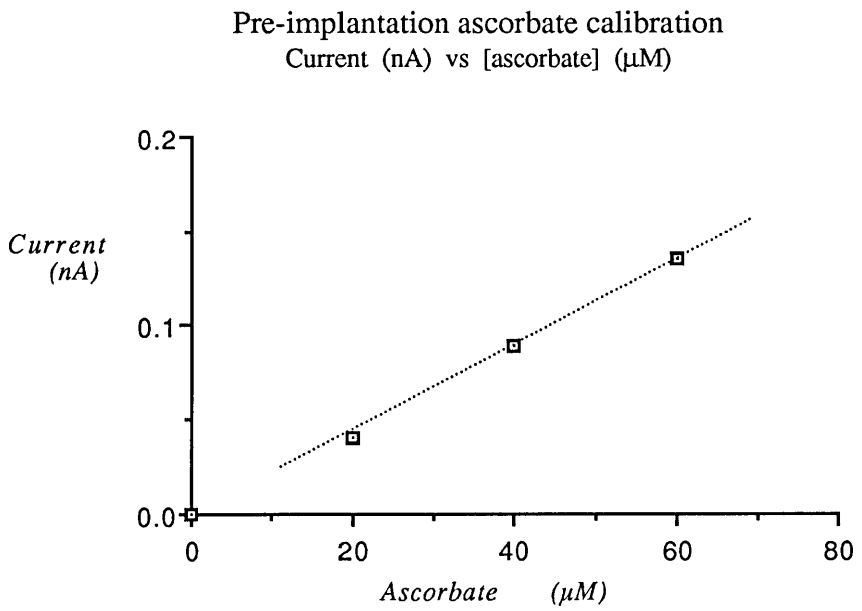


Figure 5.2 Ascorbate calibration for an implanted probe, with a nafion-coated platinum electrode held at +650 mV (vs Ag/AgCl) . The set-up is described in section 2.5

Once the current was at a low and steady value, the dentate was given some reversible stimuli, described above, and the current output from the probe is shown below in figure 5.3. Even with a stable base-line, it can be seen that the 2 Hz stimuli produce no increase in the interference. This was a very useful finding since it showed that firstly the probes were treated with sufficient nafion and had enough

ascorbate oxidase and secondly that a probe capable of measuring ≈5 μM ascorbate changes was not picking anything up.

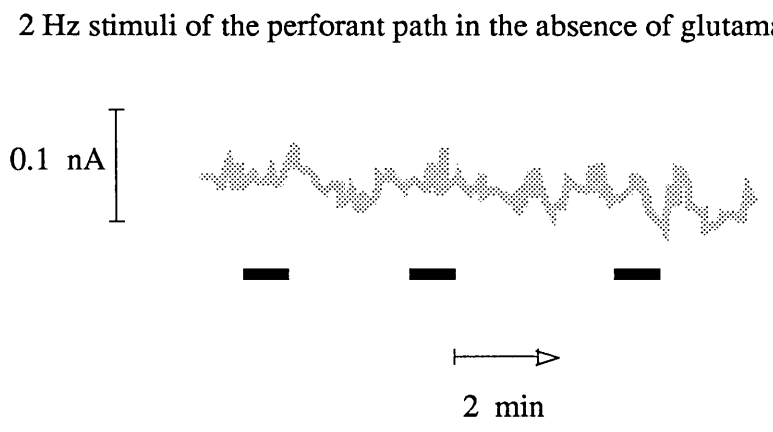


Figure 5.3 'Control' stimuli of the perforant path at 2 Hz, in the absence of glutamate oxidase. The stimulus rate before and after is 0.033 Hz. The horizontal bars represent the stimuli. (The trace is reproduced by hand from the original)

5.6 Measuring glutamate

The next step was the infusion of a solution containing 10 U/μL ascorbate oxidase with 0.6 U/μL glutamate oxidase. The perfusion is shown in figure 5.4. The important point to notice about figure 5.4 is the change in the basal currents when glutamate oxidase is added to the probe electrolyte, after the flow has stopped (the flowing causes perturbations in the electrode area giving rise to peaks seen). As it can be shown that changing the electrolyte does not change the background current (results not shown), the current change of 0.2 nA can be attributed to the enzyme catalysed oxidation of either glutamate or glutamine.

Glutamine levels in the hippocampus ECF have been estimated by various groups and their value appears to lie close to 200 μM: 195 μM Lerma *et al* (1986) and 181 μM (at 1 μL/min in rabbit) Jacobson *et al* (1985). These concentrations would produce a saturation of the enzyme's putative glutamine activity as shown in section 3.6, accounting for 0.1 nA of this 0.2 nA increase. With the glutamine activity saturated, it can be inferred that the remaining 0.1 nA is due to enzyme

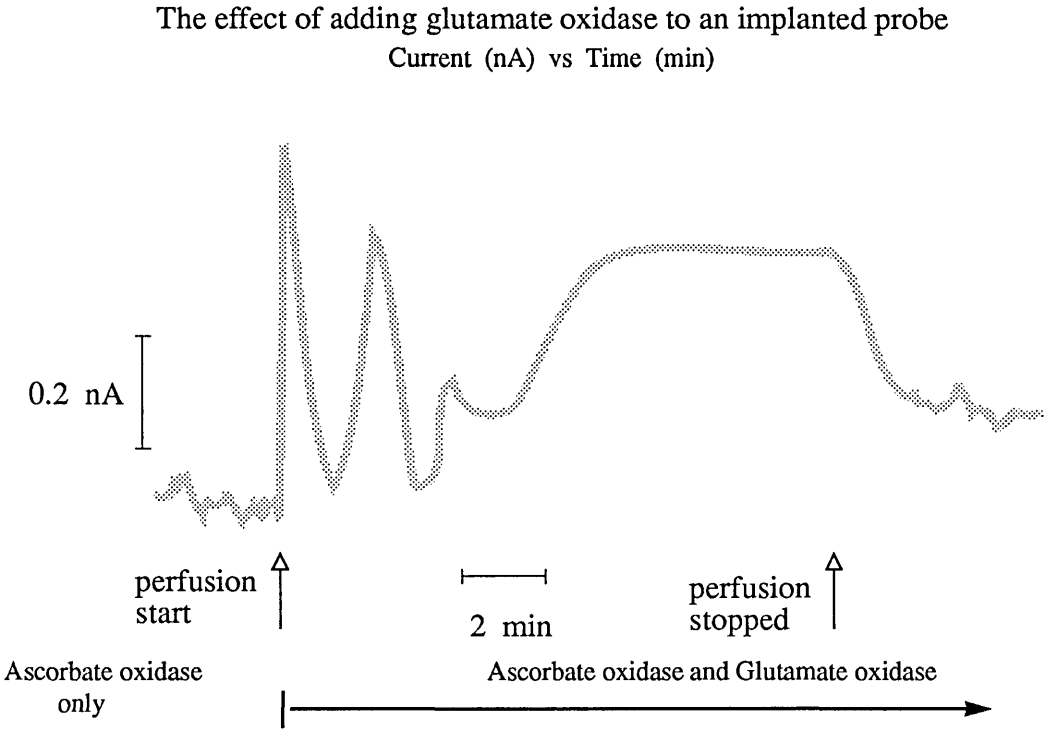


Figure 5.4 Perfusion of 10 U/μL ascorbate oxidase with 0.6 U/μL glutamate oxidase at 0.5 μL/min, with a probe implanted in the dentate. The new enzyme solution enters the probe at the point marked 'start', and remains in the probe until the rest of the experiment, as indicated by the arrow. (The trace is reproduced by hand from the original)

catalysed oxidation of glutamate; a corresponding glutamate concentration is assigned to this value later.

With glutamate oxidase in the probe and a flat control value established, the reversible stimuli were repeated using similar frequencies and durations as before. Figure 5.5 shows the increases in current measured for five increases in stimulating frequency, with the 'control' stimuli, those done in the asbsence of glutamate oxidase, below. The difference in traces is immediately apparent. Unfortunately the currents were not recorded digitally so no averaging could be done. After these stimuli, the probe was removed and calibrated with both ascorbate and glutamate. This calibration, shown in figure 5.6, not only provides a basal glutamate concentration, from the perfusion experiment, but also values for the increase in glutamate concentration from the stimulus dependent release.

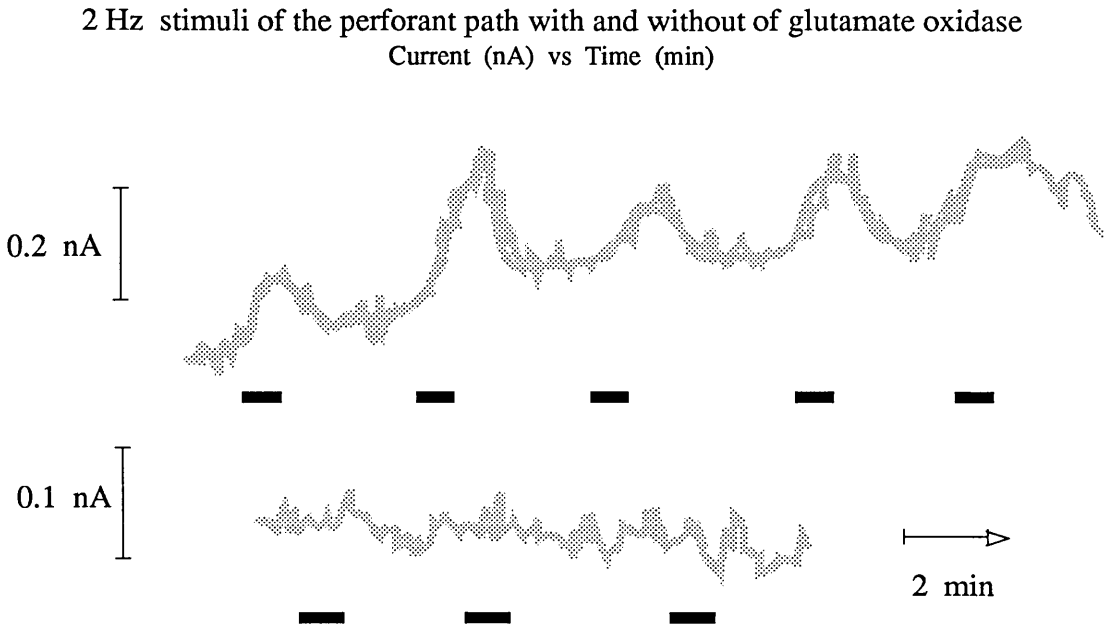


Figure 5.5 Stimuli at 2 Hz. The stimulus rate before and after each stimulation is 0.033 Hz. The horizontal bars represent the stimuli. The peaks represent increases in released glutamate. The lower trace is from the 'control' runs, in the absence of glutamate. (The traces are reproduced by hand from the originals)

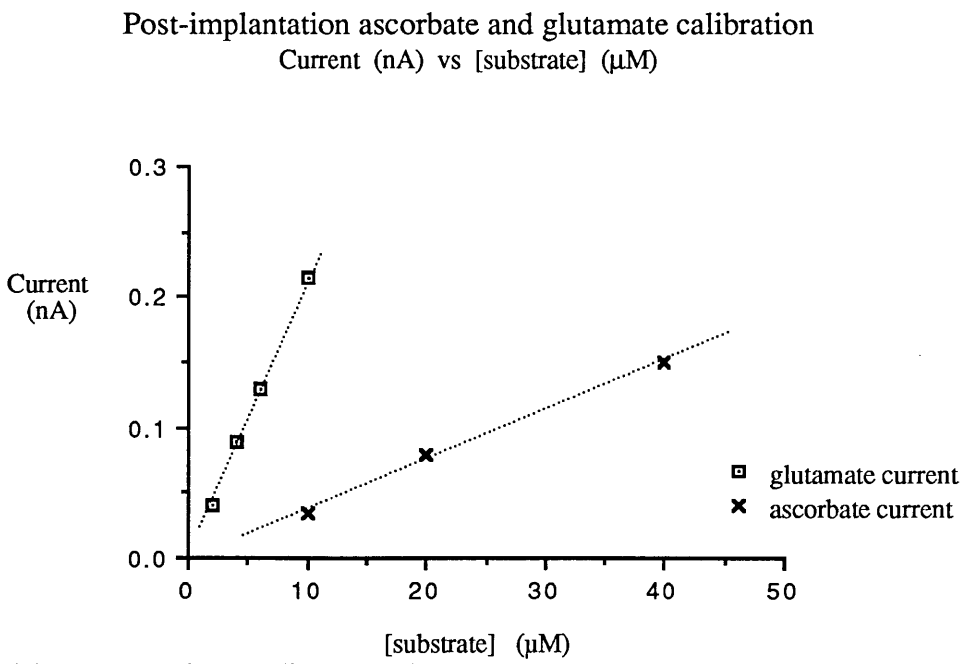


Figure 5.6 Post-experiment calibration, with ascorbate and glutamate, of the probe used for the perfusion experiments. The electrode was held at +650 mV (vs Ag/AgCl) and the set-up is described in section 2.4.

From this graph, basal levels can be estimated as 5 μM and the stimulus-dependent glutamate release as peaking at 2 μM. This basal level is higher than other published values: 2.9 μM (Lerma *et al* 1986) and 1.9 μM (Benveniste 1989). It must be stressed however, that this type of experiment was only performed once and that at least six repetitions of this type should be repeated before any working value can be obtained. However, the experiment does show that the probe is measuring glutamate concentrations of the same order.

5.7 Glutamate release during long term potentiation (LTP)

Having established the validity of the probes to measure stimulus-dependent glutamate release, the next and more important stage was to try and measure any neurotransmitter release during and after the induction of LTP. For these experiments probes were perfused with 10 U/μL ascorbate oxidase and 0.5 U/μL glutamate oxidase, left overnight and briefly calibrated, to check their activity, and then implanted in the usual manner. After a settling period of six hours or so, the hippocampus was given normally five reversible stimuli (2 Hz) to check the probe was detecting released glutamate.

Once the probe was established as working properly, the perforant path was stimulated with the 'resting' 0.033 Hz for a period of an hour, before an LTP-inducing train was given. Figure 5.7 shows the pre-LTP and post-LTP reversible 2 Hz stimuli and figure 5.8 shows the time course for the LTP. Figure 5.9 shows a post-experiment calibration for the probe used.

The stainless steel recording electrodes confirm the presence of LTP and a schematic diagram illustrating a typically recording of the evoked response is shown in figure 5.10. These two traces, (see figure 5.1), show recordings 5 minutes before and 30 minutes after induction of LTP. The increase in synaptic efficacy is shown by

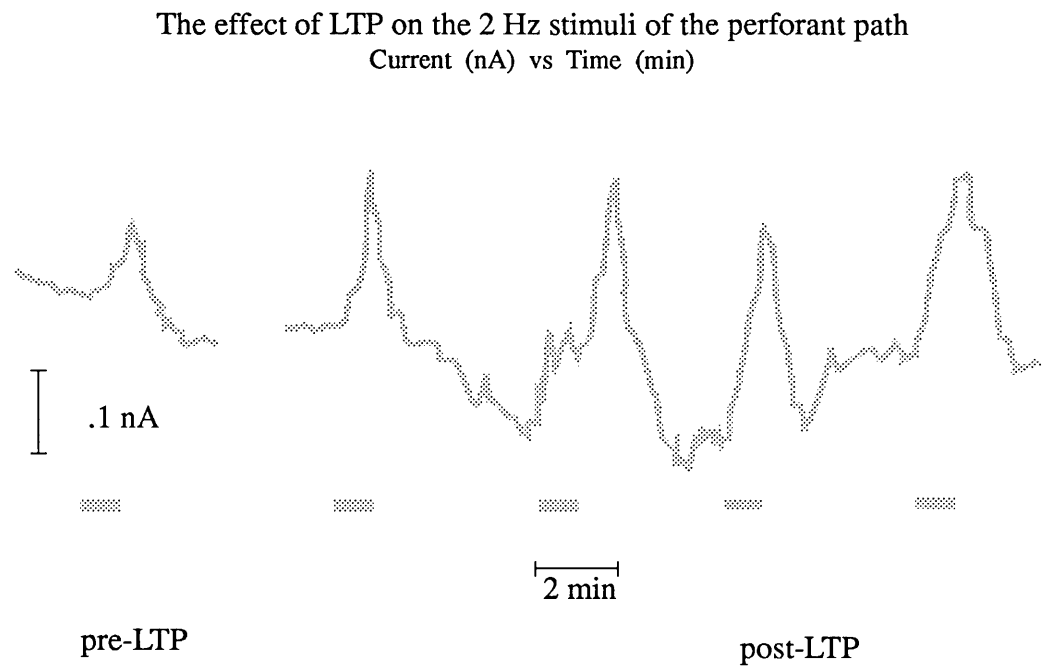


Figure 5.7 Pre- & post-LTP stimulations at 2 Hz. The stimulation rate before and after each stimulation was 0.033 Hz. The horizontal bars represent the stimuli. The post-LTP 2 Hz stimuli were performed one hour after LTP. (The traces are reproduced by hand from the originals)

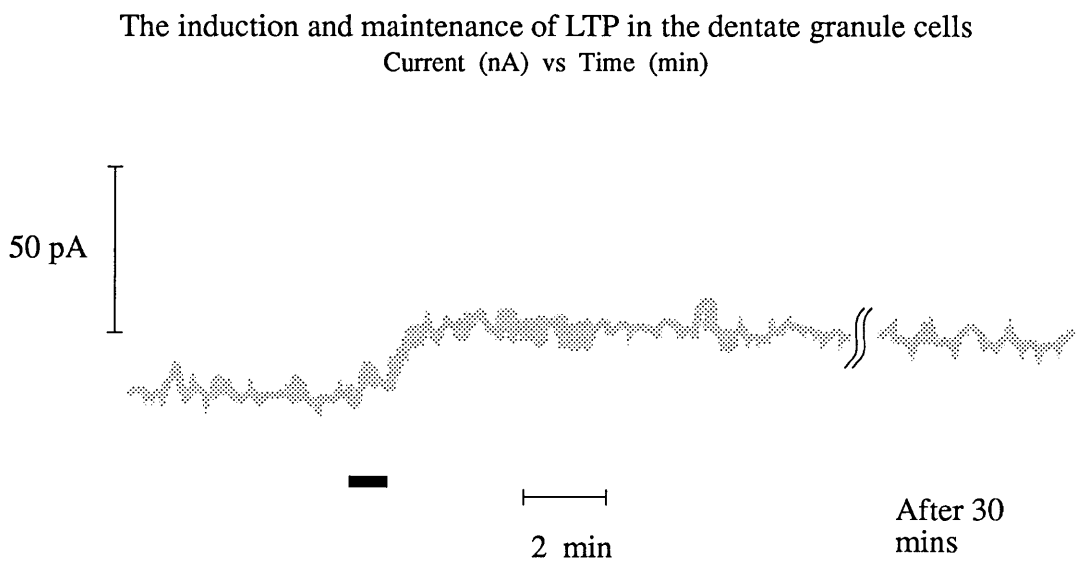


Figure 5.8 Long term potentiation in the rat hippocampus. The LTP-inducing train, shown by the bar, is described in section 5.2. The properties of the probe are given above and the electrode was held at +650 mV (vs Ag/AgCl).(The trace is reproduced by hand from the original)

a steeper component of the population EPSP, peak 1. Peak 2 represents the cells 'discharging'. (figure 5.10).

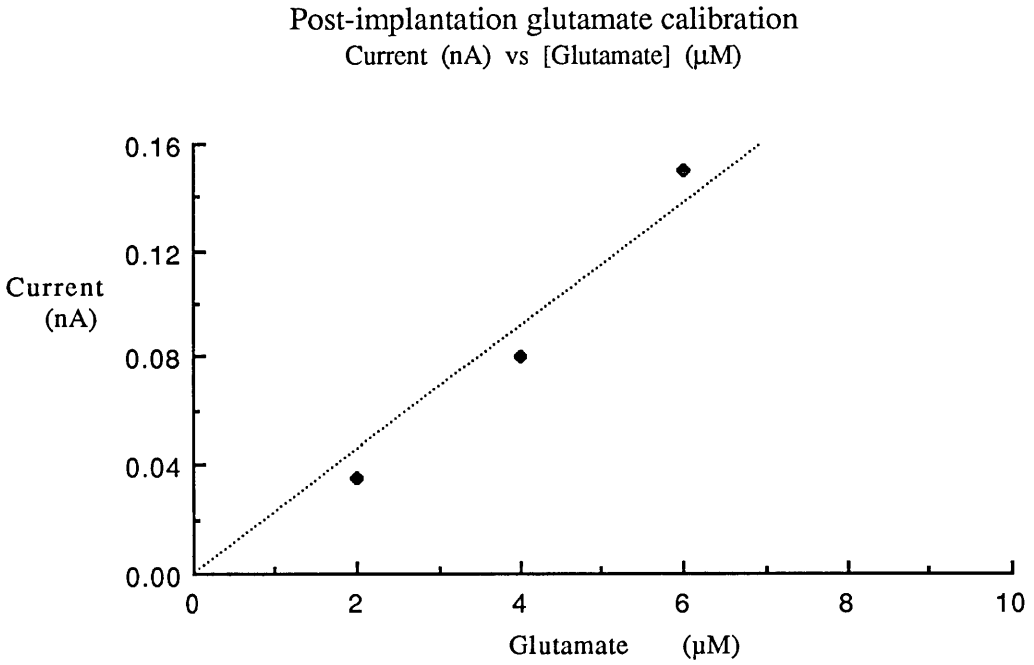


Figure 5.9 Post-experiment glutamate calibration, of the probe used for the perfusion experiments. The electrode was held at +650 mV (vs Ag/AgCl) and the set-up is described in section 2.4.

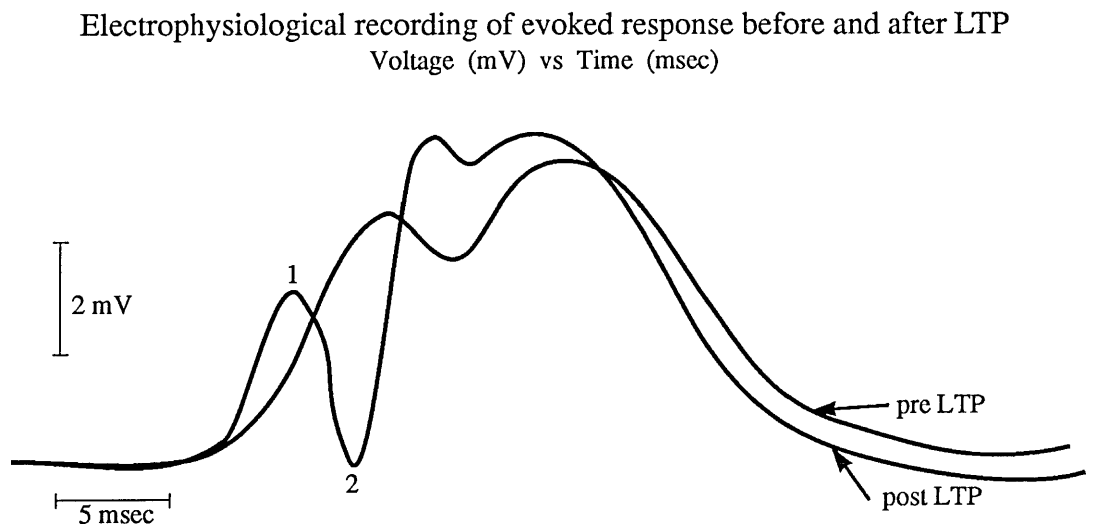


Figure 5.10 A schematic diagram of the evoked response, recorded from the granule cell layer, before and after LTP. The increased synaptic efficacy of LTP is demonstrated by the difference in the initial rise, the positive going population EPSP (peak 1), which is larger in the post-LTP evoked response. (the trace is reproduced by hand from a photograph of the oscilloscope trace). Peak 2 is the negative-going 'discharge' as the cells 'fire'.

Figure 5.7 shows an interesting point to emerge for the reversible 2 Hz stimulus work and that is an apparent increase in peak height after LTP induction. This is an increase in the stimulus-dependent component of the glutamate release associated with LTP. However, for conformation, these pre- and post-LTP stimuli need to be recorded digitally and average over eight runs.

The small increase in current observed straight after the LTP buzz, ≈25 pA (figure 5.8), confirmed the findings of Bliss and his colleagues that long term potentiation of the perforant path is associated with an increase in glutamate release. When converted to a glutamate concentration using the calibration plot in figure 5.9, this gives an increase of ≈1 μM, which on a basal glutamate concentration of 5 μM, gives an increase of 20%. Previous work has shown the increase to be 20 - 50% above basal levels (Bliss *et al* 1990), and so initial findings with the glutamate probe show it to be consistent.

5.8 Epileptic activity in the hippocampus

Epileptic discharges are due to abnormal synchronous bursts of activity in neuronal populations and result from a rapid recruitment of cells, which are normally under tight control by inhibitory neurons, into spontaneous firing. Localized seizures have been observed in both the neocortex and the hippocampus (Gutnik *et al* 1982 and Jefferys & Williams 1987) and the latter has been associated with the onset of a number of focal epilepsies (Jefferys 1990). Various theories have been proposed that are responsible for the onset of this activity and a number of methods have been described for inducing experimental epilepsy.

Synchronization of neurons by excitatory synapses is one such mechanism where a small number (2%) of recurrent excitatory collaterals provide a positive feedback, recruiting neighbouring neurons into synchronous bursting (Christian &

Dudek 1988). The absence or decrease in inhibiton would seem a likely feature of seizures, but cases have been found where inhibition is intact and the activity is caused by 'rebound excitation', where the excitation is caused by the synchronous decay of inhibition. Paradoxically too much excitatory circuitry can lead to seizures as too much inhibition of the inhibitory neurons occurs.

Many experimental models have been described: application of tetanus toxin which produces a reduction in the inhibitory post synaptic potentials and a reduction in released GABA (Jefferys & Williams 1989, Jefferys *et al* 1988); and models where inhibition has been preserved such as application of 4-aminopyridine (Buckle & Haas 1982) or removal of extracellular Mg^{2+} (Coan & Collingridge 1985).

Another model is 'kindling', where it has been suggested that repeated sub-convulsive stimulation gives rise to a progressive decrease in the GABA-mediated inhibition, reducing the seizure threshold (Morimoto & Goddard 1986). The kindling is linked to LTP in that it is a extreme form of neuronal plasticity, producing pathological results. Although kindling experiments are usually performed more subtly epileptic seizures can be generated instantly with prolonged high frequency

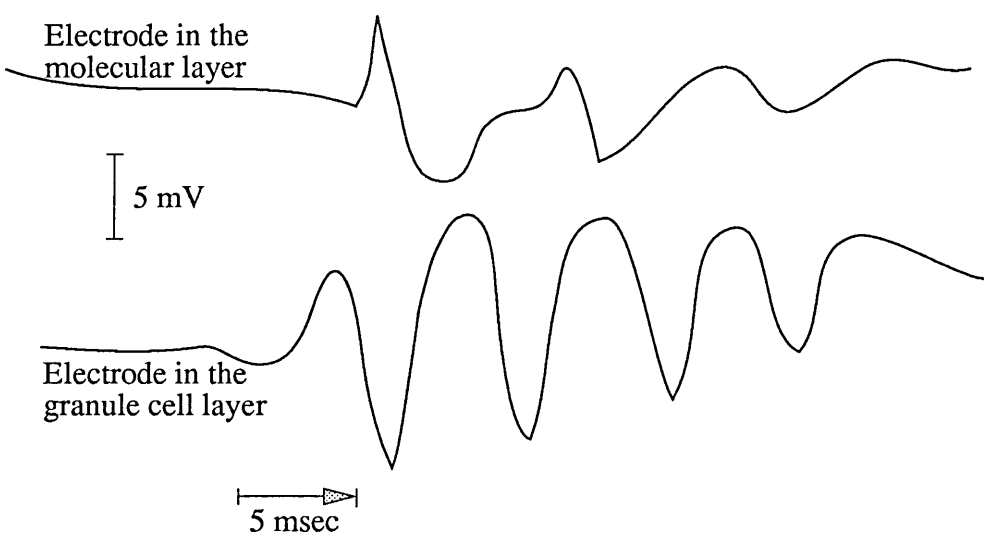


Figure 5.11 Epileptic activity in the rat dentate gyrus. The recording electrodes were attached to the probe in the usual methods and the seizure was induced by 3 minutes of 2Hz stimulus frequency.

stimulation and this was tried with a probe implanted in the dentate gyrus. By stimulating the perforant path with a stimulus frequency of 2 Hz for periods over 3 minutes, epileptic activity was observed in the granule cells. The schematic diagram below, figure 5.11, shows the evoked response on the two stainless steel recording electrodes.

The downward, negatively going peaks on the lower trace represent the cells discharging rapidly. The response from the glutamate electrode confirmed there was an increase in glutamate, which was to be expected with the high amount of neuronal activity, figure 5.12.

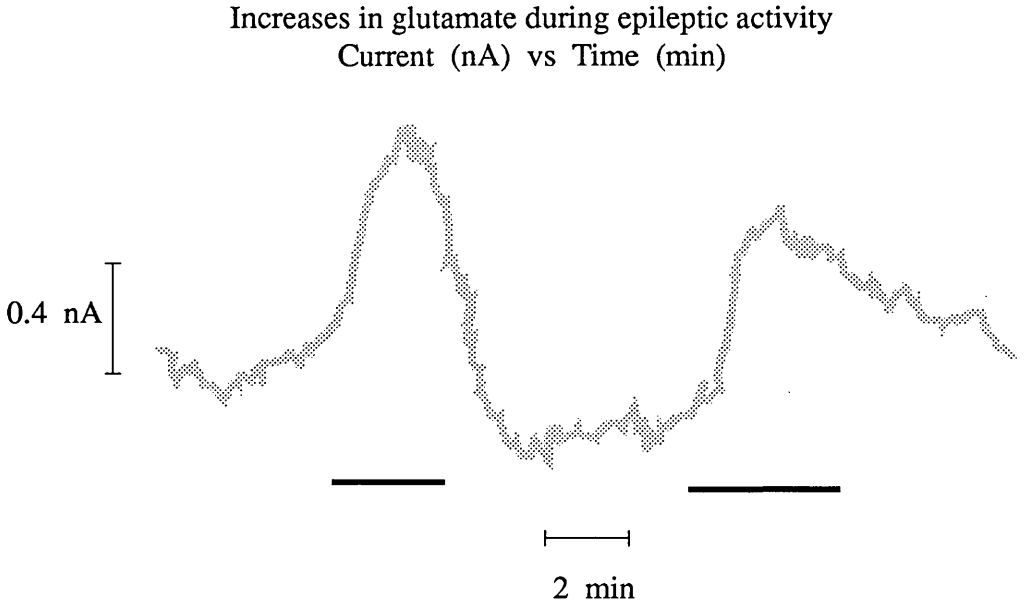


Figure 5.12 Glutamate increases during epileptic activity. The bars represent 3 and 5 minutes of 2 Hz stimulus frequency. The probe was situated in the dentate gyrus and the electrode was recording at +650 mV (vs Ag/AgCl).

5.9 Conclusions

The results presented here show that the glutamate probe, with its the high sensitivity and the fast time resolution, has great potential for studying the neurophysiology of processes such as LTP and epilepsy. Although the work has only been performed in a small number of rats, the initial success is encouraging.

The overall success rate of these probes was similar to the previous chapter, except that some of the difficulties, such as air bubble blockage, had been 'ironed out'. Out of twenty electrodes made and implanted during the period spent on the hippocampal work, twelve responded well with the best of the results shown above. The others gave little in the way of intelligible results and this was often due to sudden drift in the background traces, noisy electrical interference and spiking. The success rate was improving but better quality electrical components would be required to remove these difficulties.

References

Abdul-Ghani A S, Coutinho-Netto J & Bradford H F (1981) in *Glutamate: Transmitter in the Central Nervous System*, Roberts P J, Storm-Mathisen J, Johnston G A R (Eds), Wiley, New York

Abercrombie E D & Keefe K A (1991), 5th International Conference on *in vivo* monitoring, Noordwijkerhout, Holland p308-310

Albery W J & Bartlett P N (1985), *J. Electroanal. Chem.* **194** 211-222

Alexander G E & Crutcher M D (1990), *Trends in Neurosci* . **13** 266-272

Angevine J B & Cotman C W (1981) in Principles of Neuroanatomy , Oxford University Press, New York

Aniksztejn L, Roisen M P, Amsellem R & Ben-Ari Y (1989), *Neuroscience* **28** 387-392

Antelman S M, Szechtman H, Chin P & Fischer (1975), *Brain Res.* **99** 319-337

Armstrong-James M & Millar J, (1979) *J. Neurosci. Methods* **1** 279-287

Benveniste H (1989), *J. Neurochem.* **52** 1667-1678

Benveniste H, Drejer J, Schousboe A, Diemer N H (1984), *J. Neurochem.* **52** 1369-1374

Bliss T V P & Lømo T (1973), *J. Physiol.* **232** 357-374

Bliss T V P, Erringto M L, Lynch M A & Williams J (1990) in Cold Spring Harbour Symposium on Quantitative Biology, Vol. LV 119-129

Boutelle M G, Svensson L & Fillenz M (1989), *Neuroscience* **30** 11-17

Boutelle M G, Stanford C A, M Fillenz, Albery W J & Bartlett P N (1986) *Neurosci. Lett.* **72** 283-288

Boutelle M G (1991) personal communication

Bradford H F (1986) in Chemical Neurobiology, Freeman Press

Brazell M P & Marsden C A (1982), *Brain Res.* **249** 167-172

Buckle P J & Haas H J (1982)*J. Phsyiol.* **326** 109-122

Carlsson M & Carlsson A (1990), *Trends in Neurosci* . **13** 272-277

Cass A E G, Davis G, Francis G D, Hill H A O, Aston W J, Higgins I J, Plotkin E V, Scott L D L & Turner A P F (1984), *Anal. Chem.* **56** 667-671

Cass A E G & Kenny E (1887), in *Biosensors: Fundamentals and Applications*, Turner A P F, Karube I & Wilson G S (Eds.), Oxford Scientific Publications 113-132

Choi D W & Rothman S M (1990) *Annu. Rev. Neurosci.* **13** 171-182

Christian E P & Dudek F E (1988), *J. Neurophyiol.* **59** 110-123

Coan E J & Collingridge G L (1985), *Neurosci. Lett.* **53** 21-26

Gollingridge G L, Kehl S J & McLennan (1983), *J. Phsyiol.* **334** 19-31

Gollingridge G L & Bliss T V P, (1987) *Trends in Neurosci.* **10** 288-293

Crespi F (1990) *J. Neurosci. Methods* **34** 53-66

Delgado J M R, Lerma J, Martín del Río & Solís J M, (1984) *J. Neurochem.* **42** 1218-1228

Dolphin A C, Errington M L & Bliss T V P (1982), *Nature* **297** 496-498

Driscoll B J (1988), Ph D Thesis, University of London

Durrant S L (1988), Ph D Thesis, University of London

Errington M L, Lynch M A & Bliss T V P (1987), *Neuroscience* **20** 279-284

Ferraris J, Cowan D O, Walatka V & Perlstein (1973), *J. Amer. Chem. Soc.* **95** 948-949

Fillenz M, O'Neill R D & Grunewald (1986), in *Monitoring neurotransmitter release during behaviour* (Joseph M H, Fillenz M, Macdonald I A & Marsden C A, Eds.), Ellis Horwood Heath Science Services

Fillenz M (1991) personal communication

Fillenz M, Wheeler D B & Boutelle M G (1991), 5th International Conference on *in vivo* monitoring, Noordwijkerhout, Holland 315-316

Finch D M & Jackson M B, (1990), *Brain Res.* **518** 269-273

Gonon F, Buda M, Cespuglio R, Jouvet M & Pujol J F (1981) *Brain Res.* **223** 69-80

Girault J A, Barbeito L, Spampinoto U, Gozlan H, Glowinski A & Besson M J (1986). *J. Neurochem.* **47** 98-106

Graybiel A M (1990), *Trends in Neurosci.* **13** 244-253

Gutnik M J, Connors B W & Prince D A (1982), *J. Neurophysiol.* **48** 1321-1335

Gustafsson B & Wigström (1988), *Trends in Neurosci.* **11** 156-162

Halliwell J V& Whitaker M J, (1987) in *Microelectrode techniques* (eds Standen N B, Gray P T A & Whitaker M J), The Company of Biologists Ltd.

Havekes L, Bückmann F & Visser J (1974), *Biochem. Biophys. Acta* **334** 272-286

Heller A (1990), *Acc. Chem. Res.* **23** 128-134

Hernandez L, Fernandez R Parada M, Baptista T, Murzi E & Hoebel B(1991) 5th International Conference on *in vivo* monitoring, Noordwijkerhout, Holland p216-218

Hill H A O & Sanghera(1990) in *Biosensors: A practical approach*, Cass A E G (Ed.) pp 17

Jacobson I, Sandberg M & Hamberger A (1985), *J. Neurosci. Methods* **15** 263-268

Joseph M H, Young A M J & Gray J A (1991) 5th International Conference on *in vivo* monitoring, Noordwijkerhout, Holland p200-202

Jefferys J G R & Williams S F (1987), *Brain* **110** 517-532

Jefferys J G R, Mitchell P, O'Hara L, Hardy J, Jordan S, Lynch M A & Wadsworth J (1988), *Society for Neuroscience Abstracts* **14** 882

Jefferys J G R (1990) *Experimental Physiology* **75** 127-162

Jordan S & Jefferys J G R (1989), *Eur. J. Neurophysiol.* Supp **2** 274

Kalia Y N (1990), Ph D Thesis, University of London

Kawashima K, Hayakawa T, Kashima Y, Suzuki T, Fujimoto K & Oohata H (1991), *J. Neurochem.* **57** 882-887

Kissinger P T, Refshuage C J, Dreiling R, Blank L, Freeman R & Adams R N, (1973) *Anal. Lett.* **6** 465-477

Kissinger P T & Shoup R E (1990), *J. Neurosci. Methods* **34** 3-10

Klein J, Köppen A & Löffelholz (1990), *J. Neurochem.* **55** 1231-1236

Korenbrot J I, Perry R & Copenhagen D R (1987), *Anal. Biochem.* **161** 187-199

Korf J & Venema K (1985), *J. Neurochem.* **45** 1341-1348

Kuhr W G (1991), 5th International Conference on *in vivo* monitoring, Noordwijkerhout, Holland 117 - 120

Kusakabe H, MidorikawaY, Fujimisha T, Kuninaka A & Yoshino H (1983), *Agric. Biol. Chem.* **47** 1323-1328

Lerma J, Herranz A S, Herreras O, Abraira V & Martín del Río (1986), *Brain Res.* **384** 145-155

Lynch M A, Errington M L & Bliss T V P (1989), *Neuroscience* **30** 693-701

Madison D V, Malenka R C & Nicoll R A (1991) *Annu. Rev. Neurosci.* **14** 379-397

Magner E (1991) Unpublished results

Marsden C A, Joseph M H, Kruk Z L, Maidment N T, O'Neill, Schenk J O & Stamford J (1988), *Neuroscience* **25** 389-400

Melby L R (1965), *Can. J. Chem.* **43** 1448-1453

Miles & Wong (1986), *J. Physiol.* **373** 397-418

Morimoto K & Goddard G V (1986), *Experimental Neurology* **94** 571-584

Nicholls D G (1989), *J. Neurochem.* **52** 331-341

Nicholls D G, Shira T & Sanchez-Prieto J (1987), *J Neurochem.* **55** 1231-1236

Nicholson R S & Shain I (1964), *Anal. Chem.* **36** 706

Nilsson O G, Kalén P, Rosengren E & Björklund A (1990) *Neuroscience.*

O'Neill R D, Grunewald R A, Fillenz M & Albery W J, (1982) *Neurosci.* **7** 1945-1954

Pei Q, Zetterström T & Fillenz M (1990), *Neurosci.* **35** 133-138

Prohaska O (1987), in *Biosensors: Fundamentals and Applications*, Turner A P F, Karube I & Wilson G S (Eds.), Oxford Scientific Publications 377 - 389

Rao (1990), Ph D Thesis, University of London

Sigma (1990) enzyme specifications leaflet

Sternberg R, Bindra D S, Wilson G S & Thévenot D R (1988), *Anal. Chem.* **60** 2781-2786

Teyler T J & DiScenna P (1987), *Annu. Rev. Neurosci.* **10** 131-162

Tossman U, Jonsson G & Ungerstedt U (1986), *Acta Scand. Physiol.* **127** 533-545

Turner A P F, (1991) RSC Symposium, Imperial College

Ungerstedt U (1984) in Measurement of Neurotransmitter release in vivo , Marsden C A (Ed.), John Wiley & Sons, Chichester. 81 - 107

Warner A E & Bate C M, (1987) in *Microelectrode techniques* (eds Standen N B, Gray P T A & Whitaker M J), The Company of Biologists Ltd.

Wheeler D B (1991) MSc Thesis, University of Oxford

Wilson G S & Thévenot D R (1990), in *Biosensors: A practical approach*, Cass A E G (Ed.) 1-16

Young A M J & Bradford H F (1986), *J. Neurochem.* **47** 1399-1404

Zeman W & Innes J R M (1963), in Craigies Neuroanatomy of the Rat, Academic Press.

Zetterström T (1986), Pharmacological analysis of central dopaminergic neurotransmission using a novel brain perfusion method, Karolinska Institute. p19

Zetterström T, Wheeler D B, Boutelle M G & Fillenz M (1991) Eur. J. Neurosci. 3 940-947